

1. Introduction

In this review we wish to relate effective forces in nuclear matter and in nuclei back to the interaction between two isolated nucleons. Low-brow meson theory is used to derive the nucleon-nucleon interaction, with dispersion theoretical calculations as a guide, and a certain amount of phenomenology to pin down the parameters. A chiral picture is in the back of our mind, but since the main approach here is a semi-phenomenological one, chiral invariance is not developed in detail.

The nucleon-nucleon interaction in free space is used as a starting point to discuss effective forces in nuclear matter and in nuclei. This discussion is carried out within the framework of the Landau Fermi liquid theory, initially along the lines begun by Migdal [1], although our philosophy is somewhat different in that we wish to explicitly calculate, as far as possible, Fermi liquid parameters from the nucleon-nucleon interaction. We use certain crucial nuclear phenomena as a guide in this calculation, which cannot really be carried out from first principles, but must be continuously monitored by comparison of calculated results with empirical data.

Information that we gain about effective nuclear interactions makes it possible for us to discuss the problem of the binding energy of nuclear matter, although this latter quantity is not easily calculated within the framework of Fermi liquid theory.

2. The nucleon-nucleon interaction

The nucleon-nucleon interaction is understood, in considerable detail, as arising from the exchange of various mesons. The longest-range part results from the exchange of the lightest possible exchanged particle, the π -meson. The intermediate-range part of the interaction can be understood as arising from the exchange of scalar mesons with various masses, really systems of two pions coupled to $S = 0$, $T = 0$, as we shall discuss in more detail later.

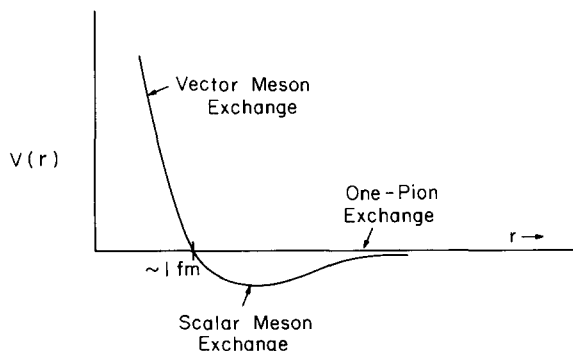


Fig. 1. Schematization of the nucleon-nucleon potential.

We shall discuss the nucleon-nucleon interaction, even the short-range repulsion, as arising from meson exchange. The quarkish constitution of the nucleons must manifest itself at short distances. There is considerable controversy, at the moment, as to how to include the quarkish composition of the nucleon. Many particle physicists wish to obtain nearly all of the nucleonic properties from those of the three constituent quarks, and therefore have "largish" quark distributions, ~ 1 fm in radius. There has been very little success in understanding low-energy nucleon-nucleon forces in such pictures. Even

signal successes of the picture, such as the description of nucleon magnetic moments, have faded somewhat when these models were applied to the strange baryons where magnetic moments, especially those of the cascade particles, differ strongly from predictions.

An alternative approach [2] pictures the quark confinement region as small in extent, compressed by pressure from the pion-cloud exterior to this region. Much of the charge distribution and of the magnetic moment are given by the meson cloud. The coupling of the pion to the interior quarks is determined by continuity of the axial-vector current. This gives, in the region outside of the core of confined quarks, the conventional one-pion-exchange interaction, which has the usual interpretation as the linear interference between two pion clouds as the nucleons come within each other's proximity.

Let us now discuss the heavier mesons, especially the ρ and ω . Quark fanatics would leave no room for these at all. We would claim that a deeper wisdom is afforded by thinking of QCD in the way proposed by 't Hooft [3]. He considered QCD generalized from SU(3) to an $SU(N_c)$ gauge group; i.e., he imagined that there could be N_c , not only 3, colors. In this generalization, $1/N_c$ is the coupling constant. If one assumes confinement*, then, in the large N_c limit, QCD is equivalent to a local field theory of mesons (and glueballs). In this way, QCD is equivalent, in a well-defined way, to a meson theory. Indeed, for any N_c , including $N_c = 3$, QCD is equivalent to a meson theory in which $1/N_c$ is the coupling constant [4]. Only, for $N_c = 3$, this coupling constant is not terribly small, and one has to estimate $1/N_c$ corrections to the lowest-order terms, calculated from simple meson theory. Sometimes these corrections are appreciable.

If QCD is equivalent to a local meson field theory in the large N_c limit, then where do the baryons come from? Witten has given strong arguments that they must arise as soliton solutions of the meson field equations [5] and, indeed, more than twenty years ago Skyrme [6] invented a model, now known as the nonlinear sigma model, in which baryons emerged as such solutions of a nonlinear meson theory.

A shortcoming of Skyrme's theory was, that in addition to the well-determined second-order meson terms of the nonlinear sigma model, which we shall discuss, a fourth-order term had to be introduced in an ad hoc way to stabilize his solution. More in line with the large N_c limit of QCD, Adkins and Nappi [7] introduce the ω -meson, coupled in the Lagrangian to the baryon density B^0 ,

$$\delta\mathcal{L} = g_\omega \omega B^0(r) . \quad (2.1)$$

They then find that the action coming from the second-order nonlinear sigma model has an additional term

$$\delta S = -\frac{1}{2} \frac{g_\omega^2}{4\pi} \int_0^\infty 4\pi r^2 dr \int_0^\infty 4\pi r'^2 dr' B^0(r) \frac{\exp(-m_\omega |\mathbf{r} - \mathbf{r}'|)}{|\mathbf{r} - \mathbf{r}'|} B^0(r') . \quad (2.2)$$

Thus, the ω -exchange provides the repulsion which keeps the nucleon from collapsing, which it would otherwise do in order to maximize the magnitude of its (attractive) pionic self-energy. The contribution (2.2) is not unlike that from the Coulomb potential in the Lorentz electron. The Poincaré stresses, which were needed to keep Lorentz's electron from flying apart, are now replaced by the pion field, which holds the nucleon together.

* We shall leave the proof of confinement to particle physicists; for our purposes, the fact that we don't see quarks is strong circumstantial evidence for confinement.

Now it is very natural to consider $B^0(r)$ and $B^0(r')$ not to be limited to both being within the same nucleon, but that they can be in different nucleons. Then one has the usual ω -exchange nucleon–nucleon interaction, after integrating over the B^0 ’s. This unifies the boson-exchange interaction with the structure of the nucleon. One has in this way a natural means for regularizing the ω -exchange potential at short distances. This program has not yet been carried out, but is in progress [8].

It has been shown [9] that effects from the ρ -meson are included in the Skyrme fourth-order term. We shall discuss later in this chapter how the ρ -meson is introduced in bag models.

So far, there is not much of a role for quarks. Yet, we know that asymptotic freedom must set in at short distances, and consequently, they should be built in. A convenient way of doing this was given by Vento et al. [10] within the framework of the chiral bag model. Independently of Skyrme and Witten, they found a soliton solution for the nucleon, consisting of a small bag of quarks coupled to the nonlinear pion cloud, the same cloud as Skyrme’s. Indeed, in the limit of bag radius R going to 0, one recovers the Skyrme model [11].

Calculations of the nucleon–nucleon potential energy have been carried out in the Skyrme model [12], as we shall discuss. The short-range repulsion is about the same as that in the chiral bag model [13]. If two small bags, each of radius R , come together, the bags will not merge into a bag of radius $2R$, but the individual bags will contract for quite a time. The argument is a simple one [14], which we shall now restate. In the bag model, the kinetic energy of each quark is

$$T_q = 2.04/R \quad (2.3)$$

where R is the bag radius. Thus, if $R = 0.5$ fm, a typical chiral bag radius, then the kinetic energy of three quarks is

$$3T_q = 6.12/R = 2.4 \text{ GeV}. \quad (2.4)$$

The attractive energy from coupling to the pion cloud must then be -1.4 GeV, for the nucleon to have net energy ~ 1 GeV. Corrections to the kinetic energy for spurious center of mass motion will decrease (2.4) somewhat, but it is clear that the energy from coupling to the meson cloud will be ~ -1 GeV. Thus, this energy for two nucleons will be ~ -2 GeV.

Now the energy from coupling of the 6-quark bag to the meson cloud will be only $2/9$ of this; to obtain this number one needs a detailed calculation [15], but one can easily see that this number is reasonable. The pion couples to the quarks through the operator $\sigma \cdot \nabla \tau \cdot \phi_\pi$. Now, 12 quarks form a “closed shell”, so that the pion coupling is zero. It turns out the coupling decreases linearly from 3 to 12 quarks [15]. Thus, for 6 quarks, it is $2/3$ of that for three quarks. The energy goes as the square of the coupling; thus

$$|E_\pi(6 \text{ quark})|/|E_\pi(3 \text{ quark})| = \frac{4}{9} \quad (2.5)$$

from which the ratio of $2/9$ follows for $|E_\pi(6 \text{ quark})|/2|E_\pi(3 \text{ quark})|$.

Consequently, rather than give up the large attractive coupling of the two bags to the pion clouds by merging into a 6-quark bag, the bags will become smaller, for a time, each keeping its identity. At a distance of $\sim 0.4\text{--}0.5$ fm, they will finally merge. The repulsion at this distance given by merging chiral bags [13] is about the same as from merging Skyrmions [12], so there is hardly any reason to shift description. Thus, the interaction can be calculated as the Skyrmion–Skyrmion interaction, with an

important addition of an interaction from scalar exchange, which results from the addition of quantum fluctuations to the Skyrme picture. We show these in fig. 5b and will discuss them later. In other words, we are back to using boson-exchange potentials, but with a definite prescription for regularization at short distances and with a much deeper understanding of them.

One should remark that having a small defect with these quarks in it is useful, in spite of what was said above, for several reasons. First, it gives us a line on corrections of order $1/N_c$; this gives, for example, a factor of $5/3$ in the pion coupling to the nucleon [12]. Second, the quarks build in the underlying SU(3) group structure. The quarks can be considered as quasiparticles, each with a large pion cloud. Indeed, for a bag radius $R = 0.57$ fm, the quarks go to zero energy [10, 11] and one regains, in this sense, the constituent quark model.

We now discuss the various components of the nucleon–nucleon interaction according to their range.

2.1. The long-range interaction

The longest-range part of the nucleon–nucleon interaction is mediated by the exchange of the lightest particle coupling strongly to the nucleons, the π -meson. The one-pion exchange potential can be obtained by standard procedures [16]. In momentum space it is

$$V_{\text{OPEP}}(k) = -\frac{f^2}{m_\pi^2} (\tau_1 \cdot \tau_2) \frac{(\sigma_1 \cdot k)(\sigma_2 \cdot k)}{k^2 + m_\pi^2} \quad (2.6)$$

$$= -\frac{f^2}{m_\pi^2} (\tau_1 \cdot \tau_2) \left\{ \left[\frac{(\sigma_1 \cdot k)(\sigma_2 \cdot k) - \frac{1}{3}(\sigma_1 \cdot \sigma_2)k^2}{k^2 + m_\pi^2} \right] + \frac{1}{3}\sigma_1 \cdot \sigma_2 - \frac{1}{3} \frac{m_\pi^2 \sigma_1 \cdot \sigma_2}{k^2 + m_\pi^2} \right\} \quad (2.7)$$

where in the second step we have broken $V(k)$ up into tensor force, spin–spin δ -function and spin–spin Yukawa. Here $f^2/4\pi = 0.081$. This interaction can be transformed into configuration space, giving*:

$$\begin{aligned} V_\pi(r) &= \frac{f^2}{4\pi m_\pi^2} (\tau_1 \cdot \tau_2) (\sigma_2 \cdot \nabla) (\sigma_2 \cdot \nabla) \frac{\exp(-m_\pi r)}{r} \\ &= \frac{f^2}{4\pi} m_\pi (\tau_1 \cdot \tau_2) \left\{ S_{12} \left[\frac{1}{(m_\pi r)^3} + \frac{1}{(m_\pi r)^2} + \frac{1}{3m_\pi r} \right] \exp(-m_\pi r) \right. \\ &\quad \left. - \frac{4\pi(\sigma_1 \cdot \sigma_2)}{3m_\pi^3} \delta(r) + \left(\frac{\sigma_1 \cdot \sigma_2}{3} \right) \frac{\exp(-m_\pi r)}{m_\pi r} \right\} \end{aligned} \quad (2.8)$$

where r is the interparticle distance, $r = |\mathbf{r}_1 - \mathbf{r}_2|$, and

$$S_{12} = 3 \frac{(\sigma_1 \cdot r)(\sigma_2 \cdot r)}{r^2} - (\sigma_1 \cdot \sigma_2). \quad (2.9)$$

As can be seen from the above, averages over either spin or isospin will make the expectation value zero in spin-saturated or charge-conjugate nuclei or nuclear matter. Some contributions from the

* We employ relativistic units $\hbar = c = 1$.

exchange terms will be left, but these are not large. Thus, the lowest-order contributions from the tensor interaction to the binding energies of nuclei or nuclear matter are not large.

We know, however, that second-order effects of the tensor force are large. The main difference between the bound deuteron system, which has $S = 1$, and the unbound proton–proton or neutron–neutron $S = 0$ system is that the tensor force is operative in the former. Since the tensor interaction introduces mainly intermediate states of high momentum and energy when used in perturbation theory, we can choose some effective energy \bar{E} for the energy of a typical intermediate state [17, 18] and represent the higher-order effects of the tensor interaction by

$$\begin{aligned} V_{\text{eff}}(r) &= -\frac{(V_{\text{tensor}})^2}{\bar{E}} \\ &= -\frac{1}{\bar{E}} (3 - 2\tau_1 \cdot \tau_2) [6 + 2\sigma_1 \cdot \sigma_2 - 2S_{12}] V_{t\pi}^2(r) \end{aligned} \quad (2.10)$$

where $V_{t\pi}(r)$ is the radial part of the pion-exchange tensor force. In the $S = 1$, $T = 0$ state,

$$V_{\text{eff}}(r) \cong -\frac{72}{\bar{E}} V_{t\pi}^2(r) \quad (2.11)$$

where we drop now the S_{12} term. The factor of 72 compensates for the smallness of $(f^2/4\pi)$, so that $V_{\text{eff}}(r)$ is

$$V_{\text{eff}}(r) \cong -\frac{0.47}{\bar{E}} (m_\pi)^2 \left[\frac{1}{(m_\pi r)^3} + \frac{1}{(m_\pi r)^2} + \frac{1}{3m_\pi r} \right]^2 \exp(-2m_\pi r). \quad (2.12)$$

Taking* $m_\pi/\bar{E} \cong \frac{2}{3}$ and evaluating $V_{\text{eff}}(r)$ at $r = m_\pi^{-1}$ to get a rough idea of its size, we find

$$V_{\text{eff}}(\hbar/m_\pi c) \cong -0.23 m_\pi c^2 = -32 \text{ MeV} \quad (2.13)$$

where we have here put in an \hbar and c to make clear that m_π^{-1} is a length. If we estimate the strengths of Yukawa potentials of range m_π^{-1} appropriate for the ${}^1\text{S}$ and ${}^3\text{S}$ states by converting potentials which give the correct scattering lengths and effective ranges [16] to this range using

$$\text{Depth} \times (\text{Range})^2 = \text{Const.},$$

we find a depth of ~ 33 MeV for the ${}^1\text{S}$ potential, ~ 60 MeV for the ${}^3\text{S}$ potential†. Our V_{eff} of eq. (2.13), which acts only in the ${}^3\text{S}$ state, is about right to account for this difference.

We cannot take the expression (2.12), which would imply a range of $(2m_\pi)^{-1}$ for V_{eff} , literally, since the closure approximation does not handle the range correctly. (Proper account of the intermediate state propagator leads to most of the weighting being at shorter distances.)

* See the discussion in chapter 6.

† The “rule of thumb”, is that in shell-model calculations the ${}^3\text{S}$ interaction should be chosen $\sim (10/6)$ times the ${}^1\text{S}$ one, as in the Rosenfeld interaction.

2.2. The intermediate-range attraction

The intermediate-range attraction in the nucleon–nucleon interaction is now understood as chiefly coming from the exchange of correlated pairs of pions which are in a $J = 0$, $T = 0$ state. This potential looks like [19]

$$V_\sigma(r) = -\frac{1}{2\pi} \int \rho(t) \frac{\exp(-\sqrt{t} r)}{r} dt \quad (2.14)$$

where $\rho(t)$ is a weighting function governing the amount of exchange of each $J = 0$, $T = 0$ system of mass \sqrt{t} . Given the amplitudes for pion–nucleon scattering $V_\sigma(r)$ is straightforward to compute by dispersion relations although complex technology is involved since the iterated one-pion-exchange potential must be removed.

Most of the contribution to $V_\sigma(r)$ comes from processes involving virtual isobars, as shown in fig. 2 provided pion–pion rescattering is put in as shown in fig. 3. Contributions to the isospin-dependence from crossed and uncrossed pion exchange cancel to a good accuracy [20] so that, practically speaking, the processes of fig. 2 give an interaction of the form (2.14), which is independent of spin and isospin. Such an interaction is of the type envisaged in the σ -model as arising from the exchange of the isoscalar $S = 0$, σ -meson; therefore we label the interaction V_σ but the “ σ ” has nothing to do with the spin operator.

Indeed, allowing for rescattering of the π -mesons, which is accomplished in the σ -model through their coupling to the σ -meson, one would more realistically have processes like those shown in fig. 3. Even though the input σ -mass in the σ -model may be large, ≥ 1 GeV, processes such as those shown in fig. 3 where it couples to pions will lower considerably the effective mass with which it enters into the nucleon–nucleon interaction. Although the σ -meson may be heavy, and cannot propagate far (only a distance $\sim m_\sigma^{-1}$), the two pions may form a system of much lower mass. Indeed, explicit calculations [21] give for processes such as shown in fig. 3 the weighting function $\rho(t)$ shown in fig. 4.

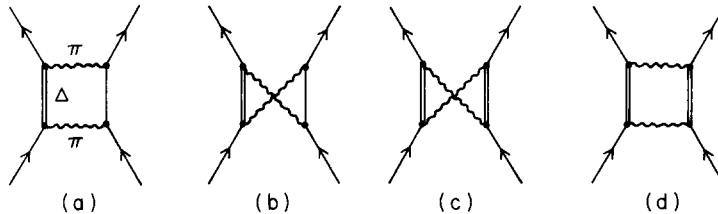


Fig. 2. Contributions to the intermediate-range potential $V_\sigma(r)$.

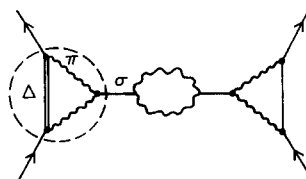


Fig. 3. The process, fig. 2a, extended to include pion rescattering. The pion scattering is envisaged here as occurring through the coupling of the pions to a σ -meson, although a more general description may be necessary. The part of the graph encircled by the dashed line may be described as a vertex correction to the σ NN coupling.

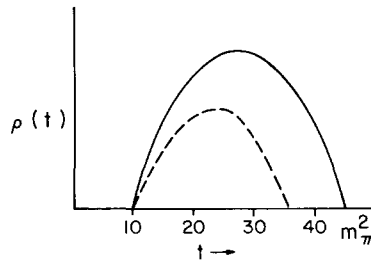


Fig. 4. The weighting function $\rho(t)$ for the exchange of two-pion system coupled to $J = 0$, $T = 0$. The dashed line represents the weighting function after subtraction of the iterated one-pion-exchange potential and therefore, the true weighting function for the potential corresponding to σ -exchange.

It should be noted that processes involving intermediate isobars are not the only ones contributing to $V_\sigma(r)$ of (2.14). After removal of the iterated one-pion-exchange interaction, one has processes in which two pions are “in the air at the same time”. Such processes are properly included in the dispersion-theoretical calculations [22] and in the considerations of [21].

The Skyrme-Skyrmion interaction [12] does not have any contribution from scalar exchange. In order to see why not, we must develop the nonlinear sigma model, which is the basis of the Skyrme theory.

In the underlying chiral-invariant σ -model, the π - and σ -mesons are built in as a four-vector. In addition to the usual coupling to nucleons as pseudoscalar and scalar mesons, i.e.

$$\delta\mathcal{L}_{NN\pi} = ig\bar{\psi}\gamma_5\tau \cdot \pi\psi \quad (2.15)$$

$$\delta\mathcal{L}_{NN\sigma} = g\bar{\psi}\sigma\psi \quad (2.16)$$

(where $g = (2m_N/m_\pi)f$ in terms of the f used previously) there is a “field potential”; i.e., a potential involving the π - and σ -fields

$$V = \frac{\lambda}{4} [(\sigma^2 + \pi^2)^2 - f_\pi^2]^2. \quad (2.17)$$

The form of this field potential is shown in fig. 5a; it looks like a roulette wheel.

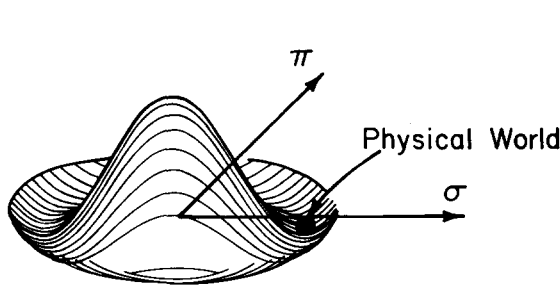


Fig. 5a. Form of “field potential” as function of π - and σ -fields.

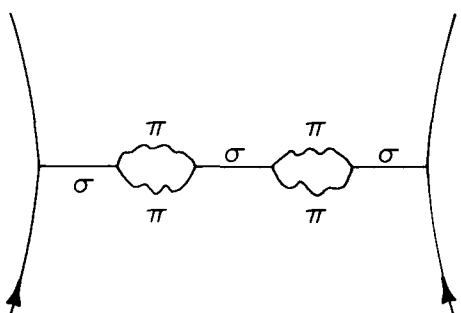


Fig. 5b. Summation of quantum fluctuations, here consisting of pion bubbles, which give the intermediate-range scalar exchange.

Our discussion of pion–nucleon interactions up to this point has been in terms of weak pion fields, single pions being emitted and absorbed as fluctuations about zero pion field. Hence, the point labelled “physical world” in fig. 5a lies on the σ -axis, with $\pi = 0$.

The system (world) will obviously wish to minimize the field potential, but since it is quantal, not classical, it will vibrate about the minimum. We can write

$$\sigma = f_\pi + \varepsilon \quad (2.18)$$

and, taking $\pi = 0$, we see that

$$V \cong \lambda f_\pi^2 \varepsilon^2 \quad (2.19)$$

correct through terms of order ε^2 ; for the moment we drop the ε^3 and ε^4 terms. We now write

$$V = \lambda f_\pi^2 \varepsilon^2 = \frac{1}{2} m_e \varepsilon^2 \quad (2.20)$$

treating ε as the usual scalar field for small fluctuations. This shows that the mass is simply related to λ ; i.e.,

$$m_e = 2\lambda f_\pi^2. \quad (2.21)$$

The Skyrme model, which has later been called the nonlinear σ -model, is obtained as the limit of the σ -model as $\lambda \rightarrow \infty$. From (2.21) it is seen that this implies $m_e \rightarrow \infty$. The classical interaction of two nucleons is equivalent to the lowest-order (second-order) exchange of the ε . But the range of this interaction is $\hbar/m_e c$. In the limit $m_e \rightarrow \infty$, the interaction becomes a zero-range (contact) one, and is completely hidden inside the ω -repulsion. Thus it follows that the classical Skyrme–Skyrmion interaction contains no scalar attraction.

Quantum fluctuations, however, restore an intermediate-range attraction. Processes such as those shown in fig. 5b or earlier in fig. 3 produce the potential V_σ of eq. (2.14) with weighting function such as shown in fig. 4. Boson exchange models, of course, replace the continuous spectrum of masses shown in eq. (2.14) by a single one. Typically, the mass is $m_e \sim 550$ MeV and

$$g_{eNN}^2/4\pi \sim 6-7. \quad (2.22)$$

From looking at either the process, fig. 5b, or that of fig. 3, one could estimate the value of m_e quite simply. The two-pion system essentially gives this mass. Each of the pions has its rest mass and, just from phase space arguments, a kinetic energy about equal to its rest mass. Thus, the total mass of the two-pion system is about $4m_\pi = 560$ MeV, and this is to be identified with the mass of the ε . It is harder to estimate the coupling constant g_{eNN} ; a calculation has to be carried out.

All of the discussion so far assumes that the quantization of the fluctuations is carried out in the perturbative vacuum; in particular, that the average π -field (see fig. 5a) is zero, and that fluctuations in the π -field are about zero-field. However, it is now understood that the chiral angle θ , the angle measured from the σ -axis, (see fig. 5a) grows as the distance r from the center of a nucleon decreases. Indeed, in the Skyrme theory [6] the chiral angle increases to π in the center of a nucleon. With introduction of a defect [10] corresponding to the little bag of quarks, the chiral angle increases only to

$\sim \pi/2$ at the bag radius R . This occurs for $R \sim 0.5$ fm. Since this is the chiral angle at R for a single nucleon, in the case of two nucleons a distance of 1 fm apart, the chiral angle at either of the bag surfaces will be $> \pi/2$, probably considerably greater than $\pi/2$ at the midpoint of the line joining the two nucleons.

Looking at fig. 5a, consider now what happens when $\theta = \pi/2$. The soft fluctuations, those requiring no energy change, are now back and forth in the σ -direction, around the roulette wheel; those in the π -direction involve going up and down the roulette wheel. Thus, fluctuations in the pion direction perpendicular to the roulette wheel are now hard, and the one-pion exchange and processes such as shown in fig. 3 will be cut out for this particular pion direction. The wheel in fig. 5a is actually the cross section of a sphere in four-dimensional space, and fluctuations in two of the three isospin directions of the pion will remain soft. Fluctuations in the σ -direction are now soft, the σ behaving as if massless. Thus, for $\theta = \pi/2$ there will be a σ -exchange interaction

$$V_\sigma = -g_{\sigma NN}^2/4\pi r. \quad (2.23)$$

Remember that the σ - and π -fields are coupled as a 4-vector, as that* $g_{\sigma NN} = g$ of eq. (2.16) or, in other words,

$$g_{\sigma NN}^2/4\pi = 14. \quad (2.24)$$

This is not yet the interaction between two physical nucleons, however. If three valence quarks are put into the vacuum with $\theta = \pi/2$, half of the baryon number goes into completing the vacuum, and only half remains in the valence states [23]. Thus, the interaction between two physical nucleons is only 1/4 of (2.23), in other words,

$$V_\sigma = -3.5/r \quad \text{for } \theta = \pi/2, \quad (2.25)$$

the θ being $\theta(R)$, the value of θ at the bag radius. This is substantially larger in magnitude than one would obtain from the boson-exchange scalar interaction $V_e = (g_{e NN}^2/4\pi) \exp(-m_e r)$ which, with the values for $g_{e NN}$ and m_e quoted above, would give $V_e \approx -1/r$ for $r = 1$ fm.

On the other hand, as the chiral angle θ becomes larger than $\pi/2$, the soft σ -mode will get rotated out. Thus, whereas the correctly calculated V_σ is substantially larger in magnitude than the V_e used in boson-exchange models for $r \approx 1$ fm, for smaller r it will soon drop below the V_e .

The above discussion indicates that the actual scalar interaction obtained from calculations which correctly quantize about the soliton will have a different shape from the boson-exchange V_e , being larger in magnitude at distances $r \sim 1$ fm, smaller in magnitude at small distances, but that, on the average it will be of roughly the magnitude of V_e . It is unlikely that experiments, at this stage, can distinguish the correct shape from the Yukawa-like V_e . Any such effects can probably be taken into account by small changes in $g_{e NN}$ or in m_e .

2.3. The short-range interaction

Originally, the existence of vector mesons was postulated in order to account for the spin-orbit

* In fact, in bag calculations the $g_{\sigma NN}$ is replaced by $1/(2f_\pi R)$ where R is the bag radius.

interaction in nuclei [24]. In the hydrogen atom one has a spin-orbit force, of the Thomas form,

$$V_{\text{s.o.}} = \frac{\hbar^2}{m_e^2 c^2} \boldsymbol{\sigma} \cdot \mathbf{L} \frac{1}{r} \frac{dV_c}{dr}, \quad (2.26)$$

where V_c is the central Coulomb potential. This spin-orbit interaction results from employing the Coulomb interaction in the relativistic Dirac equation. Vector mesons behave like heavy photons, and when the vector-meson-exchange potential is used in a relativistic two-particle equation a short-range spin-orbit interaction (of range m_ω^{-1}) results. This turns out to be what is needed in the shell model. From empirical properties of the spin-orbit force, especially as seen in nucleon–nucleon scattering, Breit predicted approximately the mass of the ω -meson, which was discovered only later. The attractive feature of the relation between short-range repulsion and spin-orbit force in the boson-exchange model has not been reproduced yet in the quark model.

In terms of quarks, p and n, the ω -meson can be written as

$$|\omega\rangle = \frac{1}{\sqrt{2}} [p\bar{p} + n\bar{n}] \quad (2.27)$$

so that the coupling of the ω to any particular hadron depends only on the number of p and n quarks in the hadron. Thus, the coupling of the ω to the Λ -particle is 2/3 of its coupling to the nucleon. Similarly, the ρ -meson can be written

$$|\rho^0\rangle = \frac{1}{\sqrt{2}} [p\bar{p} - n\bar{n}] \quad (2.28)$$

insofar as the isospin behavior is concerned. From the above scheme, one finds for the ratio of couplings to nucleons

$$\left. \frac{g_{\omega NN}^2}{4\pi} \right|_{\text{SU}(3)} = 9 \frac{g_{\rho NN}^2}{4\pi}. \quad (2.29)$$

From the known $g_{\rho NN}^2$ this gives

$$\left. \frac{g_{\omega NN}^2}{4\pi} \right|_{\text{SU}(3)} = 9 \frac{g_{\rho NN}^2}{4\pi} \cong 4.5. \quad (2.30)$$

We have used here the subscript “SU(3)” since the factor of 9 is unchanged by the introduction of strange quarks.

Aside from the spin-orbit interaction, the main effect from ω -meson exchange is the short-range repulsion

$$V_\omega(r) = \frac{g_{\omega NN}^2}{4\pi} \frac{\exp(-m_\omega r)}{r}. \quad (2.31)$$

Although the coupling constant given by (2.30) is large, analysis of empirical data, especially from nucleon–nucleon scattering, has consistently demanded a $g_{\omega NN}^2/4\pi$ much larger than given by the above argument namely [25, 26],

$$(g_{\omega NN}^2/4\pi)_{\text{emp}} \sim 10-12. \quad (2.32)$$

The large effective ω -coupling can be understood by realizing [20] that combined π - and ρ -exchange, such as that shown in fig. 6, contributes in the ω -channel. Inclusion of the additional repulsions brings one up to the empirically required strengths.

Nucleon–nucleon interactions involving intermediate vector mesons such as the spin–orbit one shown in (2.26), are singular for short r , going as r^{-3} . These singularities are regularized in calculations with the Skyrme model [12]. We will now discuss an alternative phenomenological way of regularizing them, by introducing vertex functions $\Gamma_{\omega NN}$ or $\Gamma_{\rho NN}$ of finite range, since this is quite instructive. A good idea of the range of these vertex functions can be obtained [27] by looking at the nucleon form factors, which in the so-called vector-meson dominance model, can be viewed as arising from the γ -ray first coupling to the vector mesons, as shown in fig. 7. From the empirical behavior of the form factors at high momentum transfer one can obtain the $\Gamma_{\omega NN}$ and $\Gamma_{\rho NN}$ as functions of momentum transfer.

In the Little Bag Model [2] the above ideas (and those of [27]) can be made explicit. In good approximation, the electromagnetic form factor of the proton can be described as

$$F^v(q^2) = \frac{e}{2} \left(\frac{m_v^2}{q^2 + m_v^2} \right)^2, \quad (2.33)$$

as regards the isovector part, with a similar expression for the isoscalar form factor; i.e.,

$$F(q^2) = F^s + \tau_3 F^v \quad (2.34)$$

where τ_3 is the third component of isospin. Empirically, m_v is slightly larger than m_ρ or m_ω , the vector meson masses. In the little bag picture, one power of $m_v^2/(q^2 + m_v^2)$ would come from the vector meson

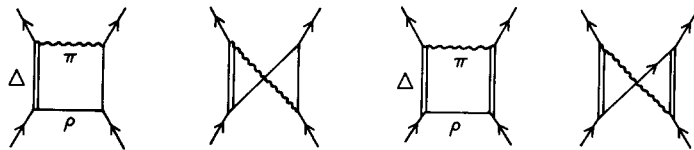


Fig. 6. Combined π - and ρ -exchange processes involving intermediate isobars which contribute in the ω -exchange channel.

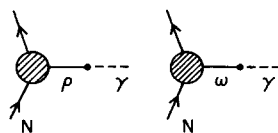


Fig. 7. Dominant contributions to the nucleon form factors.

propagator (see fig. 7) and the other, from the form factor of the bag. Thus, the bag form factor is

$$F_B(q^2) \cong m_v^2/(q^2 + m_v^2). \quad (2.35)$$

Fourier transforming this, we find $F_B(r)$ to be of extent $\sim \hbar/m_v c$, or ~ 0.3 fm, in configuration space. Of course, the Fourier transform of (2.35), taken literally, would be of Yukawa form, with a long tail, whereas in the bag model the form factor arises from quarks which are confined in a small volume with a rather abrupt surface. Thus, our above arguments should be taken only as indicative of the size of the region over which the form factor must be modified.

In the bag model, the ρ -meson is easily coupled to the nucleon, once the pion is coupled to the nucleon and isobar [28]. One starts from a basic ρ -meson constructed out of quark and antiquark coupled to spin-one and isospin-one. This ρ -meson can then decay into two pions, which are absorbed successively by the nucleon, with nucleon or Δ intermediate state. Once the ρ -meson is coupled to the two pions, the ρ -exchange potential results from one nucleon emitting two virtual pions, these two pions being scattered successively off any number of virtual basic ρ 's (described as $q\bar{q}$ states) and then being absorbed by the second nucleon.

No matter what the underlying picture, the resulting ρ -meson will be coupled to the nucleon by both a vector and a tensor coupling:

$$\delta L_\rho = \frac{g_\rho}{\sqrt{4\pi}} \left\{ \bar{\psi} \frac{(p_\mu + p'_\mu)}{2m} \tau \cdot \rho^\mu \psi + \bar{\psi} \frac{1 + K_v}{2m} [\boldsymbol{\sigma} \times \mathbf{k}] \cdot \rho \cdot \tau \psi \right\} \quad (2.36)$$

where p and p' are initial and final nucleon momenta, respectively, m is the nucleon mass and K_v is a constant which, in the vector dominance model, would be given by the anomalous moment of the nucleon

$$K_v = 3.7. \quad (2.37)$$

Effects from the vector coupling of the ρ tend to be swamped by the much larger ones from the ω , although the ρ -exchange interaction has a τ -dependence which should be distinguishable, in principle, from that of ω -exchange. Effects from the tensor coupling of the ρ tend to dominate those from the tensor coupling of the ω , which we have not discussed. The latter would involve a $(1 + K_s)$, which is very small compared with $(1 + K_v)$, if one uses the vector dominance model as a guide.

One can rewrite the tensor ρ coupling as

$$\delta L_T = \frac{f_\rho}{\sqrt{4\pi} m_\rho} \bar{\psi} [\boldsymbol{\sigma} \times \mathbf{k}] \cdot \rho \cdot \tau \psi \quad (2.38)$$

where

$$f_\rho = g_{\rho NN}(1 + K_v)m_\rho/2m. \quad (2.39)$$

From the accepted value [29],

$$g_{\rho NN}^2/4\pi = 0.5, \quad (2.40)$$

one would find

$$f_\rho^2/4\pi = 1.86 \quad (\text{vector dominance}). \quad (2.41)$$

In fact, determination of f_ρ from the nucleon form factor [30] demands a larger f_ρ ,

$$f_\rho^2/4\pi \sim 4.86, \quad (2.42)$$

and nuclear phenomena are easier to understand [31, 32] with this large value of $f_\rho^2/4\pi$. This larger f_ρ would seem to violate the vector dominance assumption; it can be understood in a simple way by assuming that there is a direct vector coupling of γ -rays to nucleons, rather than all of the coupling going through the ρ -meson [27].

The nucleon–nucleon interaction arising from ρ -exchange with tensor couplings is

$$\begin{aligned} V_\rho(k) &= -\frac{f_\rho^2}{m_\rho^2} (\boldsymbol{\tau}_1 \cdot \boldsymbol{\tau}_2) \frac{[\boldsymbol{\sigma}_1 \times \mathbf{k}] [\boldsymbol{\sigma}_2 \times \mathbf{k}]}{k^2 + m_\rho^2} \\ &= -\frac{f_\rho^2}{m_\rho^2} (\boldsymbol{\tau}_1 \cdot \boldsymbol{\tau}_2) \left\{ \frac{\boldsymbol{\sigma}_1 \cdot \boldsymbol{\sigma}_2 k^2 - \boldsymbol{\sigma}_1 \cdot \mathbf{k} \boldsymbol{\sigma}_2 \cdot \mathbf{k}}{k^2 + m_\rho^2} \right\} \end{aligned} \quad (2.43)$$

$$= \frac{f_\rho^2}{m_\rho^2} (\boldsymbol{\tau}_1 \cdot \boldsymbol{\tau}_2) \left\{ -\frac{[\boldsymbol{\sigma}_1 \cdot \mathbf{k} \boldsymbol{\sigma}_2 \cdot \mathbf{k} - \frac{1}{3} \boldsymbol{\sigma}_1 \cdot \boldsymbol{\sigma}_2 k^2]}{k^2 + m_\rho^2} + \frac{2}{3} \boldsymbol{\sigma}_1 \cdot \boldsymbol{\sigma}_2 - \frac{2 \boldsymbol{\sigma}_1 \cdot \boldsymbol{\sigma}_2 m_\rho^2}{3 (k^2 + m_\rho^2)} \right\} \quad (2.44)$$

where, in the last step, decomposition into irreducible tensors has been carried out. Writing V_ρ in configuration space,

$$\begin{aligned} V_\rho(r) &= \frac{f_\rho^2}{4\pi} m_\rho \boldsymbol{\tau}_1 \cdot \boldsymbol{\tau}_2 \left\{ -S_{12} \left[\frac{1}{(m_\rho r)^3} + \frac{1}{(m_\rho r)^2} + \frac{1}{3m_\rho r} \right] \exp(-m_\rho r) \right. \\ &\quad \left. - \frac{8\pi}{3} \frac{(\boldsymbol{\sigma}_1 \cdot \boldsymbol{\sigma}_2)}{m_\rho^3} \delta(r) + \frac{2}{3} (\boldsymbol{\sigma}_1 \cdot \boldsymbol{\sigma}_2) \frac{\exp(-m_\rho r)}{m_\rho r} \right\}. \end{aligned} \quad (2.45)$$

Comparison of the above with the pion-exchange potential, (2.8), shows the ρ -exchange tensor interaction to have opposite sign. This means that the radial part of the $\boldsymbol{\tau}_1 \cdot \boldsymbol{\tau}_2$ tensor potential will be of the form shown in fig. 8a. The effective interaction at short distances ($r < 0.6$ fm) will be modified by the highly repulsive central interaction coming from ω -exchange. The fact that the ρ -exchange tensor potential cuts off the singular π -exchange tensor potential at short distances is very important for a number of phenomena which we shall discuss in the next chapters.

A convenient way to remember the strength of ρ -coupling to the nucleon is to note that

$$f_\rho^2/m_\rho^2 \approx 2f_\pi^2/m_\pi^2 \quad (2.46)$$

with the strong ρ -coupling, eq. (2.42).

Love, Franey and Petrovich have deduced [33] empirical interactions which fit nucleon–nucleon scattering data at various energies. They plot the contribution of their tensor interactions for spins

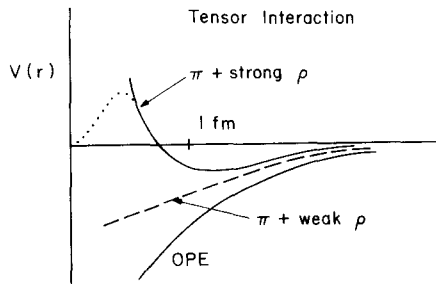


Fig. 8a. Radial behavior of the $\tau_1 \cdot \tau_2$ tensor potential from strong ($f_\rho^2 = 4.86$) and weak ($f_\rho^2 = 1.86$) exchange. The dotted line indicates the sort of modification that short-range correlations will have on the effective potential from strong ρ -exchange.

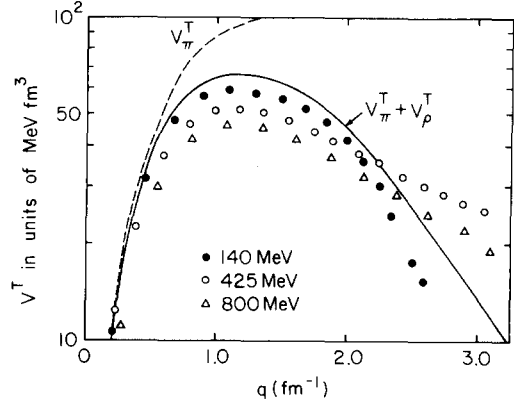


Fig. 8b. Empirical direct tensor terms compared with the theoretical V^T , eq. (2.30). A strong ρ -exchange was used.

transverse to k , essentially (see eqs. (2.7) and (2.44))

$$V^T = \frac{1}{3} \left\{ \frac{f^2}{m_\pi^2} \frac{k^2}{k^2 + m_\pi^2} - \frac{f_\rho^2}{m_\rho^2} \frac{k^2}{k^2 + m_\rho^2} \right\}. \quad (2.47)$$

We show in fig. 8b the theoretical curve corresponding to this expression; we have chosen $m_\rho = 650$ MeV rather than the empirical 770 MeV in order to take into account roughly the large width of the ρ -meson. Given the roughness of our approximations, the agreement is satisfying. We have no explanation for the apparent energy-dependence in the empirical points.

We noted earlier, following eq. (2.36), that the tensor coupling of the ρ -meson would have a factor of $(1 + K_v)$ in the vector dominance model and, in fact, is somewhat larger than would be given by this model. The tensor coupling of the ω -meson is much smaller and can, for most purposes, be ignored. A deeper understanding of which invariants are large and which are small is afforded by the Skyrme model.

The Skyrmiion-Skyrmion interaction is treated in ref. [12]. The Skyrme solution for the combined nucleon and Δ system—the nucleon must be projected from this—has the quantum number $K = 0$, where \mathbf{K} is

$$\mathbf{K} = \frac{1}{2}\boldsymbol{\sigma} + \frac{1}{2}\boldsymbol{\tau}. \quad (2.48)$$

In general \mathbf{K} will also include the orbital angular momentum \mathbf{L} , but \mathbf{L} is zero for the nucleon and Δ . Since $K = 0$, this means that the spin and isospin, neither of which is a constant of motion in the Skyrmiion, are coupled together to make a singlet state. Therefore, the interactions between two Skyrmiions involving the spins $\boldsymbol{\sigma}/2$ or the isospins $\boldsymbol{\tau}/2$ separately, will vanish. The tensor coupling of the ω involves only the spins. The tensor coupling of the ρ involves both $\boldsymbol{\sigma}$ and $\boldsymbol{\tau}$; interactions of this form will not vanish, because $\boldsymbol{\sigma}$ and $\boldsymbol{\tau}$ are (anti) correlated in the ground state of the nucleon.

In short, we have the table for Skyrmiion-Skyrmion interactions:

<u>Allowed</u>	<u>Forbidden</u>
$1_1 1_2$	$\sigma_1 \cdot \sigma_2$
$\sigma_1 \cdot \sigma_2 \tau_1 \cdot \tau_2$	$\tau_1 \cdot \tau_2$
$\sigma_1 \cdot k \sigma_2 \cdot k \tau_1 \cdot \tau_2$	

At first sight it might seem troublesome that no $\tau_1 \cdot \tau_2$ component is allowed, because the nuclear symmetry energy involves just such an invariant. However, in chapter 6 we shall show that the nuclear symmetry energy arises chiefly from second-order effects of the $\sigma_1 \cdot \sigma_2 \tau_1 \cdot \tau_2$ and $\sigma_1 \cdot k \sigma_2 \cdot k \tau_1 \cdot \tau_2$ interactions.

3. Nuclear matter as a Fermi liquid

We shall formulate the problems of nuclear matter within the framework of the Landau Fermi liquid theory. Our aim is to make a microscopic theory, in which we calculate the Landau Fermi liquid parameters, beginning from the nucleon–nucleon force. Of course, such a calculation cannot be made rigorously at the present time, but by keeping one hand on empirical quantities, we can make connections.

Our approach here is different from that of Migdal [1], whose theory of finite Fermi systems is a derivative of the Landau theory, with certain (major) added assumptions. The Migdal theory is strictly phenomenological, fitting the parameters of a quasiparticle interaction of assumed form, so as to reproduce empirical phenomena, much in the spirit of Landau’s discussion of liquid ^3He , although matters are more complicated in nuclei because of the finite nature of the system.

We are admittedly not on firm ground in calculating Landau parameters from a microscopic model in the case of nuclear matter, because there is not really any small parameter to expand in. We shall try to make plausible a picture of interacting quasiparticles and collective excitations, showing that both single-particle and collective features must be treated on an equal footing. We shall appeal to the richness of experimental data which has accumulated in recent years, for confirmation of this approach.

A great deal of work has gone into calculating the ground-state properties of nuclei from various many-body approaches: Brueckner theory, which we shall discuss later on, hypernetted chain calculations, parquet-diagram approach, various cluster expansions. One may ask why we don’t directly use one of these approaches, making a straightforward calculation of the various quantities needed. The answer is that none of these approaches is successful in reproducing the empirical saturation density or nuclear binding energy. Thus, various basic stability conditions of many-body theory would not hold for these theories at the empirical nuclear matter density.

The solution to the nuclear matter problem seems to require both the attractive nonlinear terms found [34] in the chiral σ -model Lagrangian, and the repulsive, highly density-dependent interaction resulting from the distortion of negative energy states by the σ -meson [35], essentially the meson of section 2.2. A recent review of this material has been given by A.D. Jackson [36]. It will be clear to the reader of this review that it is useful to rely heavily on experimental data in determining Fermi liquid parameters, because the theory is not yet sufficiently unambiguous to give definite results.

There are many excellent reviews of the Landau Fermi liquid theory [37, 38], in addition to the elegant original articles of Landau [39], so we shall not try to rereview this subject, but shall indicate operationally how it can be applied to give a description of nuclear matter.

Landau started from a kinetic equation for quasiparticles

$$\frac{\partial n_p}{\partial t} + \frac{\partial n_p}{\partial \mathbf{x}} \frac{\partial \varepsilon}{\partial \mathbf{p}} - \frac{\partial n_p}{\partial \mathbf{p}} \frac{\partial \varepsilon}{\partial \mathbf{x}} = I(n), \quad (3.1)$$

where n_p is the quasiparticle number*, ε and p are the energy and momentum of the quasiparticle, respectively, and I is the collision term. In the process of writing down a momentum flux tensor π_{ik} for quasiparticles, so as to obtain the conservation of total momentum

$$\frac{\partial}{\partial t} \int d^3x \int p_i n_p d\tau = 0 \quad (3.2)$$

where

$$d\tau = g d^3p / (2\pi)^3 \quad (3.3)$$

g being the degeneracy, Landau was led to the assumption: (see the discussion of section 2 of [40])

$$\delta E / \delta n(p) = \varepsilon(p), \quad (3.4)$$

where E is the total energy of the system. It is clear that this assumption is true in a Hartree–Fock theory; however, the import is much more general, although the idea of quasiparticles moving in average fields due to other particles is back of the Landau theory.

We reiterate that Landau was led to the central assumption (3.4) by conservation laws; in this case, conservation of energy and momentum. This shows what a powerful tool conservation laws can be.

Landau considered the total energy of the system to be a functional of occupation number $n(p)$ of all of the quasiparticles

$$E = \{n(p_1), n(p_2), \dots\}. \quad (3.5)$$

Thus, the $\varepsilon(p)$ in (3.4) are a functional of the $\delta n(p)$'s. To describe collective phenomena, where many of the δn 's enter, one needs to carry out the variation of E to second order,

$$\delta E = \sum \varepsilon^{(0)}(\mathbf{p}) \delta n(\mathbf{p}) + \frac{1}{2} \sum_{\mathbf{p}, \mathbf{p}'} f(\mathbf{p}, \mathbf{p}') \delta n(\mathbf{p}) \delta n(\mathbf{p}') \quad (3.6)$$

defining $f(\mathbf{p}, \mathbf{p}')$. Here we have indicated vectors explicitly, since the dependence of f on the angle between \mathbf{p} and \mathbf{p}' is crucial. Spin and isospin variables have been suppressed here, as elsewhere, for simplicity. It follows from (3.6) that

$$\varepsilon(\mathbf{p}) = \frac{\delta E}{\delta n(\mathbf{p})} = \varepsilon^{(0)}(\mathbf{p}) + \sum_{\mathbf{p}'} f(\mathbf{p}, \mathbf{p}') \delta n(\mathbf{p}'). \quad (3.7)$$

The quantity $f(\mathbf{p}, \mathbf{p}')$ is clearly the interaction between quasiparticles, since it is the change in energy

* The above n_p can be generalized [38] to $n_p \rightarrow n_p(q) = a_{p+q}^+ a_p$, where a_{p+q}^+ and a_p are Fermi creation and annihilation operators, respectively. In this way the above equation is extended to describe particle-hole excitations.

with removal of quasiparticles in states \mathbf{p} and \mathbf{p}' . It is crucial that in this removal, the occupation numbers of the other quasiparticles, $n_{\mathbf{p}''}$, $\mathbf{p}'' \neq \mathbf{p}$ or \mathbf{p}' , be kept constant. It turns out then, that $f(\mathbf{p}, \mathbf{p}')$ is the quasiparticle–quasihole interaction. This will be clear from examples worked out later, if the reader is not already familiar with this point.

The reader may have difficulty with the following conceptual point: what does one mean by functional differentiation with respect to quasiparticle number? Landau made the crucial assumption that there is a one-to-one correspondence between quasiparticle excitations in the interacting system and particle excitations in the noninteracting system. Consequently, in order to make functional differentiations in the interacting system, one can simply remove bare particles in the noninteracting system and see how the resulting changes propagate through the interacting system.

Explicit models are easily worked out when the energy is expressed in Rayleigh–Schrödinger perturbation theory, because in this theory the connection with bare-particle occupation number is clear.

We shall here work out the connection between the Brueckner–Bethe theory, which begins from Rayleigh–Schrödinger perturbation theory and makes partial summations, and the Landau theory. If one wishes to make a microscopic description of nuclear matter or nuclei, one must, in some way, get from the bare forces with extremely strong repulsive cores, which cannot be handled in perturbation theory, to effective interactions (pseudopotentials) which are well-behaved at short distances. The Brueckner–Bethe theory shows how to combine the strong short-range repulsion with correlations in the wave function which keep the particles apart over the range of this repulsive interaction, so as to give a well-behaved effective interaction.

The Brueckner–Bethe theory is only a starting point, and we must then go on to include collective effects. These turn out to be very important. The questionable part of our formalism is probably whether we include these to sufficient accuracy.

4. The Brueckner–Bethe theory

In the Brueckner theory, it is realized that, because of the strong short-ranged interactions between nucleons, ordinary perturbation theory cannot be used, and the pair interactions must be summed to all orders. One defines a G -matrix by

$$(\mathbf{k}_1 \mathbf{k}_2 | G | \mathbf{k}_1 \mathbf{k}_2) = (\mathbf{k}_1 \mathbf{k}_2 | V | \mathbf{k}_1 \mathbf{k}_2) - \sum_{|\mathbf{k}_3|, |\mathbf{k}_4| > k_F} \frac{(\mathbf{k}_1 \mathbf{k}_2 | V | \mathbf{k}_3 \mathbf{k}_4) (\mathbf{k}_3 \mathbf{k}_4 | G | \mathbf{k}_1 \mathbf{k}_2)}{k_3^2/2m + k_4^2/2m - \varepsilon_1 - \varepsilon_2} \quad (4.1)$$

where the Pauli principle has been put in explicitly. Exchange is assumed to be included, i.e., the matrix elements of V are direct minus exchange terms. Here ε_1 and ε_2 are hole energies, inclusive of self-energy insertions,

$$\varepsilon(\mathbf{k}) = \frac{k^2}{2m} + \sum_{|\mathbf{k}_2| < k_F} (\mathbf{k} \mathbf{k}_2 | G | \mathbf{k} \mathbf{k}_2). \quad (4.2)$$

The second-order self-energy insertion is shown in fig. 9; we shall not include it in our calculations here. It is usually convenient not to put self-energy insertions in particle lines, but rather to group them with other many-body clusters and to evaluate the entire sum [18]. There is then an energy gap between hole

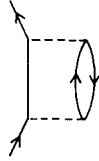


Fig. 9. Second-order self-energy insertion for a single particle. The dashed lines here represent the interactions V .

and particle states, which turns out to be awkward for making connection with the Landau theory [41]. This difficulty can be overcome by introduction of a model space [40].

In order to show the connection to Landau theory, we write the Brueckner expression for the energy

$$E = \sum_{\mathbf{k}_1} (k_1^2/2m) n(\mathbf{k}_1) + \frac{1}{2} \sum_{\mathbf{k}_1, \mathbf{k}_2} (\mathbf{k}_1 \mathbf{k}_2 | G | \mathbf{k}_1 \mathbf{k}_2) n(\mathbf{k}_1) n(\mathbf{k}_2) \quad (4.3)$$

in which we explicitly write the dependence on particle occupation number, and then carry out the variations to obtain $\epsilon(p)$ and $f(p, p')$. Here $n(k) = \theta(k_F - k)$ where θ is the step function. Equations (4.1) and (4.2) are then rewritten

$$(\mathbf{k}_1 \mathbf{k}_2 | G | \mathbf{k}_1 \mathbf{k}_2) = (\mathbf{k}_1 \mathbf{k}_2 | V | \mathbf{k}_1 \mathbf{k}_2) - \sum_{\mathbf{k}_3, \mathbf{k}_4} \frac{(\mathbf{k}_1 \mathbf{k}_2 | V | \mathbf{k}_3 \mathbf{k}_4) (1 - n(\mathbf{k}_3)) (1 - n(\mathbf{k}_4)) (\mathbf{k}_3 \mathbf{k}_4 | G | \mathbf{k}_1 \mathbf{k}_2)}{(k_3^2/2m) + (k_4^2/2m) - \varepsilon_1 - \varepsilon_2}, \quad (4.4)$$

$$\varepsilon(k) = \frac{\delta E}{\delta n(k)} = \frac{k^2}{2m} + \sum_{\mathbf{k}_2} (\mathbf{k} \mathbf{k}_2 | G | \mathbf{k} \mathbf{k}_2) n(\mathbf{k}_2) + \frac{1}{2} \sum_{\mathbf{k}_1, \mathbf{k}_2} (\mathbf{k}_1 \mathbf{k}_2 | \delta G / \delta n(k) | \mathbf{k}_1 \mathbf{k}_2) n(\mathbf{k}_1) n(\mathbf{k}_2). \quad (4.5)$$

The $\varepsilon(k)$ above in (4.5) is distinguished from that in (4.2) and from those to be used in the denominator of (4.4) by the last term involving $\delta G / \delta n(k)$. This is often called a rearrangement term, and enters into the Landau $\varepsilon(k)$, so that the Landau $\varepsilon(k_F)$ corresponds to the actual removal energy of the quasiparticle, whereas the Brueckner $\varepsilon(k_F)$ in (4.2) does not.

Now the variations can be carried out to obtain $f(\mathbf{k}, \mathbf{k}')$. Whereas the $n(k)$ refer to the occupation numbers in the noninteracting, reference state (think of Rayleigh–Schrödinger perturbation theory), removal of a particle in this state leads to the removal of a quasiparticle, since particles are assumed to transform smoothly into quasiparticles as the interaction is switched on.

Note that in (4.5) the variation

$$\delta \varepsilon(k) / \delta n(k)$$

has to be carried out with respect to

- (i) the $n(\mathbf{k}_2)$,
- (ii) the $n(\mathbf{k}_3)$ and $n(\mathbf{k}_4)$ in (4.4) for G ,
- (iii) the $n(k)$ appearing in ε_1 and ε_2 in the denominator of (4.4).

Terms arising from (ii) and (iii), which are, respectively, corrections to the Pauli operator, and self-energy coming from removal of a particle in state k' , are often called rearrangement terms.

Let us carry out these variations, replacing, for simplicity, G by V on the right-hand side of (4.4) and (4.5). This gives a theory which is essentially second-order Rayleigh-Schrödinger perturbation theory, but with the Hartree-Fock single-particle energies for the holes, i.e., we simplify (4.5) to

$$\varepsilon(\mathbf{k}) = (\mathbf{k}^2/2m) + \sum_{\mathbf{k}_2} (\mathbf{k}\mathbf{k}_2|V|\mathbf{k}\mathbf{k}_2) n(\mathbf{k}_2). \quad (4.6)$$

An example of processes we neglect in $\varepsilon(\mathbf{k})$ is pictured in fig. 9.

We obtain the following contributions to $f(\mathbf{k}, \mathbf{k}')$ from the variations listed as (i), (ii), (iii):

$$\begin{aligned} f_{(i)}(\mathbf{k}, \mathbf{k}') &= (\mathbf{k}\mathbf{k}'|V|\mathbf{k}\mathbf{k}') + \frac{1}{2} \sum_{\mathbf{k}_3, \mathbf{k}_4} \frac{(\mathbf{k}\mathbf{k}'|V|\mathbf{k}_3\mathbf{k}_4)(\mathbf{k}_3\mathbf{k}_4|V|\mathbf{k}\mathbf{k}')}{\varepsilon_k + \varepsilon_{k'} - (\mathbf{k}_3^2/2m) - (\mathbf{k}_4^2/2m)} (1 - n_3)(1 - n_4) \\ f_{(ii)}(\mathbf{k}, \mathbf{k}') &= - \sum_{\mathbf{k}_2 \mathbf{k}_4} \frac{(\mathbf{k}\mathbf{k}_2|V|\mathbf{k}\mathbf{k}_4)(\mathbf{k}'\mathbf{k}_4|V|\mathbf{k}\mathbf{k}_2)}{\varepsilon_k + \varepsilon_{k'} - (\mathbf{k}^2/2m) - (\mathbf{k}_4^2/2m)} n_2(1 - n_4) - \sum_{\mathbf{k}_2, \mathbf{k}_4} \frac{(\mathbf{k}_2\mathbf{k}'|V|\mathbf{k}\mathbf{k}_4)(\mathbf{k}\mathbf{k}_4|V|\mathbf{k}_2\mathbf{k}')}{\varepsilon_{k'} + \varepsilon_{k''} - (\mathbf{k}^2/2m) - (\mathbf{k}_4^2/2m)} \\ &\quad \times n_2(1 - n_4) + \frac{1}{2} \sum_{\mathbf{k}_1, \mathbf{k}_2} \frac{(\mathbf{k}_1\mathbf{k}_2|V|\mathbf{k}\mathbf{k}')(\mathbf{k}\mathbf{k}'|V|\mathbf{k}_1\mathbf{k}_2)}{\varepsilon_1 + \varepsilon_2 - (\mathbf{k}^2/2m) - (\mathbf{k}'^2/2m)} n_1 n_2, \end{aligned} \quad (4.7)$$

$$\begin{aligned} f_{(iii)}(\mathbf{k}, \mathbf{k}') &= -(\mathbf{k}\mathbf{k}'|V|\mathbf{k}\mathbf{k}') \sum_{\mathbf{k}_2, \mathbf{k}_3, \mathbf{k}_4} \frac{(\mathbf{k}\mathbf{k}_2|V|\mathbf{k}_3\mathbf{k}_4)(\mathbf{k}_3\mathbf{k}_4|V|\mathbf{k}\mathbf{k}_2)}{[\varepsilon_k + \varepsilon_{k'} - (\mathbf{k}_3^2/2m) - (\mathbf{k}_4^2/2m)]^2} n_2(1 - n_3)(1 - n_4) \\ &\quad - \sum_{\mathbf{k}_2, \mathbf{k}_3, \mathbf{k}_4} \frac{(\mathbf{k}_2\mathbf{k}'|V|\mathbf{k}_2\mathbf{k}')(\mathbf{k}\mathbf{k}_2|V|\mathbf{k}_3\mathbf{k}_4)(\mathbf{k}_3\mathbf{k}_4|V|\mathbf{k}\mathbf{k}_2)}{[\varepsilon_k + \varepsilon_{k'} - (\mathbf{k}_3^2/2m) - (\mathbf{k}_4^2/2m)]^2} n_2(1 - n_3)(1 - n_4). \end{aligned} \quad (4.8)$$

We draw these terms graphically as shown in fig. 10. Terms with two internal hole lines, except for fig.

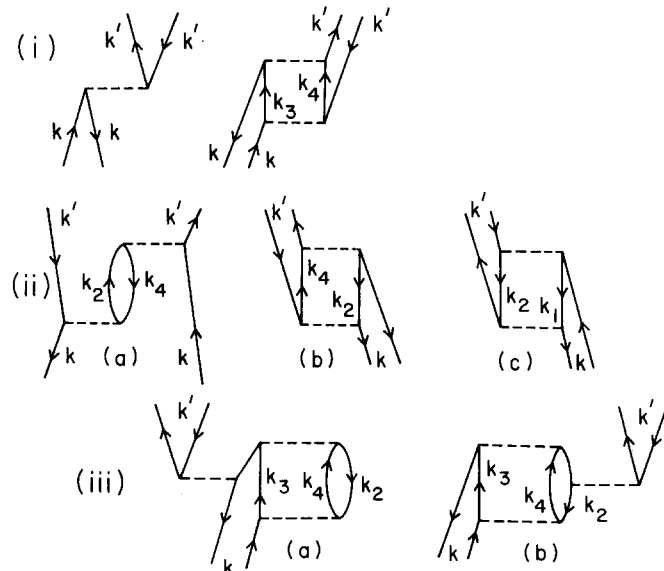


Fig. 10. Graphical representation of the terms entering into $f(\mathbf{k}, \mathbf{k}')$, (4.8). Exchange terms have not been drawn.

10(ii)c, have been consistently dropped. The graphs, figs. 10(i), would both be included in the G -matrix ($\mathbf{k}\mathbf{k}'|G|\mathbf{k}\mathbf{k}'$), but otherwise one can go directly to the G -matrix case with full G in the right-hand side of (4.1), simply by changing all matrix elements of V into those of G .

The $f(\mathbf{k}, \mathbf{k}')$ is the particle-hole interaction in the long-wavelength limit, we have drawn it that way in fig. 10, both the particle and hole having momentum k (or k'), so that the total momentum is zero. The magnitude of k (or k') must be k_F , since only on the Fermi surface can a particle and a hole have equal momentum. One can think of f as the limit of a particle-hole interaction between excitations of momentum q , as $|\mathbf{q}| \rightarrow 0$.

The fact that $f(\mathbf{k}, \mathbf{k}')$ is the particle-hole interaction in the long wavelength limit can be made clearer by the following argument in which we think of a problem involving a weak interaction V which need be handled only to first order. Consider first the particle-hole interaction connecting particle-hole states of total momentum q as shown in fig. 11. One can think of this interaction as

$$\Gamma = \sum_{\mathbf{k}', \mathbf{k}} (\mathbf{k}' + \mathbf{q}, \mathbf{k} | V | \mathbf{k}', \mathbf{k} + \mathbf{q}) (a_{\mathbf{k}'}^\dagger a_{\mathbf{k}+q})^\dagger (a_{\mathbf{k}'}^\dagger a_{\mathbf{k}+q}), \quad (4.9)$$

with the $(a_{\mathbf{k}'}^\dagger a_{\mathbf{k}+q})$ acting to the right, the $(a_{\mathbf{k}'}^\dagger a_{\mathbf{k}+q})^\dagger$ acting to the left. That is, the matrix element of Γ between particle-hole states $a_{\mathbf{k}_1+\mathbf{q}}^\dagger a_{\mathbf{k}_1} | 0 \rangle$ and $a_{\mathbf{k}_2+\mathbf{q}}^\dagger a_{\mathbf{k}_2} | 0 \rangle$, where $| 0 \rangle$ is the vacuum, will give the interaction

$$(\mathbf{k}_2 + \mathbf{q}, \mathbf{k}_1 | V | \mathbf{k}_2, \mathbf{k}_1 + \mathbf{q})$$

shown in fig. 11.

Such matrix elements enter into the description of collective excitations, the collective excitation being a linear combination of particle-hole states with coherent phases. For example, plasma oscillations are described in the random-phase approximation in such a way, where the interparticle Coulomb interaction is V . The momentum of the excitation is q , so that in the long wavelength limit, $q \rightarrow 0$. In this limit, the operator pair $(a_{\mathbf{k}}^\dagger a_{\mathbf{k}+q})$ in (4.9) becomes $(a_{\mathbf{k}}^\dagger a_{\mathbf{k}}) = n_{\mathbf{k}}$; similarly, $(a_{\mathbf{k}'}^\dagger a_{\mathbf{k}+q})$ becomes $n_{\mathbf{k}'}$. Consequently, the expectation value of Γ becomes

$$(0 | \Gamma | 0) = \sum_{\mathbf{k}', \mathbf{k}} (\mathbf{k}' \mathbf{k} | V | \mathbf{k}' \mathbf{k}) n(\mathbf{k}') n(\mathbf{k}) \quad (4.10)$$

i.e., it has the same form as the potential energy term in (4.3). Thus, removing the n 's by functional differentiation gives the matrix element $(\mathbf{k}_2, \mathbf{k}_1 | V | \mathbf{k}_2, \mathbf{k}_1)$.

To this order, we could have carried out the same considerations for the particle-particle interaction with the same conclusions. However, the second-order particle-particle interaction will have terms like those in fig. 12. Whereas the matrix element corresponding to the process fig. 12b is just that of fig.

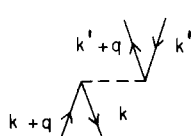


Fig. 11. Particle-hole interaction connecting two states of total momentum q .

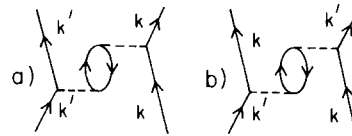
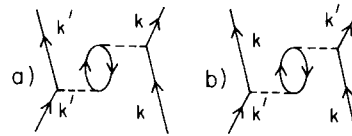


Fig. 12. Typical terms in the second-order particle-particle interactions.



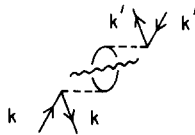


Fig. 13. Figure 12a redrawn as a particle-hole interaction.

10(ii)a, with the left-hand line pointing up instead of down, the matrix element corresponding to the process fig. 12a is missing in (4.8). The reason is simple. If we redraw fig. 12a as a particle-hole interaction as is done in fig. 13, it is reducible; that is, it can be obtained by putting together two first-order interactions of the type shown in fig. 11. But when the interaction, fig. 11, is used as the kernel in an integral equation such as occurs in the random-phase approximation, it is automatically iterated to all orders. Thus, reducible diagrams should not (and do not) occur in f .

In nuclear matter, the expression for $f(\mathbf{k}, \mathbf{k}')$ must be generalized to a matrix in spin and isospin space, because of the two spins and two kinds of particles. It can be written (m^* is the effective mass at the Fermi surface)

$$f(\mathbf{k}, \mathbf{k}') = (\pi^2/2m^*k_F) \{F + F' \boldsymbol{\tau}_1 \cdot \boldsymbol{\tau}_2 + G \boldsymbol{\sigma}_1 \cdot \boldsymbol{\sigma}_2 + G' \boldsymbol{\tau}_1 \cdot \boldsymbol{\tau}_2 \boldsymbol{\sigma}_1 \cdot \boldsymbol{\sigma}_2\} \quad (4.11)$$

where F, F', G and G' are dimensionless functions of the Landau angle between \mathbf{k} and \mathbf{k}' (remember that $|\mathbf{k}| = |\mathbf{k}'| = k_F$) and $2m^*k_F/\pi^2$ is the density of states on the Fermi surface*. In general, tensor invariants must also be introduced [32, 42, 43]. However, those do not seem to be quantitatively important for the applications we consider here and, for simplicity, we suppress them. We shall discuss the effective mass m^* which appears in the density of the states shortly.

Each of the above coefficients is expanded in a Legendre series

$$F = \sum F_l P_l(\cos \theta_L) \quad (4.12)$$

where we label the Landau angle by θ_L . The angle θ_L has nothing to do with the scattering angle; thus far we have considered only forward scattering. It has to do with the velocity dependence of the interaction, as we make clear in the following example.

Let us take a simple schematic interaction

$$f(\mathbf{k}, \mathbf{k}') = f_0 + \hat{\mathbf{k}} \cdot \hat{\mathbf{k}}' f_1 \quad (4.13)$$

where f_0 and f_1 are constants. This interaction is then a special example of the interaction, (4.12), where only the first two terms are nonzero. The term with f_1 describes the full momentum dependence of this simplified force. Let us now compute the effective mass of a quasiparticle at the Fermi surface interacting with other quasiparticles.[†] To obtain this, we calculate the difference in self-energies, Σ ,

* Migdal [1] uses the symbols f, g for the dimensionless quantities we call F, G . Our notation is more usual in other applications of the Landau theory. Migdal employs the density of states m^*k_F/π^2 appropriate to liquid ${}^3\text{He}$. Thus $F = 2f$ etc.

[†]This calculation has been carried out very elegantly by Landau using Galilean invariance.

$$\Sigma(k_F + \delta k) - \Sigma(k_F) = \frac{(k_F + \delta k)^2 - k_F^2}{2} \left(\frac{1}{m^*} - \frac{1}{m} \right) \quad (4.14)$$

of a quasiparticle slightly displaced off the Fermi surface and a quasiparticle on it (see fig. 14).

In calculating $\Sigma(k_F + \delta k)$, we can change to a calculation of $\Sigma(k_F)$, shifting the Fermi sea δk to the left, as shown in fig. 14. Such a shift will not change the interaction between a single quasiparticle and quasiparticles in the Fermi sea, since it is Galilean invariant. In calculating the interaction now one must take into account that $\delta n = \pm 1$ in the regions shown. We find

$$\begin{aligned} \Sigma(k_F + \delta k) - \Sigma(k_F) &= -\frac{4}{(2\pi)^3} f_1 \int_{-1}^1 \frac{\hat{k} \cdot \hat{k}'}{k_F^2} 2\pi k_F^2 \delta k \cos \theta d(\cos \theta) \\ &= -\frac{2k_F^2}{3\pi^2} f_1 \delta k = k_F \delta k \left(\frac{1}{m^*} - \frac{1}{m} \right) \end{aligned} \quad (4.15)$$

where $\hat{k} \cdot \hat{k}' = \cos \theta$. From (4.15) we find

$$m^*/m = 1 + F_1/3 \quad (4.16)$$

where

$$F_1 = 2k_F m^* f_1 / \pi^2. \quad (4.17)$$

The expansion (4.12) is assumed to converge rapidly. In liquid ${}^3\text{He}$, the first two terms are found to be sufficient for most applications, and we shall assume the same to be true for nuclear matter.

Our strategy in finite nuclei will be somewhat different. In chapter 2 it was shown that the long-range part of the nucleon-nucleon force comes from pion exchange. As will be shown in chapter 5, exchange terms from this interaction give the main part of F_1 , although the $V_\rho(r)$, (2.45), also makes contributions. It seems to be a good approximation to handle the interaction from all other exchanges in zero-range approximation, treating it as a $\delta(\mathbf{r}_{12})$ function; e.g., note that the weighting function for σ -exchange, fig. 4, peaks for a mass of $\sim 5m_\pi$, corresponding to a range of $(\hbar/5m_\pi c)$, small compared with the average interparticle spacing. Those interactions treated as δ -functions will contribute only to the $l = 0$ multipoles: F_0 , F'_0 , G_0 , G'_0 . Rather than introducing the F_1 which would arise from the V_π of (2.8) and the V_ρ of (2.45), we shall handle these two interactions explicitly, in a shell-model basis.

The coefficient F_0 can be related to the compression modulus K , F'_0 to the symmetry energy β . These relations are standard, and we refer the reader to [1]. We summarize them below.

Table 1
Relations between Landau parameters and observables

Quantity	Expressions
Compression modulus	$K = 6 \frac{k_F^2}{2m^*} (1 + F_0)$
Effective mass m^*	$m^*/m = 1 + F_1/3$
Symmetry energy β	$\beta = \frac{1}{3} \frac{k_F^2}{2m^*} (1 + F'_0)$

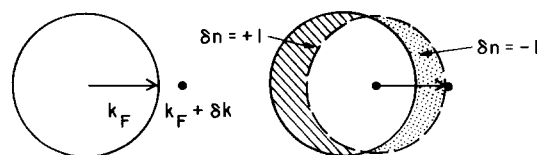


Fig. 14. Calculation of the self-energy of a particle of momentum $k_F + \delta k$ by shifting the Fermi sea, as in b) so the particle is at k_F .

The compression modulus

$$K = r_0^2 d^2 E / dr_0^2 \quad (4.18)$$

is that used in Brueckner theory; it is a factor of 9 larger than in Migdal's formula, which corresponds to defining K as $\rho_0^2(d^2E/d\rho_0^2)$, ρ_0 being the equilibrium density. The r_0 in the above formula is given by $(4\pi/3)r_0^3 = \rho_0^{-1}$.

The symmetry energy is defined in the following way: If one has an excess of neutrons, then a term appears in the energy per particle

$$\delta E_\tau = \beta \left(\frac{N - Z}{A} \right)^2. \quad (4.19)$$

Empirical values of K , m^* and β are somewhat subject to interpretation; we shall discuss them in detail later.

4.1. Brueckner's reaction matrix

In chapter 2 we discussed the properties of the free nucleon–nucleon interaction. In this section we shall see that much of the properties of the particle–hole interaction approximated by a reaction matrix can be understood knowing the properties of the free nucleon–nucleon interaction. We recall a number of previous results which suggest that F and G' in (4.11) receive large contributions from the one-pion-exchange interaction in the Born approximation and from exchange of a single ρ -meson.

Our strategy will be to remove the one-pion-exchange terms, whose functional form we know explicitly, and then to approximate the remaining G -matrix. Aside from the OPEP, the remaining contributions to the nucleon–nucleon interaction are of short range, so that one might try a zero-range approximation for these components. This has been the philosophy of the Jülich–Stony Brook [44] approach to effective interactions in finite nuclei. In this approach, one associates the ρ -meson exchange potential, suitably corrected for short-range correlations, together with the OPEP. This is for convenience, since the tensor interaction from ρ -exchange cuts off the highly singular tensor interaction from π -exchange, the total tensor interaction going through zero at $r \approx 0.7$ fm as shown in fig. 8. Furthermore, the π - and ρ -exchanges essentially exhaust* the $\sigma_1 \cdot \sigma_2 \tau_1 \cdot \tau_2$ degrees of freedom.

A less restrictive approximation than that of zero-range, is to represent the G -matrix, after removal of the OPEP, as a local operator. We shall show in this section how this can be done.

Neglecting tensor degrees of freedom, the contribution from one-pion exchange to the particle–hole interaction is given by

$$\begin{aligned} N_0^{-1} F_\pi(\mathbf{k}_1 \mathbf{k}_2) &= \frac{1}{3} \frac{f^2}{m_\pi^2} \boldsymbol{\sigma}_1 \cdot \boldsymbol{\sigma}_2 \boldsymbol{\tau}_1 \cdot \boldsymbol{\tau}_2 \frac{m_\pi^2}{m_\pi^2 + k^2} \\ &+ \frac{1}{12} \frac{f^2}{m_\pi^2} (-9 + 3 \boldsymbol{\sigma}_1 \cdot \boldsymbol{\sigma}_2 + 3 \boldsymbol{\tau}_1 \cdot \boldsymbol{\tau}_2 - \boldsymbol{\sigma}_1 \cdot \boldsymbol{\sigma}_2 \boldsymbol{\tau}_1 \cdot \boldsymbol{\tau}_2) \frac{m_\pi^2}{m_\pi^2 + (\mathbf{k}_1 - \mathbf{k}_2)^2}. \end{aligned} \quad (4.20)$$

* Some contribution to these come from iterated pion exchange, esp. in second order. As we shall see later, the second-order pion exchange has an important “ ρ -like” component.

The corresponding contribution from exchange of a single ρ -meson is

$$\begin{aligned} N_0^{-1} F_\rho(\mathbf{k}_1 \mathbf{k}_2) = C & \left\{ \frac{2}{3} \frac{f_\rho^2}{m_\rho^2} \boldsymbol{\sigma}_1 \cdot \boldsymbol{\sigma}_2 \boldsymbol{\tau}_1 \cdot \boldsymbol{\tau}_2 \frac{m_\rho^2}{m_\rho^2 + k^2} \right. \\ & \left. + \frac{1}{6} \frac{f_\rho^2}{m_\rho^2} (-9 + 3\boldsymbol{\sigma}_1 \cdot \boldsymbol{\sigma}_2 + 3\boldsymbol{\tau}_1 \cdot \boldsymbol{\tau}_2 - \boldsymbol{\sigma}_1 \cdot \boldsymbol{\sigma}_2 \boldsymbol{\tau}_1 \cdot \boldsymbol{\tau}_2) \frac{m_\rho^2}{m_\rho^2 + (\mathbf{k}_1 - \mathbf{k}_2)^2} \right\}. \end{aligned} \quad (4.21)$$

Above we have omitted the contributions from the δ -functions in (2.8) and (2.45) since, due to the strong short-range repulsion from the ω -meson, the wave function vanishes at zero distance between the nucleons. Such minimal correlations are not enough for the ρ -meson because not only is the main part of the ρ -meson exchange interaction as long range as the ω -exchange, since $m_\rho \approx m_\omega$, but also the ρ -meson has a large width, $\Gamma_\rho \approx 150$ MeV, so that substantially smaller masses enter into the exchange. In the model calculation of ref. [31] C in (4.21) was found to be ~ 0.4 . In that calculation it was shown that G' may be described qualitatively as due to the direct terms, fig. 15a, in (4.20) and (4.21). The contribution from the exchange terms, fig. 15b, was small. We see from (4.20) and (4.21) that the contribution to F from the exchange terms is a factor of 9 bigger than to G' . In ref. [45] this was used to obtain reasonable estimates for the Brueckner effective mass. We note that the tensor invariants in the particle-hole interaction are mostly due to the exchange terms, fig. 15b, of the one-pion exchange and the ρ -exchange tensor forces [32, 42]. Now, if the models mentioned above are correct, we would expect the reaction matrix to be essentially local. This has been shown to be true by Dickhoff et al. [46] and in ref. [47]. We here follow the presentation of ref. [47].

Let us consider a direct interaction in a plane wave basis defined in accordance with fig. 15a. If we can write (we suppress tensors)

$$V_d(\mathbf{k}, \boldsymbol{\sigma}, \boldsymbol{\tau}) = f_d(\mathbf{k}) + f'_d(\mathbf{k}) \boldsymbol{\tau}_1 \cdot \boldsymbol{\tau}_2 + g_d(\mathbf{k}) \boldsymbol{\sigma}_1 \cdot \boldsymbol{\sigma}_2 + g'_d(\mathbf{k}) \boldsymbol{\sigma}_1 \cdot \boldsymbol{\sigma}_2 \boldsymbol{\tau}_1 \cdot \boldsymbol{\tau}_2 \quad (4.22)$$

where the functions on the right of eq. (4.22) are functions only of the momentum transfer, \mathbf{k} , we shall consider the interaction local. The Fourier transform of eq. (4.22) to configuration space will yield an interaction which depends only on the relative coordinate, \mathbf{r}_{12} . Above we have chosen notation consistent with that of fig. 15. The exchange term fig. 15b can be obtained by applying the usual exchange operator to the direct term:

$$V_e(\mathbf{q}, \boldsymbol{\sigma}, \boldsymbol{\tau}) = P V_d(\mathbf{k}, \boldsymbol{\sigma}, \boldsymbol{\tau}) = -P_{12} P_\sigma P_\tau V_d(\mathbf{k}, \boldsymbol{\sigma}, \boldsymbol{\tau}). \quad (4.23)$$

The momentum transfer appearing in the exchange term is $\mathbf{q} = \mathbf{k}_1 - \mathbf{k}_2$. The effect of P is to change the

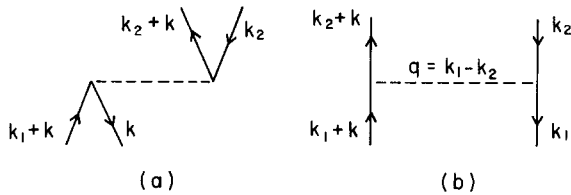


Fig. 15. The direct (a) and exchange (b) parts of a particle-particle interaction drawn as particle-hole diagrams. The Landau limit is $k \rightarrow 0$.

identity of the outgoing particles. Writing V_e in the form of eq. (4.22) we obtain

$$V_e(\mathbf{q}, \boldsymbol{\sigma}, \boldsymbol{\tau}) = f_e(\mathbf{q}) + f'_e(\mathbf{q}) \boldsymbol{\tau}_1 \cdot \boldsymbol{\tau}_2 + g_e(\mathbf{q}) \boldsymbol{\sigma}_1 \cdot \boldsymbol{\sigma}_2 + g'_e(\mathbf{q}) \boldsymbol{\sigma}_1 \cdot \boldsymbol{\sigma}_2 \boldsymbol{\tau}_1 \cdot \boldsymbol{\tau}_2. \quad (4.24)$$

The various terms on the right of eq. (4.24) can be expressed in terms of the direct functions of eq. (4.22) by carrying out the operations of eq. (4.23) explicitly. After some algebra one obtains

$$\begin{aligned} f_e(\mathbf{q}) &= -\frac{1}{4}f_d(\mathbf{q}) - \frac{3}{4}f'_d(\mathbf{q}) - \frac{3}{4}g_d(\mathbf{q}) - \frac{9}{4}g'_d(\mathbf{q}) \\ f'_e(\mathbf{q}) &= -\frac{1}{4}f_d(\mathbf{q}) + \frac{1}{4}f'_d(\mathbf{q}) - \frac{3}{4}g_d(\mathbf{q}) + \frac{3}{4}g'_d(\mathbf{q}) \\ g_e(\mathbf{q}) &= -\frac{1}{4}f_d(\mathbf{q}) - \frac{3}{4}f'_d(\mathbf{q}) + \frac{1}{4}g_d(\mathbf{q}) + \frac{3}{4}g'_d(\mathbf{q}) \\ g'_e(\mathbf{q}) &= -\frac{1}{4}f_d(\mathbf{q}) + \frac{1}{4}f'_d(\mathbf{q}) + \frac{1}{4}g_d(\mathbf{q}) - \frac{1}{4}g'_d(\mathbf{q}). \end{aligned} \quad (4.25)$$

We see that the central degrees of freedom are described by four functions. Above we have satisfied the Pauli principle by construction. In what follows we shall use the Pauli principle as a test of the consistency of the local representations.

For a central force the Pauli constraints, applied to $F(k, q)$, give

$$\begin{aligned} F(0, 0) + F'(0, 0) + G(0, 0) + G'(0, 0) &= 0 \\ F(0, 0) - 3F'(0, 0) - 3G(0, 0) + 9G'(0, 0) &= 0 \end{aligned} \quad (4.26)$$

where, for example, we have defined $F(k, q)$ as the sum of $F_d(k)$ and $F_e(q)$. The first constraint tells us that, when the momenta \mathbf{k} and \mathbf{k}' of the particles are equal, the interaction must vanish in triplet odd waves while the second constraint guarantees this for singlet odd waves. In a Fermi liquid these constraints are the Born approximants to the sum rules of ref. [48], which we shall discuss in appendix A.

In the calculations the Reid soft-core potential was used. This potential is expressed as a set of local potentials fit to nucleon–nucleon phase shifts in each partial wave with $J \leq 2$. In the case of the 3S_1 – 3D_1 channel, some deuteron properties are also fitted. From this potential a reaction matrix, G , is obtained in each partial wave channel following standard prescriptions. These include the use of an angle-averaged Pauli operator and the following single particle spectrum

$$\begin{aligned} \varepsilon(k) &= -\frac{\hbar^2 k_F^2}{m} \Delta + \frac{\hbar^2 k^2}{2m^*}, \quad k < k_F \\ &= \frac{\hbar^2 k^2}{2m}, \quad k > k_F. \end{aligned} \quad (4.27)$$

The values $k_F = 1.35 \text{ fm}^{-1}$, $m^*/m = 0.63$, and $\Delta = 1.03$ were used in the calculations. The reaction matrix elements in the desired plane wave basis are given by [49, 50]

$$\begin{aligned} \langle \mathbf{p}_f; sm_s | G | \mathbf{p}_i; sm_s \rangle &= \sum_{Jl'm} (4\pi)^2 i^{(l-l')} (l' m s m_s | J m + m_s) \\ &\times (l m s m_s | J m + m_s) \langle p_f | G_{ll'}^{Jl} | p_i \rangle Y_{l'm} (\hat{t} \cdot \hat{p}_f) Y_{lm}^* (\hat{t} \cdot \hat{p}_i) \end{aligned} \quad (4.28)$$

where we have used standard notation for Clebsch–Gordon coefficients and spherical harmonics. All quantum numbers are in the particle–particle channel. Here \hat{t} denotes an arbitrary spin quantization axis, and \mathbf{p}_i and \mathbf{p}_f are the initial and final relative momenta of the interacting particles. The sum in eq. (4.28) extends over all J while the Reid potential is defined only in channels with $J \leq 2$. This truncation is not serious for the short-range components in the reaction matrix. However, it introduces serious errors in the evaluation of the longest-range and best known component of the potential, one pion exchange, which converges slowly as a function of J . Thus, we set $G_{ll''}^{J_s}$, equal to the one-pion-exchange potential for $J > 2$. In practice this is done as in ref. [42]. The contribution of the one-pion-exchange potential (in Born approximation) is removed from the reaction matrix elements in each partial wave channel with $J \leq 2$ before performing the sums required by eq. (4.28). After the truncated sums are performed the full one-pion-exchange matrix elements in a plane wave basis are added.

We can now construct the functions which appear on the right in eq. (4.11) for arbitrary \mathbf{p}_f and \mathbf{p}_i by forming the following linear combinations [42]

$$\begin{aligned} f &= \frac{1}{16} \sum_t (2t+1) \sum_{sm_s} G_{st}^{m_s} & g &= \frac{1}{16} \sum_t (2t+1) \left(\frac{1}{3} \sum_{m_s} G_{1t}^{m_s} - G_{0t}^0 \right) \\ f' &= \frac{1}{16} \sum_t (2t-1) \sum_{sm_s} G_{st}^{m_s} & g' &= \frac{1}{16} \sum_t (2t-1) \left(\frac{1}{3} \sum_{m_s} G_{0t}^{m_s} - G_{0t}^0 \right). \end{aligned} \quad (4.29)$$

Here, t denotes the isospin in the particle–particle channel.[†] The matrix elements can be calculated using any convenient quantization axis, as can be inferred from eqs. (4.28) and (4.29). For off-diagonal elements we may choose \mathbf{p}_i as a spin quantization axis.

In order to evaluate the expressions (4.29) it is necessary to relate the momenta \mathbf{k} and \mathbf{q} appearing in eqs. (4.22) and (4.23) with the momenta \mathbf{p}_i and \mathbf{p}_f of eq. (4.28). These relative momenta are given as

$$\mathbf{p}_i = \frac{1}{2}(\mathbf{q} + \mathbf{k}) \quad (4.30)$$

$$\mathbf{p}_f = \frac{1}{2}(\mathbf{q} - \mathbf{k}). \quad (4.31)$$

The momentum transfers in the direct and exchange diagrams are then \mathbf{k} and \mathbf{q} . For a given value of p_i in the Fermi sea, reaction matrix elements are obtained for a set of values of p_f corresponding to the mesh adopted for the solution of the integral equation, and the functions on the right of (4.11) may be calculated on a corresponding set of \mathbf{k} and \mathbf{q} .^{*} The sum of direct and exchange terms obtained is a general function of the two variables \mathbf{k} and \mathbf{q} (e.g., $f(\mathbf{k}, \mathbf{q})$). In the special case where a local representation is possible $f(\mathbf{k}, \mathbf{q})$ is simply the sum of a function of \mathbf{k} and a function of \mathbf{q} . In this case the difference $f(\mathbf{k}, q_0) - f(\mathbf{k}_0, q_0)$ should be a function only of k , the momentum transfer in the direct diagram fig. 15a giving $F_d(k)$ of eq. (4.22) up to a constant. Similarly, the difference $f(\mathbf{k}_0, \mathbf{q}) - f(\mathbf{k}_0, q_0)$ should be a function only of q , the momentum transfer in the exchange diagram, giving $F_e(q)$ again up to a constant.

[†] In what follows s and t denote particle–particle spin and isospin while S and T denote particle–hole spin and isospin.

^{*} We have not yet mentioned the third momentum variable of the reaction matrix, the center-of-mass momentum of the interacting particle defined as $\mathbf{P} = \mathbf{k}_1 + \mathbf{k}_2$. In these calculations $\frac{1}{2}\mathbf{P}$ is set equal to the value $\sqrt{k_f^2 - p_i^2}$ valid on the Fermi surface as in eq. (3.4) of ref. [42]. Thus, P is not an independent variable.

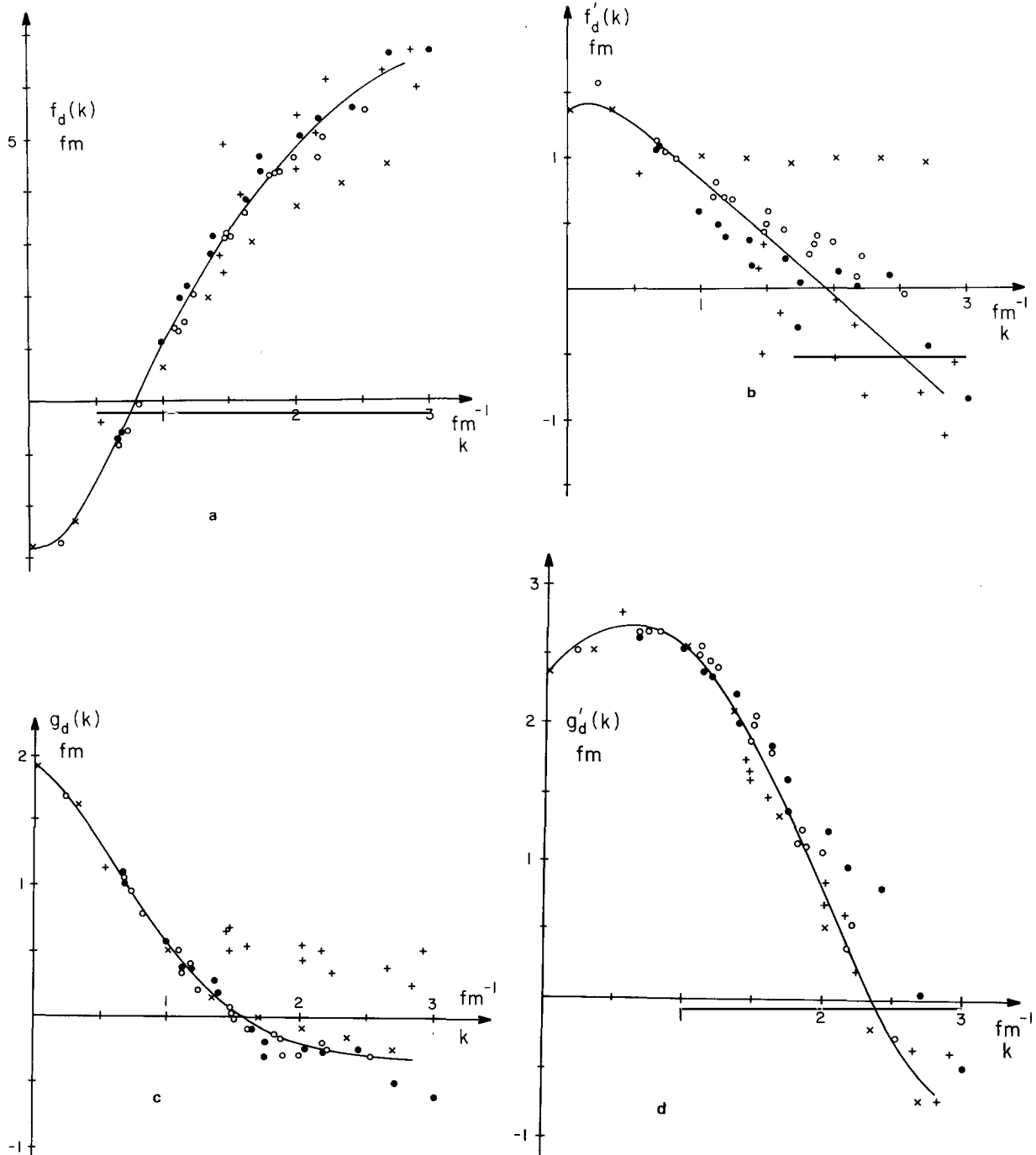
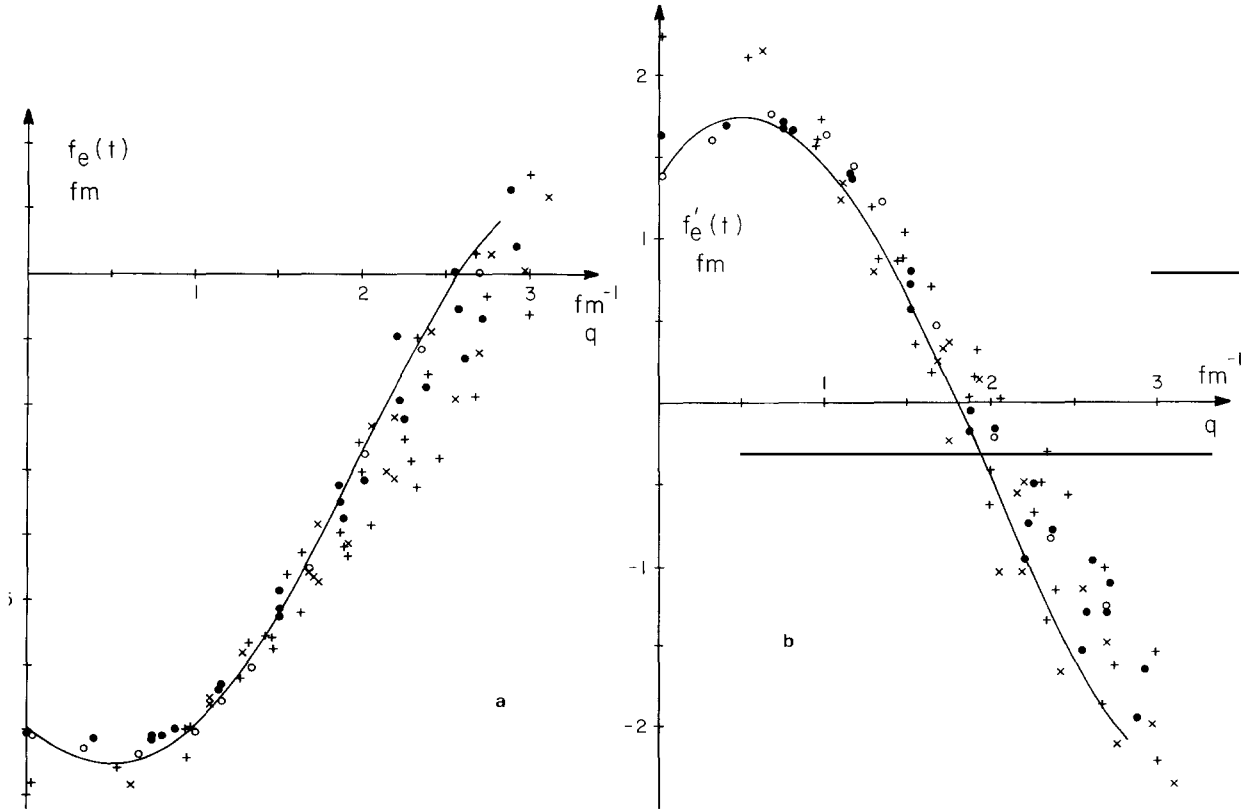


Fig. 16. The direct part of the particle-hole interaction as a function of the momentum transfer k . The points were calculated by forming the differences $f(k, q_0) - f(k_0, q_0)$ etc. as explained in the text. The fact that all points fall on essentially the same curve independent of p_i , p_f or q_0 is an indication of the validity of the local approximation. Here dots are for $q_0 = 1.169$ fm $^{-1}$, crosses are for $q_0 = 0$, plusses for $q_0 = 2.61$ fm $^{-1}$ and circles for $q_0 = 0.75$ fm $^{-1}$. The value of k_0 is 0.75 fm $^{-1}$ from which p_i and p_f can be deduced. The solid curve is a fifth-order polynomial fit to the bulk of the points. Here as in fig. 17 the OPE contribution is subtracted.

In fig. 16 we display the direct functions and in fig. 17 the exchange functions. The range over which these functions are shown is determined by the fact that we shall later need values of k and q only in the range 0 to $2k_F$. In order to emphasize the nontrivial aspect of these plots we have removed the explicitly local contribution from the one-pion-exchange potential. The results display a satisfying insensitivity to the variables k_0 and q_0 , respectively, indicating that local approximations are sensible. This conclusion becomes even firmer when the one pion exchange contributions are reintroduced. In attempting to fit these results it is useful to reduce the number of functions and constants from eight to four by imposing the constraints of eq. (4.25). The four direct functions were parameterized and roughly adjusted to pass through the calculated points shown in fig. 16. The constant terms cannot be established uniquely by returning to the original $f(k, q)$, $f'(k, q)$, $g(k, q)$ and $g'(k, q)$ since these do not determine how the constants are distributed between direct and exchange functions. Thus, it was also useful to impose the physically reasonable constraint that $f_d(k)$, $f'_d(k)$, $g_d(k)$ and $g'_d(k)$ vanish in the large k limit. The resulting direct functions are shown as solid lines in fig. 16. Using these four functions and eq. (4.25) the corresponding exchange functions were generated. These functions are shown in fig. 17 as solid lines and provide further confirmation of the validity of this local approximation.

We see that the curves for f and g' very much follow what we expected from the discussion in the beginning of this section. Reid's soft core only contains explicitly a π -exchange, with the delta-function piece omitted. However, due to the fits to phase shifts the presence of a ρ -exchange in the nucleon-nucleon force is indirectly felt. Consequently we see that, e.g., $g'_d(k)$ is quite local (a "rho-meson"), whereas the exchange term is of somewhat lesser importance. It is also tempting to interpret f_e as



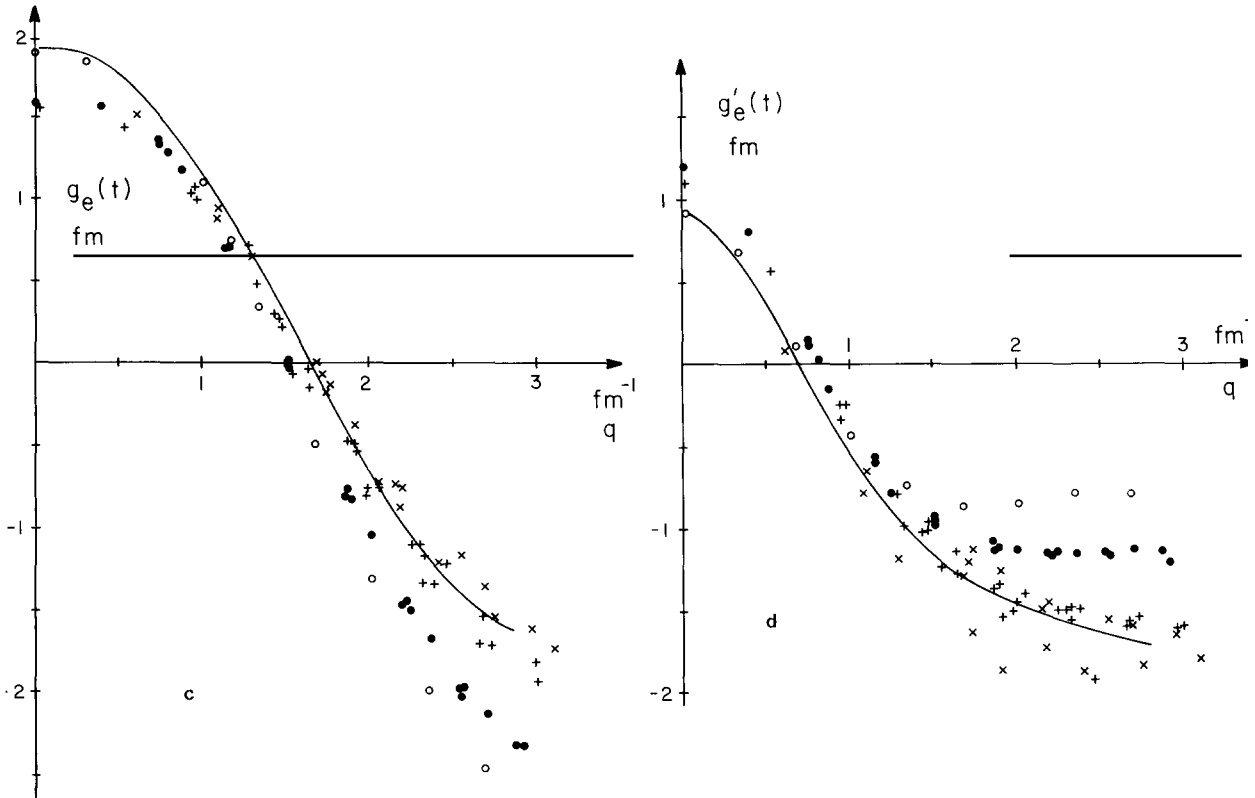


Fig. 17. The exchange part of the particle-hole interaction as a function of the momentum transfer q . Dots are for $k_0 = 0.675 \text{ fm}^{-1}$, crosses are for $k_0 = 2.04 \text{ fm}^{-1}$, plusses for $k_0 = 1.36 \text{ fm}^{-1}$, and circles for $k_0 = 0$. Here $q_0 = 1.169 \text{ fm}^{-1}$. The solid curve was calculated from the solid curve in fig. 16 by using eq. (4.25). Note that no additional fit was made.

largely due to the exchange term of a ρ -exchange, e.g. (4.21). When we come to f' the relative importance of the second-order tensor in the reaction matrix gets enhanced compared with in f as can be seen from eq. (4.21) and eq. (2.10). As long as the closure approximation (2.10) is good that does not ruin the locality of the reaction matrix. The problem is, however, that the gap used in the spectrum (see (4.27)) cuts down this important contribution. As a matter of fact the main result of introducing a model space is to enhance the contributions from coupled channels like ${}^3\text{S}_1 + {}^3\text{D}_1$, whereas the contributions from other channels remain almost unchanged [51]. Sjöberg used the approximations used here in ref. [52] and a model space approach in ref. [53]. The by far biggest change in the results came in F'_0 , i.e. the symmetry energy, see table 1, which when a model space was used rose from 25.6 MeV to 38.4 MeV. However, his calculations contain faulty spin sums for G_0 and G'_0 (see end of chapter 5). Doing the spin sums correctly gives a smaller symmetry energy than the mentioned value of 38.4 meV (see section 6.3). There is, however, no doubt that a proper F'_0 can only be obtained using a model space.

Finally a few words about the one-pion-exchange contribution. In fig. 18 we have plotted the contributions coming from the one-pion-exchange potential in various channels. These contributions have to be added to those in figs. 16 and 17. Remember that the Landau limit is $k \rightarrow 0$ and that the exchange contributions have to be projected on Legendre polynomials to give the various multipoles F_l etc. of the particle-hole interaction. The results are then those given in ref. [42].

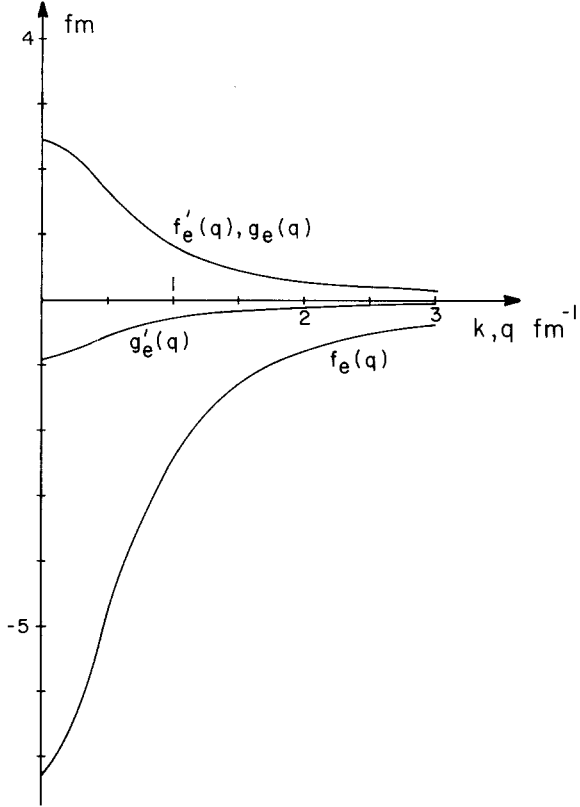


Fig. 18. Contributions from one-pion exchange to the particle-hole interaction in various channels. The momenta are defined as in fig. 15 and eq. (4.20), i.e. \mathbf{k} is the momentum transfer in the direct term and $\mathbf{q} = \mathbf{k}_1 - \mathbf{k}_2$ in the exchange term.

So, in conclusion, the reaction matrix in nuclear matter is quite local. There are two reasons for this. First, although the short-range repulsion from ω -exchange is nonlocal it is so strong that it effectively keeps the particles outside the core so that it hardly contributes to the nonlocality. Secondly, another source for a nonlocality would be the Pauli principle. Nuclear matter is, however, quite dilute so the effect of the Pauli principle is not enough to produce a substantial nonlocality when a spectrum like (4.27) is used.

Although nuclear matter is a dilute system, these are nonetheless important collective effects which we shall deal with in the next section.

5. A theory of interacting quasiparticle and collective excitations

Earlier work [54] clarified the connection between Brueckner theory and Landau theory, but was not quantitatively successful, because it did not properly include effects of collective excitations. We can think of the quasiparticle energies being composed of two types of contributions, such as shown in fig. 19.

It is clear that clothing the particle as in fig. 19b, with collective excitations will change observable quantities in important ways. The quasiparticle builds up correlations in the medium around it, so that

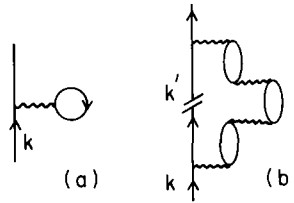


Fig. 19. The two types of contributions to the particle self-energy. Here the wavy line represents the G -matrix. There is some double counting between (a) and (b), because the G -matrix sums ladder contributions to all orders, so that the second-order term must be removed from (b).

the clothed quasiparticle is substantially larger than the bare particle, and harder to compress; thus, the compression modulus will be increased. Inclusion of the processes, fig. 19b, also changes the effective mass, since it represents processes in which the quasiparticle carries its collective-excitation clothing along with it. In the case of liquid ^3He , such processes increase the effective mass to $m^* \approx 3m$ [55, 56]. We shall indicate later that the effective mass in finite nuclei is also substantially changed by inclusion of collective effects.

From functional differentiation of the processes fig. 19b we will obtain new contributions to $f(\mathbf{k}, \mathbf{k}')$. To begin with, we consider the changes we get by differentiating with respect to $n(\mathbf{k}')$ where \mathbf{k}' refers to the intermediate particle line as shown in fig. 19b. We shall return to a discussion of other contributions later. Functionally differentiating with respect* to $n(\mathbf{k}')$ gives the contribution, fig. 20, to $f(\mathbf{k}, \mathbf{k}')$. We shall call this contribution the “Induced Interaction”.

Now, in a complete theory, f is the complete particle-hole interaction, so that it is clear that the G -matrix in the particle-hole interactions should be replaced by f to include higher-order effects. It has also been proved in the limit of $\mathbf{k}' \rightarrow \mathbf{k}$ that the vertex functions on the left- and right-hand sides should be replaced by f [57].

Thus, more generally, the induced interaction is assumed to have the form, fig. 21. The particle-hole phase space between interactions f is assumed to be described by Lindhard functions. It should be emphasized that use of the form shown for the Induced Interaction, fig. 21, away from the zero Landau angle $\mathbf{k} = \mathbf{k}'$ involves an extrapolation. We shall see that this form has certain very pleasant properties, especially with respect to preserving antisymmetry in any microscopic calculation.

We arrive then at the integral equation [57], shown graphically in fig. 22.† In this equation, we have a driving term, enclosed, consisting of processes such as one would evaluate in the Brueckner theory.

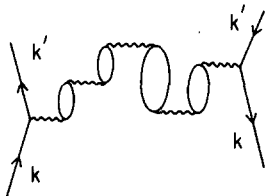


Fig. 20. Contributions of the collective effect, fig. 19b, to the particle-hole interaction $f(\mathbf{k}, \mathbf{k}')$.

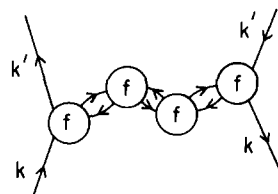


Fig. 21. Assumed general form of the induced interaction.

* Functionally differentiating one of the bubbles in fig. 19b will produce two-phonon exchange terms. It is necessary to include these when discussing spin- (or isospin-) collective modes [58].

† This equation, with first-order kernel, was used by M.W. Kirson [59]. A discussion of this equation within the framework of the schematic model was carried out by D.W.L. Sprung and A.M. Jopko [60].

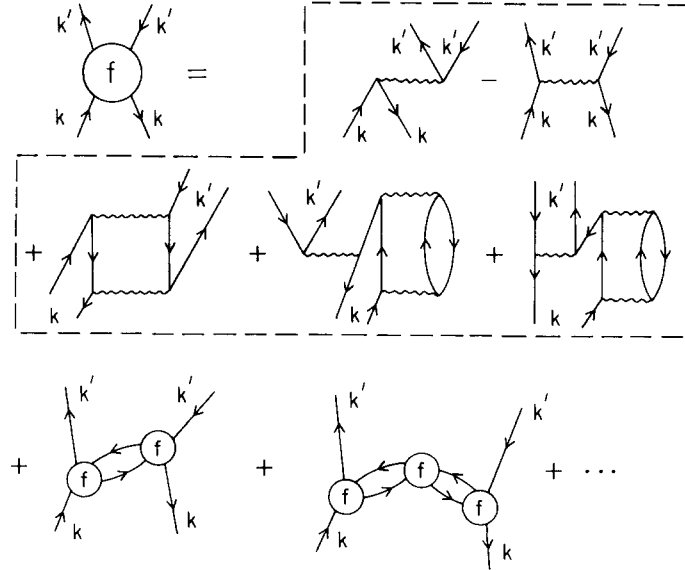


Fig. 22. Graphical representation of our integral equation. The wavy lines here denote G -matrix elements. The enclosed processes will be called the driving term.

Only those processes should be included that cannot be separated into two unlinked diagrams by cutting only one internal particle line and one internal hole line. The terms which are not enclosed, on the bottom, contain all such diagrams. For example the lowest-order bubble term is obtained within the Brueckner theory but should not be included in the driving term since it is produced by iteration of the integral equation in fig. 22.

By including all irreducible processes to all orders in the driving term we would include all processes in the solution of this integral equation, so we are essentially just rearranging the order of summation. Yet this is of importance, because the resulting equation has a much greater stability than a straightforward summation of graphs; i.e., the solution is rather insensitive to the order one goes to in the driving term.

Much of the convenience of the integral equation depicted in fig. 22 stems from the fact that calculations to any order in the driving term will give results for the particle-particle interaction which automatically satisfy the Landau sum rule, whereas a straightforward calculation of f to a given order in the G -matrix does not [41]. Some care in choosing the driving term has, however, to be exercised [41, 52], since particles and holes are not treated on equal footing in Brueckner's theory. For example the process in fig. 23a would come from differentiation of the binding energy in Brueckner's ap-

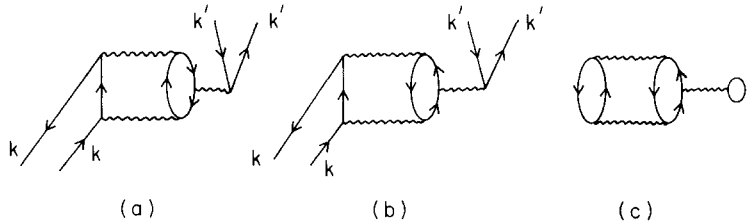


Fig. 23. The process in (a) is obtained by differentiation of Brueckner's binding energy. The process in (b) is obtained by differentiation of the binding-energy diagram (c). Inclusion of (a) but not (b) in the driving term in fig. 22 would violate the Pauli principle.

proximation. The process in fig. 23b would come from differentiation of the binding energy diagram in fig. 23c. Now the particles are off the energy shell, i.e. a self-energy insertion like the one in fig. 23c depends on the rest of the diagram. In nuclear matter one usually uses kinetic energies as self-energies for particles and incorporates the process in fig. 23c into the Bethe-Faddeev equation. For particles in the same state, $k = k'$, the processes in figs. 23a and 23b cancel each other. Hence, since we want the antisymmetry in the driving term to be preserved processes like fig. 23a should not be included in the driving term. (See the discussion immediately preceding section 6.1.)

We've not yet talked about the particle-particle interaction, so a few words of explanation would be in place here. The particle-particle (i.e. the forward scattering amplitude) interaction A between quasiparticles on the Fermi surface can be expressed as [37, 38, 39]

$$A(\mathbf{k}, \mathbf{k}') = \sum_l \frac{F_l P_l(\hat{\mathbf{k}} \cdot \hat{\mathbf{k}'})}{1 + F_l/(2l+1)} + \boldsymbol{\tau}_1 \cdot \boldsymbol{\tau}_2 \frac{F'_l P_l(\hat{\mathbf{k}} \cdot \hat{\mathbf{k}'})}{1 + F'_l/(2l+1)} \\ + \boldsymbol{\sigma}_1 \cdot \boldsymbol{\sigma}_2 \frac{G_l P_l(\hat{\mathbf{k}} \cdot \hat{\mathbf{k}'})}{1 + G_l/(2l+1)} + (\boldsymbol{\tau}_1 \cdot \boldsymbol{\tau}_2)(\boldsymbol{\sigma}_1 \cdot \boldsymbol{\sigma}_2) \frac{G'_l P_l(\hat{\mathbf{k}} \cdot \hat{\mathbf{k}'})}{1 + G'_l/(2l+1)}, \quad (5.1)$$

where

$$A = \frac{2k_F m^*}{\pi^2} a.$$

The graphical interpretation of (5.1) is straightforward, and is shown in fig. 24. The $[1 + F_l/(2l+1)]^{-1}$ in (5.1) just represents the summation of bubbles, to all orders, in the crossed channel. Note that the particle lines going in and out of the interaction f are now drawn appropriate for particle-particle scattering. Since \mathbf{k} and \mathbf{k}' are both on the Fermi sea, it is somewhat a matter of convention as to how they are to be drawn.

The final process on the right-hand side of fig. 24 is topologically like the Induced Interaction, fig. 21, except that one of the $(\mathbf{k}, \mathbf{k}')$ pairs has been interchanged. In fact, the Induced Interaction is just the exchange term corresponding to the process on the right-hand side of fig. 24. Putting this latter process and the Induced Interaction together, we have, then, both the direct and exchange terms of this interaction, so that antisymmetry of the total particle-particle interaction $A(\mathbf{k}, \mathbf{k}')$ is guaranteed, provided that antisymmetric driving terms are used in our integral equation, fig. 22.

Antisymmetry gives us the Landau sum rules. Landau pointed out that the forward scattering of identical particles (same spin and isospin) must vanish, because this amplitude must change sign under interchange of the particles (antisymmetry); on the other hand, the particles are identical and nothing is

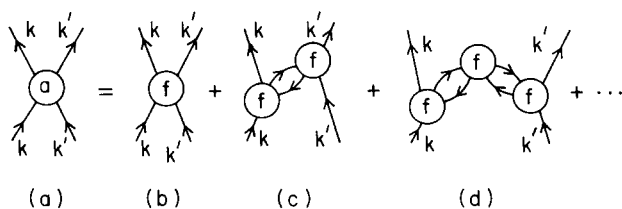


Fig. 24. Graphical interpretation of the relationship between A and f .

changed. Thus,

$$\sum_l \left\{ \frac{F_l}{1 + F_l/(2l+1)} + \frac{F'_l}{1 + F'_l/(2l+1)} + \frac{G_l}{1 + G_l/(2l+1)} + \frac{G'_l}{1 + G'_l/(2l+1)} \right\} = 0. \quad (5.2)$$

This sum rule relates, in an important way, the various parameters of the interaction. It is badly violated in [1] and in most of the applications of the Landau theory to nuclei, in fact, in [1] all of the coefficients, F_0 , F'_0 etc. are positive, so there's no chance of (5.2) being satisfied. The second sum rule [48], see appendix A, is a manifestation of that in a Fermion system with two spin degrees of freedom we have two sets of odd waves (triplet–triplet and singlet–singlet) that vanish for equal momenta. In appendix A we derive the sum rules from the requirement that the forward scattering amplitude (5.1) is antisymmetric under the exchange of, say, the outgoing particles.

Of course, the complete quasiparticle interaction A must satisfy the sum rules (5.2) and (A.15). In general, A 's that are constructed from calculations of f to some finite order, with subsequent use of (5.1) will not satisfy the sum rules. This is clear, because the polarization bubbles are included to all orders in the direct term of the phonon-induced interaction, fig. 24d, whereas if one calculates f to any finite order, the corresponding exchange part of the induced interaction will have polarization bubbles only to finite order. Our construction of the integral equation, fig. 22, ensures the satisfaction of the sum rules so long as an antisymmetric driving term is employed in the integral equation, regardless of the order one goes to in the G -matrix in the kernel. This is because the Induced Interaction just gives the proper exchange term for the phonon induced interaction in A . We shall see later that preservation of the Landau sum rules puts useful and important constraints on the calculation, and that the solution of the integral equation, fig. 22, is much more stable with respect to input than calculations are of f to some finite order.

A great advantage of the integral equation is that solutions generally obey the stability conditions, such as $F_0 > -1$, even in cases where the direct interaction* does not, as in liquid ^3He where $F_0^d \ll -1$. Thus, one has a starting point in a stable region, and it is then more likely, although not guaranteed, that further additions will lead to a convergent answer.

A disadvantage of the equation is that two-phonon exchange terms are handled on a different footing from one-phonon exchange ones. The former would come, as noted earlier, from functionally differentiating a line in one of the bubbles of fig. 19b. On the other hand, it is necessary to treat the two-phonon and one-phonon exchange terms on the same footing in the case of spin- (or isospin-) dependent interactions. Those two-phonon exchange terms which are not in our induced interaction are included in the direct term. In principle, they could be pulled out and included in a more general induced interaction, but this would complicate the latter immensely.

We first derive the form of the Induced Interaction for the simplified case where it is sufficient to keep only the $l=0$ terms in the expansions, such as (4.12), for the Landau parameters. It is straightforward to construct the term of second order in f in the Induced Interaction, and then generalize it by making the complete expression into a geometrical series. One has (see eqs. (3.12) of ref. [52])

* In section 4.1 we meant by the direct term the direct term of the potential in fig. 15 and eqs. (4.20), (4.21) and (4.22). From here on we refer by the direct term to the driving term enclosed in fig. 22. This terminology is in accordance with ref. [52].

$$\begin{aligned}
4F_i &= \frac{F_0^2 U(q, 0)}{1 + F_0 U(q, 0)} + \frac{3F_0'^2 U(q, 0)}{1 + F'_0 U(q, 0)} + \frac{3G_0^2 U(q, 0)}{1 + G_0 U(q, 0)} + \frac{9G_0'^2 U(q, 0)}{1 + G'_0 U(q, 0)} \\
4F'_i &= \frac{F_0^2 U(q, 0)}{1 + F_0 U(q, 0)} - \frac{F_0'^2 U(q, 0)}{1 + F'_0 U(q, 0)} + \frac{3G_0^2 U(q, 0)}{1 + G_0 U(q, 0)} - \frac{3G_0'^2 U(q, 0)}{1 + G'_0 U(q, 0)} \\
4G_i &= \frac{F_0^2 U(q, 0)}{1 + F_0 U(q, 0)} + \frac{3F_0'^2 U(q, 0)}{1 + F'_0 U(q, 0)} - \frac{G_0^2 U(q, 0)}{1 + G_0 U(q, 0)} - \frac{3G_0'^2 U(q, 0)}{1 + G'_0 U(q, 0)} \\
4G'_i &= \frac{F_0^2 U(q, 0)}{1 + F_0 U(q, 0)} - \frac{F_0'^2 U(q, 0)}{1 + F'_0 U(q, 0)} - \frac{G_0^2 U(q, 0)}{1 + G_0 U(q, 0)} + \frac{G_0'^2 U(q, 0)}{1 + G'_0 U(q, 0)}
\end{aligned} \tag{5.3}$$

where the lower index i denotes “induced”. Here $U(q, 0)$ is the Lindhard function $U(q, \omega)$ for $\omega = 0$,

$$U(q, 0) = \frac{1}{2} + \frac{1}{2} \left(\frac{q}{4k_F} - \frac{k_F}{q} \right) \ln \frac{k_F - q/2}{k_F + q/2} \tag{5.4}$$

with the normalization

$$U(0, 0) = 1. \tag{5.5}$$

Note that the various excitations contribute, with coefficients corresponding to their statistical weight, to the spin- and isospin-independent parameter F . Note also that although the input F ’s, etc., may have only $l = 0$ terms, the Induced Interaction will develop terms of higher order in l .

The right-hand side of (5.3) can be understood in the following way. The F_0 ’s in the numerator describe the coupling of the quasiparticle and quasihole to the density fluctuations of the exchange mode; similarly the F'_0 to the isospin fluctuation of the exchanged mode, etc. The quantity

$$\chi(q, \omega) = -\frac{U(q, \omega)}{1 + F_0 U(q, \omega)}, \tag{5.6}$$

evaluated at $\omega = 0$, since we are calculating Landau parameters, is the density-density correlation function in our approximation. This turns out to be identical with the function of Pines and Nozières [38].

This interpretation tells us how to generalize the expression (5.3) to include $l = 1$ terms. In this case, the F_1 will describe coupling of the quasiparticle or quasihole to the fluctuation in current associated with the exchanged excitation, and we shall then construct the current-current correlation function $\chi_{jj}(q, 0)$ to describe the propagation of the excitations.

This can be made explicit by considering the vertex fig. 25, in the limit $q \rightarrow 0$. Although we shall extrapolate our description to $\mathbf{k}' = \mathbf{k} - \mathbf{q}$ with $0 \leq |q| \leq 2k_F$, we can only make rigorous statements for $q \rightarrow 0$, i.e. for the long-wavelength limit in the crossed channel.

As noted earlier, it was proved in the appendix to [57] that the vertex function, fig. 25, in the limit of $q \rightarrow 0$ is just $f(\hat{\mathbf{k}}, \hat{\mathbf{p}})$, the magnitudes of both \mathbf{k} and \mathbf{p} being equal to k_F . Expanding f up to terms of $l = 1$,

$$F(\hat{\mathbf{k}} \cdot \hat{\mathbf{p}}) = f_0 + f_1(\hat{\mathbf{p}} \cdot \hat{\mathbf{k}}) = f_0 + f_1\{(\hat{\mathbf{k}} \cdot \hat{\mathbf{q}})(\hat{\mathbf{p}} \cdot \hat{\mathbf{q}}) + \sqrt{1 - (\hat{\mathbf{k}} \cdot \hat{\mathbf{q}})^2} \sqrt{1 - (\hat{\mathbf{p}} \cdot \hat{\mathbf{q}})^2} \cos \phi\} \tag{5.7}$$

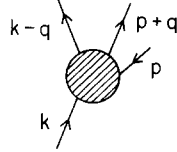


Fig. 25. Vertex function describing quasiparticle coupling to a particle-hole excitation of momentum q .

where we have used the addition theorem for Legendre polynomials in the last step. The term in $\cos \phi$ vanishes upon integration over angles.

The interaction is then

$$\Gamma = \int f(\hat{k} \cdot \hat{p}) \delta n_p 4 \frac{d^3 p}{(2\pi)^3} = f_0 \delta n_0 + \frac{f_1}{3} (\hat{k} \cdot \hat{q}) \delta n_1 \quad (5.8)$$

where

$$\delta n_p = \delta n_0 + \delta n_1 \cos(\hat{p} \cdot \hat{q}), \quad (5.9)$$

with

$$\begin{aligned} \delta n_0 &= \frac{1}{2} \int_{-1}^1 \delta n_p d(\cos(\hat{p} \cdot \hat{q})) \\ \delta n_1 &= \frac{3}{2} \int_{-1}^1 \delta n_p \cos(\hat{p} \cdot \hat{q}) d(\cos(\hat{p} \cdot \hat{q})). \end{aligned} \quad (5.10)$$

Note that $\delta n_0 = \delta \rho$. The δn_1 's are multipoles in the expansion of the δn_p 's associated with the particle-hole excitations of (vanishing) momentum q .

The current associated with the particle-hole excitation is

$$\mathbf{j} = \rho \mathbf{v}, \quad (5.11)$$

with ρ the density, and \mathbf{v} the velocity field of the excitation, given by

$$m\rho \mathbf{v} \cdot \hat{q} = \sum_p \mathbf{p} \cdot \hat{q} \delta n_p = \frac{k_F}{3} \delta n_1 \quad (5.12)$$

where we have used the fact* that each quasiparticle on the Fermi surface carries momentum k_F . From

* The current carried by a quasiparticle in the interacting system must be equal to the current carried by a bare particle in the noninteracting system, since the interactions are translationally invariant, and therefore preserve particle current.

(5.12) we find

$$\delta n_1 = \frac{3m}{k_F} j, \quad (5.13)$$

and, since j is in the direction of $\hat{\mathbf{q}}$, the interaction is

$$\Gamma = f_0 \delta n_0 + \frac{mf_1}{k_F} \hat{\mathbf{k}} \cdot \mathbf{j}. \quad (5.14)$$

In order to preserve a symmetrical treatment between \mathbf{k} and \mathbf{k}' as we move away from $\mathbf{q} = 0$, the $\hat{\mathbf{k}}$ above should be interpreted [57] as $(\hat{\mathbf{k}} + \hat{\mathbf{k}}')/2$.

The current carried by a quasiparticle of moment \mathbf{k} is proportional to \mathbf{k} , so the final term in (5.14) represents the coupling between the current carried by the quasiparticle and that carried by the particle-hole excitation. In the $\mathbf{q} = 0$ limit, the coupling can be put into the familiar form [61]

$$\frac{mf_1}{k_F} \hat{\mathbf{k}} \cdot \mathbf{j} = \frac{mf_1}{k_F} \rho \hat{\mathbf{k}} \cdot \mathbf{v} = \frac{m^* - m}{m^*} kv \quad (5.15)$$

which can be derived simply using Landau's application of the Galilean invariance. Equation (5.15) gives

$$\frac{m^*}{m} = \frac{1}{1 - \frac{1}{3} N_0^m f_1}, \quad N_0^m = \frac{2k_F m}{\pi^2} \quad (5.16)$$

which is eq. (4.16) in a different form.

In this example, we have worked out the coupling to the longitudinal particle-hole mode, the velocity field of which will be in the direction of \mathbf{q} . But $\frac{1}{2}(\hat{\mathbf{k}} + \hat{\mathbf{k}}') \cdot \mathbf{q} = 0$. However, the current-current correlation function is diagonal in the long-wavelength limit, so that exactly the same contribution as calculated above will be picked up from transverse modes.

The induced interaction, (5.3), can now be generalized to include the current-current couplings, giving:

$$\begin{aligned} 4F_i &= \frac{F_0^2 U(q, 0)}{1 + F_0 U(q, 0)} + \left(1 - \frac{q^2}{4k_F^2}\right) \frac{F_1^2 \alpha_1(q, 0)}{1 + F_1 \alpha_1(q, 0)} + \frac{3F_0'^2 U(q, 0)}{1 + F_0' U(q, 0)} + 3\left(1 - \frac{q^2}{4k_F^2}\right) \frac{F_1'^2 \alpha_1(q, 0)}{1 + F_1' \alpha_1(q, 0)} \\ &\quad + \frac{3G_0^2 U(q, 0)}{1 + G_0 U(q, 0)} + 3\left(1 - \frac{q^2}{4k_F^2}\right) \frac{G_1^2 \alpha_1(q, 0)}{1 + G_1 \alpha_1(q, 0)} + \frac{9G_0'^2 U(q, 0)}{1 + G_0' U(q, 0)} + 9\left(1 - \frac{q^2}{4k_F^2}\right) \frac{G_1'^2 \alpha_1(q, 0)}{1 + G_1' \alpha_1(q, 0)} \end{aligned} \quad (5.17)$$

where α_1 is essentially the current-current correlation function. Obvious generalizations of (5.3), involving the $\alpha_1(q, 0)$, are valid for the other parameters [52].

The factor $(1 - q^2/4k_F^2)$ arises from our symmetrization between \mathbf{k}' and \mathbf{k} in describing the quasiparticle current. For $\mathbf{k}' = -\mathbf{k}$, the average current carried by the quasiparticle is zero, as the factor $(1 - q^2/4k_F^2)$ correctly reproduces. Here $\alpha_1(q, 0)$ is given by [52]

$$\alpha_1(q, 0) = \frac{1}{2} \left[\frac{3}{2} - \frac{k_F^2}{2q^2} + \left(\frac{k_F^3}{2q^3} + \frac{k_F}{4q} - \frac{3q}{32k_F} \right) \ln\left(\frac{k_F + q/2}{k_F - q/2}\right) \right]. \quad (5.18)$$

Our integral equation takes, finally, the deceptively simple form

$$f(\mathbf{k}, \mathbf{k}') = f_{d(i)}(\mathbf{k}, \mathbf{k}') + f_{d(ii)}(\mathbf{k}, \mathbf{k}') + f_{d(iii)}(\mathbf{k}, \mathbf{k}') + f_i(f(\mathbf{k}, \mathbf{k}')), \\ |\mathbf{k}| = |\mathbf{k}'| = k_F \quad (5.19)$$

the induced interaction f_i being a function of the Landau f . The “direct interaction”, shown as the enclosed part of fig. 22, contains all terms that cannot be separated into two diagrams by cutting one internal particle-hole pair and can, in principle, be extended to any order. We have used “order” here in the sense of the number of G -matrices, but one might well use some other scheme for constructing the direct interaction.

The above eq. (5.19) can be solved by iteration. For the F_0 and F_1 it tends to be very stable, i.e., one can alter the input, in terms of the f_d 's considerably, with little alteration in the final F_0 and F_1 . We show, as example, in fig. 26 how little final results change with inclusion of $f_{d(ii)} + f_{d(iii)}$. It can be seen that an $\sim 20\%$ change in the f_d -input is translated into an $\sim 8\%$ change in F_0 .

The reasons for this stability are two-fold: (i) The important F'_l , G_l and G'_l are all positive, in nuclear matter; thus, we know the important F_l must be negative, so that the Landau sum rule (5.2) be satisfied. In practice, this implies that F_0 be negative. (ii) The Induced Interaction acts in the opposite direction to the direct interaction. To elaborate on point (ii), let us drop the spin- and isospin-dependent terms, for the moment, and consider the equation

$$F = F_d + \frac{F_0^2 U(q, 0)}{1 + F_0 U(q, 0)} + \left(1 - \frac{q^2}{4k_F^2}\right) \frac{F_1^2 \alpha_1(q, 0)}{1 + F_1 \alpha_1(q, 0)}. \quad (5.20)$$

Suppose that we put in for F_d an amplitude which is too attractive. (An example is the F_d^i of fig. 26.) Then the terms involving F_0^2 and F_1^2 on the right-hand side of (5.20) will be too large and, being repulsive, will subtract off too much from F_d , giving a final F which does not differ too much from the correct one.

One can see that all of the terms in the induced interaction, (5.17), are positive so that they all will increase the compressibility. From our discussion at the beginning of this chapter, we can understand

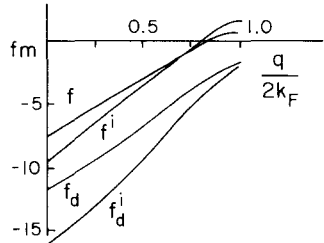


Fig. 26. The variation of the spin- and isospin-independent particle-hole interaction caused by a change in the direct interaction is illustrated. The f_d is the interaction $f_{(i)} + f_{(iii)}$ illustrated in fig. 22, and f is the solution to the integral equation. The f_d^i and f^i are the corresponding terms when only $f_{(i)}$ is used in the kernel.

this in terms of clothing of the quasiparticles; through interaction with collective modes in the environment about them, the quasiparticles build correlations into that environment and become effectively larger in size and harder to compress.

Sjöberg [52, 53] arrived at a value of the compression modulus $K \approx 200$ MeV in all of his approximations. The work of [53] should be preferable to that of [52], since a model space was used there, and single-particle energies, etc. must be continuous across the Fermi surface in order to make any sense out of a microscopic calculation within the framework of the Landau theory. The work of [53] is, however, marred by a spin sum being incorrectly carried out in the calculation of G and G' . Thus, G' turned out to be much too small and G_0 too big [42]. This reflects back on the other parameters. In ref. [42] the calculation of ref. [52] was redone with corrected spin summations.

We have so far not mentioned the influence of the tensor force. On the Fermi surface the tensor force comes largely from the exchange term of the interaction. The direct term disappears in the Landau limit. Since π - and ρ -exchange give rise to the most important tensor forces we would then expect a ratio of 3 to 1 between the strengths in $T = 0$ and $T = 1$ states, respectively. This ratio is, for the Reid soft-core potential, quite close to the results of ref. [42]. Inclusion of the tensor force in the induced interaction (5.3) has yet to be done. It may well be, for example, that some (welcome) repulsion to the symmetry energy can be obtained this way.

6. Making contact with nature

We shall now discuss the nature of the interactions in the various channels, keeping in mind the underlying nucleon-nucleon interaction outlined in chapter 2 and the resulting reaction matrix discussed in section 4.1. It seems natural to begin with the spin- and isospin-independent interaction F .

On the level of a reaction matrix we have three important contributions to F . Two of them we discussed in section 4.1, namely the exchange-term contributions fig. 15b, from exchange of a pion and a rho-meson. Let us now discuss the third important contribution, the second-order tensor. In figs. 27 and 28 we have reproduced figs. 3 and 4 of ref. [42]. The reaction matrix was calculated as explained in section 4.2 with only kinetic energies for particles, eq. (4.27). In fig. 27 the $l = 0$ Fermi liquid parameters are displayed for the Reid soft-core potential, with the Born term of the one-pion exchange subtracted. In fig. 28 the corresponding results when the one-pion exchange has been completely switched off are displayed. The difference in results shown in figs. 27 and 28 is thus almost completely due to the iterated

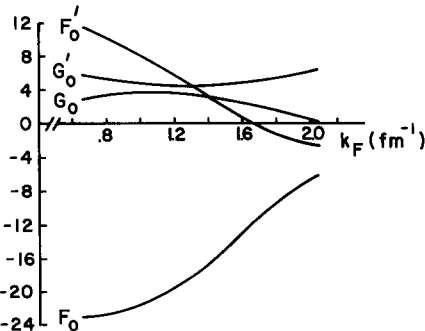


Fig. 27. The $l = 0$ Fermi liquid parameters for Reid's soft-core potential when the Born term of the one-pion exchange has been subtracted. Here $m^* = m$.

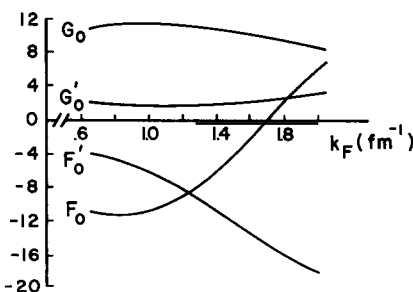


Fig. 28. The $l = 0$ Fermi liquid parameters for Reid's soft-core potential when the one-pion exchange has been completely switched off. Here $m^* = m$.

one-pion-exchange tensor (second and higher orders). We see that this contribution is very important. We also see that the shifts of the curves going from fig. 28 to fig. 27 roughly follow eq. (2.10). To put this more clearly: In eq. (2.10) the ratio of the absolute values of the contributions ΔF_0 , $\Delta F'_0$, ΔG_0 and $\Delta G'_0$ from the second-order tensor is 9:6:3:2, ΔF_0 and ΔG_0 being negative and $\Delta F'_0$ and $\Delta G'_0$ being positive. If we use* $m^* = m$ in the densities of states $\Delta F_0 \sim -1$ at $k_F = 1.35 \text{ fm}^{-1}$. To put this number in perspective, $\Delta F_0'' = -0.4$.

Now the observant reader notes that all our contributions to F_0 so far are negative and if we add them up we have, as in ref. [42], an $F_0 \approx -2$, with $m^* = m$, at saturation density. The results for some one-boson-exchange potentials, of the Bonn groups, obtained in ref. [42] were, at $k_F = 1.35 \text{ fm}^{-1}$, much the same as for the Reid soft core. Now, stability (see appendix B for stability criteria) demands $F_0 > -1$, where m^* naturally is to be used in the density of states. Before we discuss the origin of the necessary repulsion, let us say a few words about the contributions from the exchange of ω - and σ -mesons. In order to obtain a reasonable estimate of F_0 , or any other parameters, for a reaction matrix we don't need them. The reason for this is as follows. The peaks in the mass distributions for ω and ρ are at about the same mass, but this mass distribution is broader for the ρ -meson than for the ω -meson. The low mass tail of the mass distribution is significantly bigger for the ρ -meson than for the ω -meson. This means that little is left of the ω -exchange potential where the nucleon–nucleon wave function starts to differ from zero, whereas part of the ρ -exchange is left. The contribution left from ω -exchange to Fermi liquid parameters is then largely cancelled by the corresponding contributions coming from the exchange of σ -mesons.

Now to the necessary, so far missing, repulsive contributions to F_0 . If we calculate for the nucleon–nucleon interaction a reaction matrix we get for any reasonable one saturation in nuclear matter. The saturation density, i.e. the density at which a given interaction within Brueckner's theory gives a minimum in the binding energy, is different for different interactions and occurs for the Reid soft-core potential at about $k_F = 1.35 \text{ fm}^{-1}$. In the vicinity of the equilibrium density ρ_0 the compression modulus†

$$K = 9\rho_0^2 d^2E/d\rho_0^2 \quad (6.1)$$

is then guaranteed to be positive and $F_0 > -1$ (see table 1). It is the rearrangement terms that on the level of Brueckner's theory makes the system stable [54]. We have discussed these in section 4.1 and chapter 5. As pointed out in conjunction with the discussion of the induced interaction, depicted in fig. 21, some graphs like the second-order bubble have to be discarded from the direct interaction in order to avoid double counting. There is also another reason for not calculating this diagram with a Brueckner gap in the self-energy spectrum; such a calculation would lead to violation of the Pauli principle sum rules [41]. The diagram in fig. 23a we had to neglect only because of the gap in the spectrum. If we would do a model-space calculation we could and probably should keep both fig. 23a and fig. 23b. This is again a reminder of the virtues of a model-space calculation in that large contributions of opposite sign can be handled together. In Sjöberg's calculation [52] the renormalization at the quasiparticle pole ((iii) in the kernel of fig. 10) was taken into account.

* If not otherwise stated we use $m^* = m$ in the density of states.

† The factor of 9 is explained in conjunction with eq. (4.18).

6.1. Compressibility

The compression modulus K defined by (4.18) is given in terms of Fermi liquid parameters by

$$K = 6 \frac{k_F^2}{2m^*} (1 + F_0). \quad (6.2)$$

Calculations by Sjöberg [52, 53] have given $K \approx 200$ MeV. These calculations suffer from an error in spin sums in evaluating G_0 and G'_0 as mentioned earlier. The calculation of ref. [52] was repeated, with correct spin sums, in ref. [42], see fig. 6 therein. The result was essentially the same for K as in refs. [52] and [53]. That the change was that small is due to numerical stability of the integral equation discussed in chapter 5, see fig. 26.

Empirically, the situation with K has been greatly clarified by the identification of the breathing mode in ^{208}Pb [62, 63]. By composing the compression modulus in finite nuclei out of a volume term, a surface term and symmetry energy and Coulomb components, Blaizot and Grammaticos [64, 65] can perform the extrapolation to infinite nuclear matter, and obtain $K \sim 210$ MeV, a value which would seem to fit in well with Sjöberg's calculations.

6.2. Effective mass*

The history of the effective-mass calculations in nuclei and nuclear matter is interesting and instructive, in that only recently the theoretical and empirical determinations have come at all together. Brueckner theory always produced effective masses $m^*/m \sim 0.6\text{--}0.7$, which would imply that the level density, at the Fermi surface, which is proportional to m^* , is substantially lowered by the particle interactions. On the other hand, empirical descriptions using the Nilsson model, etc., begin from velocity-independent potential wells for the shell model, corresponding to $m^*/m = 1$, and then usually had to compress the levels further to achieve agreement with experiment.

The empirical behavior of the effective mass was clarified already in 1964 by Brown, Gould and Gunn [66], we reproduce this in fig. 29. The figure has been slightly redrawn to show the enhancement as symmetrical about the Fermi energy.

The theoretical reasons underlying the compression of levels at the Fermi surface were given by Bertsch and Kuo [67] and elucidated further in the work of Jeukenne, Lejeune and Mahaux [68]. In these works it was pointed out that the ω -dependence of m^* is essential for the explanation of level compression. The effective mass may be expressed as

$$\frac{m^*}{m} = \frac{1 - \partial\Sigma(k, \omega)/\partial\omega}{1 + \partial\Sigma(k, \omega)/\partial T_k} \Big|_{\omega=\epsilon_k} \quad (6.3)$$

where $\Sigma(k, \omega)$ is the self-energy, T_k is the kinetic energy

$$T_k = k^2/2m \quad (6.4)$$

* This topic is covered extensively in Physics Reports 120, Nos. 1–4 (1985) 1–274 by C. Mahaux, P.F. Bortignon, C.H. Dasso and R.A. Broglia.

and in the numerator $\partial\Sigma/\partial\omega$ is to be evaluated at the quasiparticle pole ε_k . As pointed out in refs. [68] and [69], Brueckner theory calculations treated the ω -dependence in a rough way, so that the numerator in (6.3) was close to unity; actually, it is the increase in the numerator near $\varepsilon_k = \varepsilon_F$ which causes the behavior of the effective mass shown in fig. 29.

The calculations of refs. [67] and [68] are carried out in the framework of perturbation theory. They are starting points for coupling of the single particle to vibrations, which consist of many bubbles, when described, e.g., in random phase approximation. Low-lying surface vibrations in heavy nuclei have low energies $\hbar\omega \ll \varepsilon_F$, so that through this coupling it is possible to obtain the enhancement of fig. 29 which is of short range in energy. In ^{208}Pb the enhancement has essentially disappeared by the time the single-particle energy has reached the neutron separation energy; no trace of enhancement is seen in scattering experiments. This means that the range is $\sim 8 \text{ MeV}$, much less than $k_F^2/2m$. But 8 MeV is in the range of $\hbar\omega$ for surface energies.

Bernard and Van Giai [69] calculated the single-particle energy shifts in the framework of a microscopic particle-vibration model, using the random phase approximation to construct the vibration. They find the $(2j+1)$ -averaged particle-hole energy gap at the Fermi surface of ^{208}Pb to be reduced from 8.81 MeV to 6.94 MeV from the coupling to vibrations; corresponding roughly to an effective mass enhancement of 1.27, since level spacings are inversely proportional to m^*/m .

Single-particle level shifts due to particle-vibration coupling have also been estimated by Bortignon and Broglia [70]; these are consistent with those of Bernard and Van Giai where they can be compared. Wambach, Mishra and Li Chu-hsia [71] have calculated particle-vibration coupling using as input a particle-hole interaction of Landau-Migdal form, finding an average level shift somewhat smaller. Sommerman, Kuo and Ratcliff [72] find a shift of about the same size. It is difficult to extend these calculations very far from the Fermi surface because of the great number of states one has to deal with. However, calculations [73] in liquid ^3He show that the effective mass does, indeed, change very rapidly with increasing energy from the Fermi surface, and this behavior has been confirmed experimentally [74]. In liquid ^3He the enhancement in the effective mass arises primarily from coupling to the low-lying spin fluctuations; the spin-dependence of the interaction gives considerable attraction with $G_0 \approx -0.7$, quite unlike the case in nuclei. One can follow through the liquid ^3He calculation in detail and see that the range of energy variation in m^*/m is given by the typical spin-fluctuation energy. In nuclei, this role is taken over by the typical surface vibration energy. Otherwise, the situations are quite similar.

The ω -dependence of the effective mass resolves a deep problem presented by early parameterizations of the Migdal theory [1]. In these and, indeed, in almost all of the parameterizations to date, all of the Fermi liquid parameters F_i , F'_i , G_i , G'_i are positive. With all positive parameters it is obviously impossible to satisfy the Landau sum rule eq. (A.14).

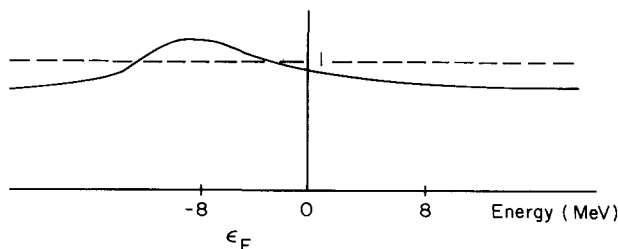


Fig. 29. Behavior of the effective mass m^*/m as a function of the distance from the Fermi surface.

In the work leading to these parameterizations it was generally assumed that $m^*/m \approx 1$, as is the situation just at the Fermi surface. Of course, most data on level spacings pertain to this energy region. If, however, m^*/m drops rapidly with increasing energy, then the compression of single-particle energies at the Fermi surface will relax, and the levels will occur at substantially higher energies than one would estimate from $m^*/m = 1$ (static potentials). Just these levels, such as those at $2\hbar\omega$ unperturbed excitation energy, enter into the giant monopole vibration; with them substantially higher in unperturbed energy, the Fermi liquid interaction F_0 must now be substantially attractive, $F_0 \sim -0.3$ [44], in order to bring the collective excitation down to its energy.

Furthermore, we have now understood much of the enhancement in m^*/m at the Fermi surface to be due to coupling to surface vibrations, which are absent in the infinite system, so it is appropriate to use in the sum rule, derived for the infinite system, a value of $m^*/m < 1$, and, therefore, a negative F_1 . The combination of negative F_0 and F_1 then makes it possible to satisfy the sum rule, all other Fermi liquid parameters being positive.

A simple model for calculating the effective mass which takes into account only the k -dependence, i.e., the denominator of the right-hand side of eq. (6.3), can be made in terms of π - and ρ -meson exchange potentials [45]; at nuclear matter density this model gives results close to Sjöberg's [52]. It is, of course, natural that at low densities pion-exchange gives the most rapid variation of f with Landau angle, because it is of longest range in configuration space, and therefore has a Fourier transform which varies most rapidly. The contributions from π - and ρ -exchange to F are given in (4.20) and (4.21), respectively. For a π -exchange we have

$$\delta F_\pi = -\frac{N_0}{4} \frac{3f^2}{m_\pi^2 + (\mathbf{k} - \mathbf{k}')^2}, \quad (6.5)$$

where the density of states N_0 is given by

$$N_0 = 2k_F m^*/\pi^2. \quad (6.6)$$

At the Fermi surface

$$(\mathbf{k} - \mathbf{k}')^2 = 2k_F^2 (1 - \cos \theta_L), \quad (6.7)$$

where θ_L is the Landau angle. Alternatively, we could also obtain (6.5) by taking expectation values π - and ρ -exchange with appropriate particle-hole wave functions. Consider the two processes shown fig. 30. From the matrix elements in fig. 30 we can make up the elements

$$\left\langle \left(\frac{p\bar{p} \pm n\bar{n}}{\sqrt{2}} \right) | \boldsymbol{\tau}_1 \cdot \boldsymbol{\tau}_2 | \left(\frac{p\bar{p} \pm n\bar{n}}{\sqrt{2}} \right) \right\rangle = \frac{2 \pm 4}{2} = \begin{pmatrix} 3 \\ -1 \end{pmatrix} \quad (6.8)$$

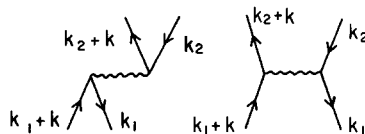


Fig. 30. Isospin matrix elements for the exchange term in the particle-hole interaction.

appropriate for the exchange terms of, respectively, isoscalar (+ sign) isovector (− sign) particle-hole matrix elements. Thus, the OPEP interaction

$$\frac{f^2}{3} \frac{(\boldsymbol{\sigma}_1 \cdot \boldsymbol{\sigma}_2)(\boldsymbol{\tau}_1 \cdot \boldsymbol{\tau}_2)}{k^2 + m_\pi^2}$$

leads to particle-hole matrix elements, in the long-wavelength limit

$$-3 \frac{f^2}{(\mathbf{k}_1 - \mathbf{k}_2)^2 + m_\pi^2},$$

an additional minus sign entering in because this is the exchange term.

We easily find the result given by (6.5). Straightforward calculation gives

$$F_{1\pi} = -\frac{9}{8} N_0 \frac{f^2}{2k_F^2} \left\{ \frac{2k_F^2 + m_\pi^2}{2k_F^2} \ln \frac{m_\pi^2 + 4k_F^2}{m_\pi^2} - 2 \right\} \quad (6.9)$$

which is easily evaluated at nuclear matter densities where $k_F \approx 2m_\pi$ to give

$$F_{1\pi} = -0.46m^*/m. \quad (6.10)$$

A similar calculation for the $\boldsymbol{\sigma}_1 \cdot \boldsymbol{\sigma}_2 \boldsymbol{\tau}_1 \cdot \boldsymbol{\tau}_2$ part of the ρ -exchange potential gives,

$$F_{1\rho} = -\frac{9}{8} N_0 \frac{\hat{f}_\rho^2}{k_F^2} \left\{ \frac{2k_F^2 + m_\rho^2}{2k_F^2} \ln \frac{m_\rho^2 + 4k_F^2}{m_\rho^2} - 2 \right\} \quad (6.11)$$

where

$$\hat{f}_\rho^2 = 0.4f_\rho^2, \quad (6.12)$$

the 0.4 taking into account [31] in a crude way effects of short-range correlation, due mainly to ω -meson exchange

$$F_{1\rho} = -0.56m^*/m \quad (6.13)$$

and

$$m^*/m = 0.75 \quad (6.14)$$

where we have used (4.16), to compare with Sjöberg's 0.74 [52]. In fact, Sjöberg used the Reid potential, which has a smaller ρ -exchange component, but the second-order tensor interaction, which is then stronger, makes up for some of the difference. In any case, our model calculation is probably adequate for not only qualitative, but also semiquantitative considerations.

Given a value of m^*/m we can deduce a value of F_0 from the known compression modulus $K \approx 220$ MeV and from eq. (6.2). If, for example, we use $m^*/m = 0.75$ from (6.14), corresponding to

$$F_1 = -0.75 \quad (6.15)$$

we find

$$F_0 = -0.28,$$

roughly the value one needs to bring the giant monopole resonance down into place. (We use $k_F = 1.36 \text{ fm}^{-1}$ in (6.2).) These give the only attractive terms in the Landau sum rule, eq. (A.14) – we shall find the other parameters to all be repulsive. With these Fermi liquid parameters one will, at least roughly, be able to satisfy (A.14), also (A.16), which we will find to put a stronger constraint on the negativity of the F_i 's.

Although the large enhancement of m^*/m at the Fermi surface comes from coupling to surface vibrations, and is a property of finite nuclei, there should be some enhancement also in nuclear matter due to the coupling to collective excitations. Thus, m^*/m should be larger than 0.75, and F_1 smaller in magnitude than (6.15); fitting the compression modulus will give an F_0 closer to zero, then. For $m^*/m = 1$, one obtains $F_0 = 0.05$. The F_0 is small because the compression modulus K is essentially that of a noninteracting Fermi gas. Since $F_1 = 0$ for $m^*/m = 1$, we are back in the quandary of the early parameterizations of Migdal theory, where all parameters in (A.14) are positive, but must add up to give zero.

The true situation must be between the above two cases, namely

$$\begin{aligned} -0.75 &< F_1 < 0 \\ -0.28 &< F_0 < 0.05, \end{aligned} \quad (6.16)$$

and the sum rule would favor the lower values (6.15). There is some “give” in the sum rule, because the higher Landau parameters have not been included. In particular, F_2 may well be substantial and negative. Also we neglected the tensor components. We believe, though, that (6.16) sets reasonable limits.

6.3. Symmetry energy

It is well known that the neutron–proton interaction is substantially more attractive than the like particle one, resulting in a term which appears in the energy per particle

$$\delta E_r = \beta \left(\frac{N-Z}{A} \right)^2 \quad (6.17)$$

where β is given by

$$\beta = \frac{1}{3} \frac{k_F^2}{2m^*} (1 + F'_0). \quad (6.18)$$

Empirically [75], $\beta \approx 25 \text{ MeV}$, which would give $F'_0 \approx 0.95$, using $m^* = m$, and $F'_0 = 0.46$ for $m^* = 0.75m$ where we have used $k_F = 1.36 \text{ fm}^{-1}$.

In appendix A of Bethe et al. [76], a summary of theoretical values of the symmetry energy is given, as well as an analysis of binding energies of Fe isotopes and what they imply for β . These authors arrive at a value

$$\beta \cong 32 \text{ MeV} \quad (6.19)$$

although it is pointed out that there is some uncertainty because the symmetry energy in known nuclei results from a combination of bulk and surface symmetry energies, and the bulk energy is not easily disentangled. Still, we feel that (6.19) is a more reliable value than 25 MeV. This would give

$$\begin{aligned} F'_0 &= 1.49 \quad \text{for } m^*/m = 1 \\ &= 0.9 \quad \text{for } m^*/m = 0.75 . \end{aligned} \quad (6.20)$$

We would expect F'_0 to be between these limits; a value of $F'_0 \sim 1$ seems reasonable.

If we go back to chapter 2 to the nucleon–nucleon interaction, we see that second- and higher-order effects of the tensor force provide the main difference between neutron–proton and like-particle interactions. This is born out by the big difference, as mentioned at the end of section 4.2, in Sjöberg’s results when using a Brueckner gap [52] or a model space [53]. Translated to nuclei this implies a strong energy dependence of the effective interaction as found in ref. [77]. The reason for the special importance of the second-order tensor for F'_0 is the following. Lowest-order meson contributions like the ones in (4.21) and (4.20) are here scaled down by a factor of three compared with the contributions to F . The combined contribution from exchange of ω - and σ -mesons is thought to be small, because of cancellations. If this is the case the largest contribution to F'_0 comes from higher-order processes, which are energy-dependent. These remarks are also to some extent true for G_0 , although the presence of tensors here complicates matters.

From our model of the last section for F_1 , we can relate F'_1 and F_1 . Equation (6.8) or eqs. (4.20) and (4.21) would give

$$F'_1 \cong -\frac{1}{3}F_1 . \quad (6.21)$$

This is only very roughly satisfied in Sjöberg’s calculations [52, 53], where F'_1 is more like $-\frac{2}{3}F_1$. Our argument should be sufficient to give the sign and general size of F'_1 , however. Inclusion of the second-order tensor interaction leads to a ratio more like Sjöberg’s.

6.4. The spin-dependent interactions

We shall treat G and G' together, since we believe them to arise mainly from common agencies, namely π - and ρ -meson exchanges and the second-order tensor. For the moment we concentrate on the central degrees of freedom, G and G' in eq. (4.11). Later in this section, and in appendix B, we will discuss the tensor invariants H and H' that couple to G and G' , respectively.

There are several reasons why we expect G'_0 to be considerably bigger than G_0 . In the first place: We get contributions from the direct term in fig. 30 to G'_0 but not to G_0 . These contributions are according to (4.20) and (4.21)

$$G'_{0\pi} = \frac{1}{3} \frac{f^2}{m_\pi^2} N_0 \quad (6.22)$$

and

$$G'_{0\rho} = \frac{2}{3} \frac{\hat{f}_\rho^2}{m_\rho^2} N_0, \quad (6.23)$$

respectively. Numerically we get*

$$G'_{0\pi} = 0.9m^*/m \quad (6.24)$$

and

$$G'_{0\rho} = 1.46m^*/m. \quad (6.25)$$

Since it is not clear, as we have discussed, what value of m^*/m to use, we express the various contributions in terms of m^*/m .

The second-order tensor (2.10) gives attraction to G_0 and repulsion to G'_0 . This is a suitable place to comment on the “ ρ -like” properties of the second-order tensor. In ref. [32] $G'_0 = 1.3m^*/m$ was obtained from a reaction matrix based on Reid’s soft-core potential. The calculation was done with a Brueckner gap in the spectrum. As we earlier mentioned, end of section 4.1, Sjöberg’s symmetry energy, and so F'_0 , was greatly enhanced when using a model space [53] instead of a Brueckner gap [52]. Let us, in a somewhat oversimplified way, assume that all of the change in F'_0 comes from the second-order tensor. According to (2.10) we would then have an increase in G'_0 by $\sim \frac{1}{3}m^*/m$ and a G'_0 of $1.6m^*/m$ to $1.7m^*/m$ for the Reid, soft-core potential. On the other hand, using a strong ρ as we have used in our estimates in this article would reduce the contribution from the second-order tensor since the ρ - and π -tensors have opposite signs. This tends to make the sum of the contributions to G'_0 fairly stable, and is one of the reasons why one can fit phase shifts with both strong and weak ρ -couplings. However, it also tells us that in order to get reliable numbers from a reaction matrix calculation a model space is needed.

Above we get an attractive contribution to G_0 from the second-order tensor. In the calculation of ref. [42] a value from the reaction matrix of $0.44m^*/m$ for G_0 was found, using a gap in the spectrum. This agrees quite well with the result found by Krewald and Speth [58]. They analyzed magnetic high spin states which are sensitive both to G_0 and G'_0 . They found that $G_0 = 0.50$ had to be used in order to reproduce the excitation energies of the M12 and M14 states. The previous values for G_0 (bigger than 1) were obtained analyzing predominantly isovector states insensitive to G_0 . We get repulsive contributions to G_0 from the exchange term in fig. 30. Making the necessary projections on Landau angles in (4.20) and (4.21) gives the following contribution from the exchange terms:

$$G_{0\pi} = 0.1m^*/m, \quad G_{0\rho} = 0.9m^*/m, \quad (6.26)$$

* Couplings to virtual isobars provide a screening and cut these numbers down somewhat [32]. See also G.E. Brown and Mannque Rho [78].

and

$$G'_{0\pi} = -0.04m^*/m, \quad G'_{0\rho} = -0.3m^*/m. \quad (6.27)$$

The large contribution $G'_{0\rho}$ from ρ -exchange can be compared with the direct $G'_{0\rho}$ -term (6.25). In the limit of a zero-range ρ -exchange, the interaction $\boldsymbol{\sigma}_1 \cdot \boldsymbol{\sigma}_2 \boldsymbol{\tau}_1 \cdot \boldsymbol{\tau}_2 \delta(\mathbf{r}_1 - \mathbf{r}_2)$ can be replaced by $-3 \delta(\mathbf{r}_1 - \mathbf{r}_2)$, using the antisymmetry of two-body wave function*. This δ -function interaction now acts only in exchange terms and does not mix neutron with proton excitations. Thus, in this limit,

$$G'_{0\rho} = G_{0\rho}. \quad (6.28)$$

Whereas the $G'_{0\pi}$ is large, the $G_{0\pi}$ is small, mirroring the long range of the pion-exchange force. Another difference between G' - and G -channels is that the second-order tensor interaction (2.10) is repulsive in the $\boldsymbol{\sigma}_1 \cdot \boldsymbol{\sigma}_2 \boldsymbol{\tau}_1 \cdot \boldsymbol{\tau}_2$ channel, attractive in the $\boldsymbol{\sigma}_1 \cdot \boldsymbol{\sigma}_2$ channel. From our earlier discussion, we expect these second-order tensor terms to be underestimated, because of the gap, in reference-spectrum calculations.

We can learn what model-space calculations should give from Brown, Speth and Wambach [77], who carried out a calculation of the second-order tensor terms without using closure as in eq. (2.10), also not a gap. These authors find a $\boldsymbol{\tau}_1 \cdot \boldsymbol{\tau}_2$ volume integrated interaction $U_t = 210$ MeV for low nucleon energy (20 MeV) from the second-order tensor terms. This corresponds, for $k_F = 1.36$ fm⁻¹, to a Fermi liquid interaction

$$F'_0 = 1.28m^*/m, \quad (6.29)$$

essentially all of F'_0 (see the last section). Indeed, these authors find that 78% of the symmetry energy comes from the second-order tensor interaction although the model is somewhat crude and the precise fraction should not be taken seriously.

The second-order tensor contribution to G'_0 is

$$G'_0 = 0.70m^*/m \quad (6.30)$$

so that the ratio

$$G'_0/F'_0 = 0.55 \quad (6.31)$$

is somewhat larger than the 1/3 which would be implied by closure, eq. (2.10). Closure implies that

$$G_0 = -\frac{3}{2}G'_0, \quad (6.32)$$

i.e.,

$$G_0 = -1.05m^*/m. \quad (6.33)$$

Note that this large negative contribution essentially wipes out the $G_{0\rho}$ of (6.26).

* The full expression for zero-range ρ -exchange is given in eq. (4.4) of ref. [42], where a misprint in ref. [32] was corrected.

The above contributions from the second-order tensor interactions appear surprisingly large; certainly they are much larger than would follow from reference spectrum calculations which suppress higher-order processes because of the gap.

The energy-dependence of the V_τ and $V_{\sigma\tau}$ terms of Brown et al. [77], the generalization to finite energies of F' and G' , has been well checked empirically [79]. With increasing proton energy, the principal value involved in second-order terms goes to zero, over an energy range corresponding to typical values of the energy denominators. The experiments show this range to be ~ 200 MeV, rather than the 400 MeV implied by the reference spectrum. This is a clear statement that model-space calculations are strongly to be preferred over reference spectrum ones.

From the above we have seen that the G_0 -parameter should be small at low energies, chiefly because of cancellation between contributions from ρ -meson exchange and from the second-order tensor interaction. One could hope to “peel” the latter off by going to higher energies in the nucleon–nucleon interaction, much as V_τ is peeled off from $V_{\sigma\tau}$ [77]. One should also encounter, at high momentum transfers, some (positive) $\sigma_1 \cdot \sigma_2$ interaction from ω -meson exchange*, the analog of the Fermi–Breit interaction in atomic physics. This will be short range, $\sim m_\omega^{-1}$, and should hold up well in going to high energies and large momentum transfers.

The fact that interactions in the $\sigma_1 \cdot \sigma_2$ channel are weak at low energies means that states of a purely spin-dependent character will not be very collective and, indeed, none are seen.

Calculations of nuclear binding energies and other properties have been carried out with an energy spectrum continuous across the Fermi surface [68], which corresponds roughly to using a model space. These give much better results than corresponding Brueckner calculations.

Before leaving this matter, we wish to comment on strong ρ versus weak ρ potentials. The Höhler–Pietarinen work [30] shows the former to be correct. The Reid soft-core potential effectively has a weak ρ exchange. The work of Brown et al. [77] quoted above, uses a strong ρ . Perturbation theory in the tensor interaction will converge much more quickly with the strong ρ than with the weak one, because the resulting tensor interaction is weaker in the strong ρ case. As far as two-body interactions are concerned, however, the net difference of using a strong or weak ρ potential is not large, in that whatever potential is used it must be adjusted to fit the nucleon–nucleon scattering phase shifts. Thus, higher-order terms must make results from the two come out about the same.

This isn’t at all true with three-body terms in the nuclear binding energy, etc., however. The three-ring term will, for example, give much more attraction with the weak ρ forces than with the strong ρ ones [80]. Thus, the Reid soft-core potential is not at all reliable for nuclear-matter calculations carried to higher than two-body order. We believe that many of the difficulties in the nuclear-matter problem have arisen from use of the wrong two-body potential.

Due to the calculation of the contributions to G_0 mentioned above, even small contributions to G_0 become relatively important. In ref. [31] an estimate of the combined contributions from σ - and ω -exchange was made; the result was a contribution ~ 0.2 to both G_0 and G'_0 . Hence we expect G_0 to be small and what is left in the $T = 0$, $S = 1$ particle–hole channel is mostly a tensor force. We shall return to G'_0 in the next section in connection with the giant Gamow–Teller resonance. Now a few words about the tensor degrees of freedom.

As pointed out by Dabrowski and Haensel [43] one should in principle add the tensor-invariants to G and G' in (4.11). The particle–hole interaction would then be in $S = 0$, $T = 1$.

* We have here in mind the so-called small components coming from ω -meson exchange.

$$G \boldsymbol{\sigma}_1 \cdot \boldsymbol{\sigma}_2 + \frac{1}{4} \frac{(\mathbf{k} - \mathbf{k}')^2}{k_F^2} H(\cos \theta_L) S_{12}, \quad (6.34)$$

and in $S = 1$, $T = 1$

$$G' \boldsymbol{\sigma}_1 \cdot \boldsymbol{\sigma}_2 \boldsymbol{\tau}_1 \cdot \boldsymbol{\tau}_2 + \frac{1}{4} \frac{(\mathbf{k} - \mathbf{k}')^2}{k_F^2} H'(\cos \theta_L) S_{12} \boldsymbol{\tau}_1 \cdot \boldsymbol{\tau}_2. \quad (6.35)$$

On the Fermi surface the tensor invariants don't vanish due to the Pauli principle. In the case of nuclear matter they have been studied in refs. [32, 42, 48], and in ^{208}Pb for example in ref. [81].

Obviously π - and ρ -exchange supplemented by the tensor part in (2.10) of the second-order tensor are the dominant sources of H and H' . Fourier transforming the tensor parts of eq. (2.8) and (2.45) and applying the exchange operator given in (4.23) gives, for the pion

$$\left(\frac{q}{2k_F}\right)^2 H = \frac{1}{2} \frac{f^2}{m_\pi^2} \frac{(\mathbf{k} - \mathbf{k}')^2}{(\mathbf{k} - \mathbf{k}')^2 + m_\pi^2} N_0, \quad (6.36)$$

$$\left(\frac{q}{2k_F}\right)^2 H' = -\frac{1}{6} \frac{f^2}{m_\pi^2} \frac{(\mathbf{k} - \mathbf{k}')^2}{(\mathbf{k} - \mathbf{k}')^2 + m_\pi^2} N_0 \quad (6.37)$$

where $\mathbf{q} = \mathbf{k} - \mathbf{k}'$. For the ρ -meson we get

$$\left(\frac{q}{2k_F}\right)^2 H = -\frac{1}{2} \frac{f_\rho^2}{m_\rho^2} \frac{(\mathbf{k} - \mathbf{k}')^2}{(\mathbf{k} - \mathbf{k}')^2 + m_\rho^2} N_0 \quad (6.38)$$

and

$$\left(\frac{q}{2k_F}\right)^2 H' = +\frac{1}{6} \frac{f_\rho^2}{m_\rho^2} \frac{(\mathbf{k} - \mathbf{k}')^2}{(\mathbf{k} - \mathbf{k}')^2 + m_\rho^2} N_0. \quad (6.39)$$

The fact that we in eqs. (6.36) through (6.39) always get

$$H_l = -3H'_l \quad (6.40)$$

is due to the operator identity

$$-P_\sigma P_\tau S_{12} \boldsymbol{\tau}_1 \cdot \boldsymbol{\tau}_2 = -\frac{3}{2} S_{12} + \frac{1}{2} S_{12} \boldsymbol{\tau}_1 \cdot \boldsymbol{\tau}_2. \quad (6.41)$$

In results calculated from the Reid soft-core potential (see table 2 below), this ratio is rather ~ 2.6 for $l \leq 2$. For $l > 2$ the ratio 3 holds, see table 2 of ref. [42]. The second-order tensor, eq. (2.10), gives contributions with the same sign as the pion. The ratio here is, however, $2H_l = -3H'_l$, which explains the deviation from the ratio given in (6.40) above. Let us now compare the models of ref. [32] with the actual calculations based on the Reid soft-core potential in ref. [42]. We have to divide the results of ref. [32] by a factor of four in this comparison (see definitions of q following eq. (1.3) of ref. [32] and eq.

Table 2
Values of H_l and H'_l obtained by projection on Legendre polynomials as in eq. (4.12)

l	H_l , total ref. [31]	H_l , OPEP alone	H_l , “strong” ρ , ref. [21]	H'_l ref. [31]	H'_l OPEP alone	H'_l , “strong” ρ , ref. [21]
0	0.65	0.91	0.66	-0.255	-0.30	-0.22
1	0.975	1.12	1.09	-0.36	-0.37	-0.365
2	0.83	0.91	0.925	-0.315	-0.30	-0.31

(1.4) of ref. [42]). The results are presented in table 2. Observe that $k_F = 1.36 \text{ fm}^{-1}$ was used in ref. [32] and $k_F = 1.35 \text{ fm}^{-1}$ in ref. [42]. In using the tensor interactions we do not need to introduce short-range correlations because they chiefly act between relative S-states and D-states, and the centrifugal barrier in the latter keeps the nucleons somewhat apart.

We see that by far the most important source for the tensor invariants is the one-pion-exchange tensor. In higher multipoles, not displayed here, other sources rapidly become completely negligible. However, the ρ -meson gives nevertheless an important contribution to H_0 . In appendix B we give some stability criteria when we take into account the tensor invariants. The $T = 0, J = 0$ nuclear matter state, which for stability must satisfy these criteria, is close to an instability even with $H_0 = 0.65$ [42], which corresponds to a strong ρ -coupling. The corresponding 0^- isoscalar state in ^{208}Pb has a high unperturbed energy due to the spin-orbit splitting. The counterpart of $J = 1, T = 0$ coupled nuclear matter state that has to satisfy stability criteria is, however, seen. In ^{208}Pb there is a low-lying isoscalar 1^+ state at 5.51 MeV very close to its unperturbed position. In ref. [81] the behavior of this state as a function of the ρ -meson coupling strength was studied. With a coupling strength of half of that corresponding to Höhler and Pietarinen’s [30] results this state went down to zero energy. This is another result that speaks in favor of a strong ρ -coupling. The calculation was done in such a way that it was only the tensor force that could cause the collapse mentioned above (and chiefly the exchange terms which entered). So the tensor invariants enter into the low-lying isoscalar states but, due to the strong ρ -exchange potential, the net effects of the tensor invariants aren’t large.

Our discussion above concerned low-lying states where the particle-hole momenta involved are small compared to k_F . In the pion-condensation game we have large particle-hole momenta $\sim k_F$. Then the direct tensor of the OPEP tensor brings down the $M_S = 0, S = 1, T = 1$ wave [82], possibly producing a pion condensate well above the saturation density [83] ρ_0 of nuclear matter. Only if one in a calculation forgets the repulsion coming from the ρ -tensor and from G'_0 critical densities around and below ρ_0 can be obtained. In fact, with inclusion of the induced interaction, the pion condensation may not occur at all [91].

6.5. The giant Gamow-Teller resonance

The most important event in nuclear structure physics in the past few years has been the “putting into place” of the giant Gamow-Teller resonance (GTR), the spin-isospin sound. This allows us to give a much better determination of the $\sigma_1 \cdot \sigma_2 \tau_1 \cdot \tau_2$ interactions, not only at low energies, but also to study their energy-dependence, as discussed in the last section and in Brown, Speth and Wambach [77].

The position of the GTR determines G'_0 to be [78]

$$G'_0 = 1.6-1.7. \quad (6.42)$$

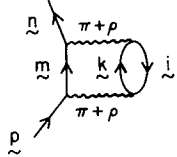


Fig. 31. Second-order effects of the $\pi + \rho$ tensor interaction, as they enter into the (p, n) reaction.

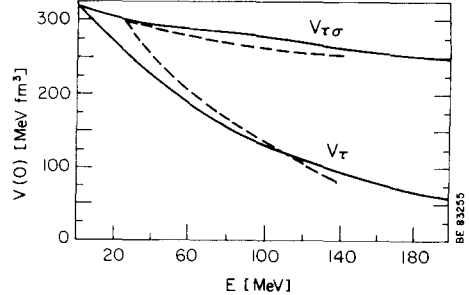


Fig. 32. Dependence of the isovector coupling potentials $V_\tau(q = 0)$ and $V_{\tau\sigma}(q = 0)$ on the energy of the incoming particle. Dashed lines give the Love-Petrovich [84] interactions.

This large value precludes pion condensation and critical opalescence at nuclear densities.

We now discuss the energy-dependences of the $\tau_1 \cdot \tau_2$ and $\sigma_1 \cdot \sigma_2 \tau_1 \cdot \tau_2$ interactions. As noted earlier, Brown, Speth and Wambach [77] calculated effects of the second-order tensor interaction. These are as is shown in fig. 31. The expression for this matrix element is

$$V_\tau(\epsilon_p) = \sum_{k, m, i} \frac{|(km| V_{\tau\pi} + V_{\tau\rho}| ip)|^2}{\epsilon_p - [\epsilon_m + \epsilon_k - \epsilon_i]} \quad (6.43)$$

where we have made the approximation that $k_n = k_p$, which is approximately true for forward scattering. The ϵ_i , which refer to hole states, are small, and are neglected here.

For $\epsilon_p \approx 0$, $V_\tau(\epsilon_p)$ is large in magnitude and attractive. In closure approximation it is (2.10). In section 6.3 we showed that it is large enough to give essentially almost all of the nuclear symmetry energy.

The energy denominator in $V_\tau(\epsilon_p)$ consists of the difference of the initial energy ϵ_p and the energy of the two particles in intermediate states $\epsilon_m + \epsilon_k$. Note that no gap is introduced here; we are essentially making a model-space calculation. As soon as the energy ϵ_p becomes comparable with typical $\epsilon_m + \epsilon_k$, the sum over intermediate energies will develop appreciable positive contributions, tending to cancel the negative ones which give the $\epsilon_p \approx 0$ value of V_τ i.e., the F' . The curve that emerges from the Brown et al. [77] calculation is shown in fig. 32, and compared with the t -matrix calculation of Love and Petrovich [84]. Figure 32 shows clearly that the typical intermediate state energy $\epsilon_m + \epsilon_k$ is ~ 200 MeV, not ~ 400 MeV as in the reference spectrum method. Below we reproduce results from ref. [77].

The effective interaction $V_{\tau\sigma}$ shown here is the one to be used in the combined nucleon-isobar space. When we use Fermi liquid parameters, we work in the purely nucleon space, and must then apply for the $\tau\sigma$ interactions a screening correction γ . Taking [78] $\gamma = 0.72$ and converting* the 20 MeV results in table 3 to Fermi liquid parameters, we have the following contributions, assuming them all to correspond to Landau $l = 0$:

$$\begin{array}{ll} \text{to } F'_0 \text{ from } V_\tau: 1.78m^*/m & \text{to } G'_0 \text{ from } V_{\tau\sigma}: 1.41m^*/m \\ U_\tau: 1.39m^*/m & U_{\tau\sigma}: 0.54m^*/m \\ W_\tau: 0.40m^*/m & W_{\tau\sigma}: 0.87m^*/m. \end{array} \quad (6.44)$$

* This conversion amounts to multiplying the above V , W and U by $2k_F m^*/\pi^2$. We use $k_F = 1.35 \text{ fm}^{-1}$.

Table 3

The contributions U_τ and $U_{\pi\pi}$ (second-order tensor) and W_τ and $W_{\pi\pi}$ (one-pion- and one ρ -exchange potential) to the isovector coupling potentials V_τ and $V_{\pi\pi}$ in MeV fm³. The calculation has been performed for two different proton energies (20 and 130 MeV)

Proton energy	V_τ	$V_{\pi\pi}$	U_τ	$U_{\pi\pi}$	W_τ	$W_{\pi\pi}$
20 MeV	270	300	210	115	60	185
130 MeV	100	265	90	60	10	205

The relatively large contributions W_τ and $W_{\pi\pi}$ arise because the ρ -exchange potential contributes strongly to the Landau angle $l = 0$ parameters. A rather schematic treatment of short-range correlations was used in ref. [77], so these numbers may not be very accurate.

The energy-dependence of the ratio

$$R(\epsilon_p) = \gamma V_{\pi\pi}/V_\tau \quad (6.45)$$

can now be compared directly with experiment [85]. This comparison is shown in fig. 33.

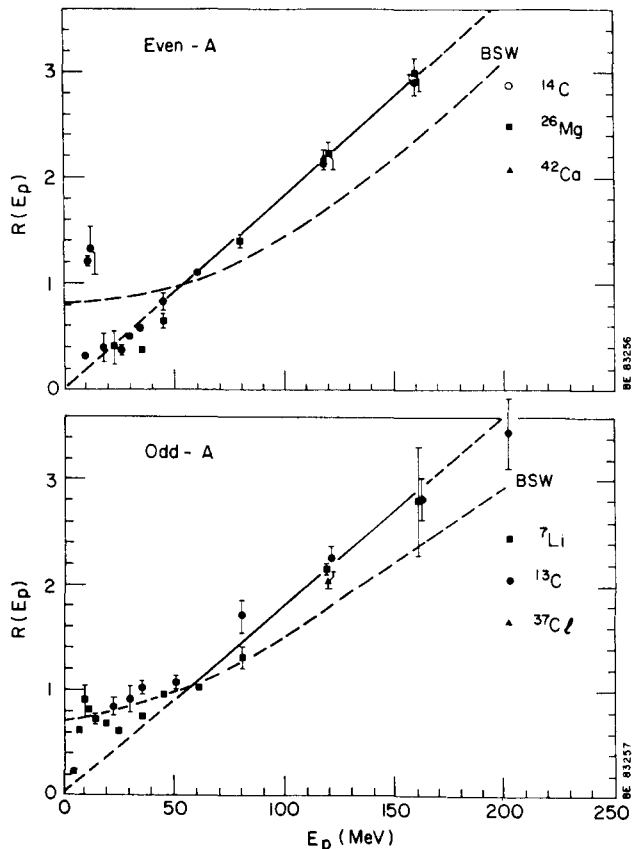


Fig. 33. Comparison of experimental and theoretical values of the ratio $R(\epsilon_p) = \gamma V_{\pi\pi}/V_\tau$ of spin-isospin to isospin interactions. The experimental points are taken from Taddeucci et al. [85]. The theoretical curve is from ref. [77].

It is clear from this figure that the model of Brown et al. [77] has the main features of this energy-dependence right. Note, however, that the second-order tensor terms and contributions from π - and ρ -exchange have pretty much the same energy-dependence, because only the exchange potentials enter in the latter case. The total G'_0 , after multiplying by the screening factor $\gamma = 0.72$, is $G'_0 = 1.41 m^*/m$, whereas the G'_0 necessary to push the giant Gamow–Teller resonance up to the correct energy is [78] $G'_0 = 1.6$ or 1.7 (see eq. (6.42)).

Goodman et al. [79] have deduced from an analysis of the experiments volume integrals of the $V_{\pi\sigma}$ interaction for 130 MeV incident proton energy, finding

$$\int dt V_{\pi\sigma} \cong 168 \text{ MeV fm}^3. \quad (6.46)$$

This is to be compared with $\gamma V_{\pi\sigma} = 191 \text{ MeV fm}^3$ from table 3, where γ is taken [78] as 0.72. This should be considered to be reasonable agreement, considering the roughness of the model [77].

It is amusing that the energy-dependence in V_τ encountered here has the same origin as that of the effective mass discussed in section 6.2. In both cases, the dependence comes from the energy moving up into a principal value integral. Of course, the scales are quite different, determined, in the case of V_τ , by typical energies involved in excitations by the tensor force, and in case of the effective mass, by energies of surface excitations.

In both cases, the energy-dependence is useful for diagnostics. In the case of m^*/m , the rapid energy-dependence can only come from coupling to the low-lying surface vibrations. In the case of V_τ , the energy-dependence tells us about typical intermediate-state energies, and comes down squarely in favor of model-space calculations.

It is not strange that V_τ should come almost completely from π - and ρ -exchange, especially from the second-order tensor interaction, but also from the exchange terms of the lowest-order interaction. These are the only mesons coupled to the nucleon by isospin; the σ - and ω -mesons are isoscalar. Exchange terms from the σ - and ω -interactions do contribute, but there is a large cancellation between them, the former predominating slightly.

6.6. Summary of Fermi liquid parameters

By a mixture of theoretical arguments and empirical data, we arrive at the following Fermi liquid parameters:

$$\begin{aligned} -0.3 &< F_0 < 0 \\ -0.75 &< F_1 < 0 \\ 0.9 &< F'_0 < 1.5 \\ G_0 &\text{ is small} \\ G'_0 &= 1.6–1.7. \end{aligned} \quad (6.47)$$

We now consider the consistency of these parameters with the sum rules (A.14) and (A.16).

In the sum rules, all Fermi liquid parameters F_l , etc., enter, whereas we have truncated with $l = 0$ or $l = 1$. This truncation may not be justified in the case of the F 's. In particular, F_2 may be appreciable and negative. As discussed earlier, the problem is in getting negative contributions to (A.14), so that from this point of view, the lower values of F_0 and F_1 are preferred. The lower value of F_0 also seems to be necessary to bring the giant monopole resonance in ^{208}Pb down to its empirical value.

As noted at the end of section 6.3, F'_1 is positive, and smaller than F'_0 . The interactions in the $\sigma_1 \cdot \sigma_2$ channel are altogether weak and for most purposes we can neglect G_0 . If G_0 has to be taken into account that's the place where one might have to take the tensor HS_{12} also into account.

The interaction in the $\sigma_1 \cdot \sigma_2 \tau_1 \cdot \tau_2$ channel is best known, $G'_0 \sim 1.6\text{--}1.7$. Most of G'_0 comes from short-range correlations in the pion exchange or from ρ -meson exchange. These are of short range in configuration space, so should give a local interaction. Thus G'_1 from these should be small. From table 3 of the last section, we see that an appreciable contribution to the $\sigma_1 \cdot \sigma_2 \tau_1 \cdot \tau_2$ interaction comes from the second-order tensor interaction. This is not, however, of longer range than the ρ -exchange potential once short-range correlations have been included in the latter; these cut out the interior part of the ρ -exchange potential, leaving the main contribution from distances $r \approx 0.7\text{--}0.8$ fm. Altogether, one would not expect G'_1 to be large.

The sum rule (A.16) is then particularly instructive. With $G'_0 = 1.6$, the right-hand side is equal to -1.85 . With our minimal values of F_0 and F_1 , eq. (6.47), the left-hand side is -1.43 . The two sides can be brought into agreement with $F_2 = -0.39$, not particularly large. This illustrates, however, our difficulty in getting enough attraction in the F -channel to satisfy the sum rules. In order to reach this agreement, we have had not only to introduce a negative F_2 , but have had to give up any enhancement of the effective mass at the Fermi surface from coupling to collective excitations in nuclear matter.

6.7. Concluding discussion

We would like to conclude by a discussion of various developments which are currently in progress and remaining problems. A recurrent difficulty has been to theoretically obtain an isospin-dependent interaction, F'_0 for the infinite system, which is strong enough to push the giant dipole state up to its empirical position. As mentioned at several places in this article (see, e.g., the end of section 4.1) just this Fermi liquid parameter is substantially increased in going over from a Brueckner calculation with a gap to a model-space one. Our arguments in section 6.5 that V_τ comes chiefly from second-order contributions from π - and ρ -exchange indicate that it will be particularly sensitive to how energy denominators in the intermediate states are handled. This is largely confirmed by recent work of Z.Y. Ma and T.T.S. Kuo [51] who find a substantial increase in the binding energy of nuclear matter in going over to a model-space calculation. Bäckman and Sjöberg [86] have corrected Sjöberg's original calculations [52, 53], and find that the symmetry energy for the Reid soft-core potential increases from 22 to 32 MeV in going over to a model-space calculation. Bethe et al. [76] find 32 MeV to be the empirical value.

Models that use the energy-dependence of the effective mass to raise the energies of giant resonances which are pushed up in energy by repulsive interactions (see, e.g., ref. [87]) have not fared so well [88]. The work of Mahaux and Sommermann indicates that little energy is to be gained by this mechanism; indeed, in their schematic model, some energy is even lost. Thus, if the increased F'_0 from the model-space calculation is insufficient to push up the giant dipole state, then there is still a difficulty.

The induced interaction has recently been receiving renewed attention [89]. The F_0 one obtains from a reaction matrix is sufficiently negative ($F_0 < -1$) to violate the stability criteria, see appendix B. The Brueckner expression for the binding energy has a minimum in symmetrical nuclear matter. For the Reid soft-core potential this occurs around a Fermi momentum ~ 1.35 fm $^{-1}$. Consequently the compressibility is positive. It is the rearrangement terms in fig. 10 that restore stability in Brueckner's theory and the renormalization at the quasiparticle pole, fig. 10(iii)a, is most crucial. See further ref. [33], where the results from a calculation from diagrams in fig. 10 are compared with the result obtained by differentiating the energy versus density curve. However, the Brueckner F_0 is too attractive and the

induced interaction is useful in bringing F_0 into the range of values found in the last section. This role of the induced interaction was implicit in the work of Sjöberg [52, 53]. Looking at eq. (5.3), one sees that the largest term, by far, in F_i is the last one involving $G'_0{}^2$. The authors of ref. [81] point out, as did Oset and Palanques-Mestre [90], that there is a rapid q -dependence of the interaction in this channel due to the fact that the pion exchange contributes here. This q -dependence is no surprise, since it was utilized as a mechanism to obtain a pion condensate in the past. See various contributions in “Mesons in Nuclei” mentioned in refs. [19, 22]. Thus, the Landau expansion used in obtaining (5.3) does not converge rapidly. Rather, the explicit π - and ρ -exchange interactions discussed in chapter 2 should be used. If the tensor degrees of freedom are kept in the calculation one sees also more directly the tendency of cancellation between the π - and ρ -contributions [80]. The induced interaction, with Δ -hole included, contributes ~ 0.2 to G'_0 making it more repulsive, in conformity with the results of Dickhoff et al. [91].

Important contributions from the induced interaction to the isobar-hole transition interaction have been noted by Nakayama et al. [92] who point out that the factor of 4 multiplying F_i , F'_i , G_i , G'_i is changed to a factor of 2. Thus, the contributions to G'_0 would be twice as large as in ref. [89].

From the foregoing it seems that the induced interaction has many beneficial effects. As is usual, not all aspects can be bright. Looking at eq. (5.3) one can see that increasing G'_0 in magnitude will tend to bring down F'_i , since F'_i involves $-\frac{3}{4}G'_0{}^2 U(q, 0)/(1 + G'_0 U(q, 0))$. Making F'_i smaller makes it harder to get the giant dipole state sufficiently high in energy. Putting in the momentum dependence of G'_0 will decrease this contribution to F'_i greatly, however.

We have some insight into how to cure this difficulty from the work of Carneiro and Pethick [93]. In working with soft spin modes in liquid ^3He , corresponding to negative Fermi liquid parameters, they find that the two-phonon (two-paramagnon in their case) exchange provides a repulsion which more than cancels the attractive induced interaction. In fact, their arguments apply directly to the $-\frac{1}{4}F'_0{}^2 U(q, 0)/(1 + F'_0 U(q, 0))$ occurring in F'_i and to the $-\frac{1}{4}G'_0{}^2 U(q, 0)/(1 + G'_0 U(q, 0))$ in G_i . (Since they work with liquid ^3He , their work applies either to the $\tau_1 \cdot \tau_2$ or to the $\sigma_1 \cdot \sigma_2$ component of the interaction, but not to the $\sigma_1 \cdot \sigma_2 \tau_1 \cdot \tau_2$ one.) The conclusion of Carneiro and Pethick is that for small q the two-phonon exchange gives four times the induced interaction and of opposite sign*.

In the small q limit, the two-phonon contribution to density modes is zero. The way in which this comes about is the following: In the two-phonon exchange process in fig. 34, each line a or b can be either a particle or a hole. Consider a. When a is a hole, the coupling of the phonon at vertex Γ has opposite sign to the case where a is a particle.

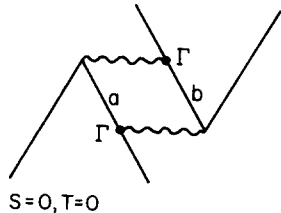


Fig. 34. The two-phonon contribution in the case of density modes. The wavy line represents a phonon; i.e., a particle-hole excitation.

* As actually presented in the paper of Carneiro and Pethick, the net contribution from soft spin-dependent modes is zero. The counting is as follows: In units in which the induced interaction is -1 , the contribution from soft phonon emission and absorption to the quasiparticle self-energy is -3 , the two-phonon contribution, $+4$.

In the case of an $S = 1(T = 0)$ excitation, the same argument holds for the $m_s = 0$ mode, where m_s is the spin projection. But in the case of $m_s = \pm 1$ modes, an additional sign comes in for the exchange of $S = 1$ modes in the crossed channel.* Hence the factor 4 remarked earlier, 2 for each $m_s = +1$ and $m_s = -1$. We believe that a similar counting will produce a factor of +8 for the exchange of two spin-isospin phonons in the case of spin-isospin direct channel excitations.

From the above (highly preliminary) discussion of the effects of two-phonon exchange, it seems likely that the exchange of two spin-isospin dependent excitations will produce repulsions in the $\sigma_1 \cdot \sigma_2, \tau_1 \cdot \tau_2$, and, especially, in the $\sigma_1 \cdot \sigma_2 \tau_1 \cdot \tau_2$ channels. It is clear from the work of Carneiro and Pethick that inclusion of two-phonon exchange is necessary for consistency. The “hard” excitations being considered here may not be relatively as important as the soft excitations considered by them, however.

As mentioned earlier inclusion of Z-factors and, as in refs. [53, 42], an effective mass of $m^*/m \sim 0.75$ in nuclear matter produces too small values for F'_0 and G'_0 . The above-mentioned repulsive contributions are hence welcome. As long as one uses approximations that satisfy the Pauli principle sum rules (A.14) and (A.15) we will instead obtain attraction somewhere else.

The title of chapter 5 is “A theory of interacting quasiparticles and collective excitations”. It should by now be clear that what was outlined there was the beginning of a theory, but that much more needs to be done. We believe that we have established the importance of effects from exchange of collective excitations.

In addition to two-phonon exchange, the ω -dependence of the effective interaction will have to be better understood. Since we have found spin-isospin sound, i.e., $S = 1, T = 1$ excitations, to be particularly important in the induced interaction, we consider their effect in the crossed channel on the direct channel $S = 1, T = 1$ excitation, see fig. 35. The complete expression for the process, fig. 35, is complicated, but consider the exchange of the collective excitation in the crossed channel in the following way: The matrix elements for coupling to the hole and particle each involve G'_0 , hence the

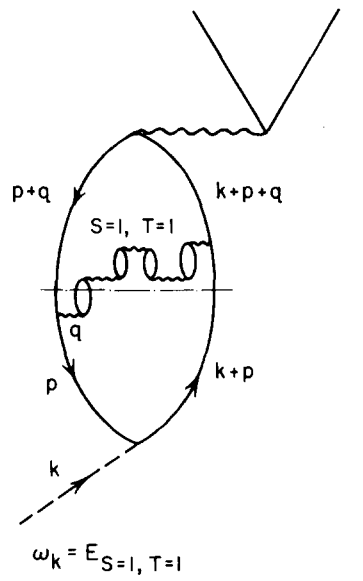


Fig. 35. Effective interaction in the spin-isospin sound channel from the exchange of spin-isospin sound in the crossed channel.

* We use here the terminology of field theory.

G'_0 in the numerator of the induced interaction. There will be an energy denominator for the process shown, evaluated at the position of the dash-dot line, fig. 35, of

$$\text{Den.} = \omega_k - [\varepsilon_{k+p} - \varepsilon_{p+q} + E_q]$$

where $\varepsilon_{k+p} - \varepsilon_{p+q}$ is the quasiparticle energy minus the quasi-hole energy, necessarily positive, and E_q is the energy of the exchanged collective excitation.

Now the prescription we have used to date is to evaluate the induced interaction at $\omega_k = 0$. We kept both particle and hole in the Fermi surface, so $\varepsilon_{k+q} - \varepsilon_{p+q}$ cancelled out. Thus our energy denominator was, effectively, E_q . After inclusion of the process in which the collective excitation is first emitted by the quasiparticle and absorbed by the quasi-hole, and the phase space integrations, we would recover the induced interaction. However, when ω_k is the energy of the collective excitation, ω_k is larger than a typical particle-hole energy $\varepsilon_{k+p} - \varepsilon_{p+q}$ and comparable with E_q , so a correct calculation of this interaction at the right ω_k would have $\varepsilon_{k+q} - \varepsilon_{p+q}$, a typical particle-hole energy, as denominator rather than E_q . In the case E_q refers to the giant Gamow–Teller resonance, $E_q \cong 2(\varepsilon_{k+q} - \varepsilon_{p+q})$. Thus, the G'_0 would be roughly doubled.

As noted earlier, the question of ω -dependence has been found to be very important in the quasiparticle effective mass, both in liquid ^3He [73, 74] and in nuclei [68–72]. This involves its effect on the Landau parameter F_1 , i.e., $F_1 = F_1(\omega)$ and the dependence on ω is appreciable. It would be strange, if there were not large effects on other Landau parameters. However, these effects may cancel out to a large extent in combinations of Landau parameters describing physical observables such as the susceptibility or compression modulus [93] and that might explain why they have not been discovered to date.

In chapter 2 the connection between (old-fashioned?) meson theory for the nucleon–nucleon interaction and the chiral σ -model was touched upon. Jackson et al. [34] have shown within such a model that many-body forces may eliminate the discrepancy between calculated and empirical values of the binding energy and saturation density of nuclear matter. In terms of a meson picture this is accomplished by a density-dependent enhancement of the attractive contribution from the σ -meson to the binding energy. Playing with the exchange operators of chapter 4 it is easy to see that such a scalar will give repulsive contributions to F'_0 , G_0 and G'_0 . Indeed, Sjöberg [94] has found within a model-space calculation that the symmetry energy, on the level of the Brueckner’s reaction matrix, is increased by several MeV with $m^* = m$ in the density of states.

We seem to have ended by pointing out more problems than we have solved; this may be in the nature of considerations of strongly interacting systems.

We would like to thank John Durso, Andy Jackson, Claude Mahaux, Josef Speth and Jocham Wambach for many helpful discussions and useful criticism.

Appendix A. Pauli principle sum rules

In section 4.1 we presented the Pauli principle constraints

$$\begin{aligned} F(0, 0) + F'(0, 0) + G(0, 0) + G'(0, 0) &= 0, \\ F(0, 0) - 3F'(0, 0) - 3G(0, 0) + 9G'(0, 0) &= 0, \end{aligned} \tag{A.1}$$

which the particle-hole interaction satisfies when approximated by a reaction matrix. Let us recast these constraints into a more familiar form. Assume we calculate Landau's

$$\mathcal{F} = F(\mathbf{k}, \mathbf{k}') + F'(\mathbf{k}, \mathbf{k}') \boldsymbol{\tau}_1 \cdot \boldsymbol{\tau}_2 + G(\mathbf{k}, \mathbf{k}') \boldsymbol{\sigma}_1 \cdot \boldsymbol{\sigma}_2 + G'(\mathbf{k}, \mathbf{k}') \boldsymbol{\sigma}_1 \cdot \boldsymbol{\sigma}_2 \boldsymbol{\tau}_1 \cdot \boldsymbol{\tau}_2 \quad (\text{A.2})$$

for a reaction matrix. The momenta \mathbf{k} and \mathbf{k}' are on the Fermi surface. We make the standard expansions on Legendre polynomials of F , F' , G and G' ,

$$F(\mathbf{k}, \mathbf{k}') = \sum_l F_l P_l(\cos \theta_L) \quad (\text{A.3})$$

and correspondingly for the other functions. For equal momenta all $P_l(1) = 1$ and we have

$$\mathcal{F}(\mathbf{k}, \mathbf{k}) = \sum_l (F_l + F'_l \boldsymbol{\tau}_1 \cdot \boldsymbol{\tau}_2 + G_l \boldsymbol{\sigma}_1 \cdot \boldsymbol{\sigma}_2 + G'_l \boldsymbol{\sigma}_1 \cdot \boldsymbol{\sigma}_2 \boldsymbol{\tau}_1 \cdot \boldsymbol{\tau}_2). \quad (\text{A.4})$$

Now assume the particles have the same spin and isospin. Since the reaction matrix is antisymmetrical in the particles we get

$$\sum_l (F_l + F'_l + G_l + G'_l) = 0 \quad (\text{A.5.1})$$

expressing the fact that the triplet odd wave functions vanish in this special case. However, also the singlet odd wave functions vanish in the limit of equal momenta. In this case the expectation values of $\boldsymbol{\sigma}_1 \cdot \boldsymbol{\sigma}_2$ and $\boldsymbol{\tau}_1 \cdot \boldsymbol{\tau}_2$ is -3 . We get

$$\sum_l (F_l - 3F'_l - 3G_l + 9G'_l) = 0. \quad (\text{A.5.2})$$

We emphasize that (A.5.1) and (A.5.2) are correct only if we approximate the particle-hole interaction by a reaction matrix or a potential. Antisymmetrical Skyrme interactions, for example, satisfy (A.5.1) and (A.5.2). As pointed out in chapter 5 a reaction-matrix alone is in many cases not a satisfactory approximation. Let us now proceed to derive the Pauli principle sum rules for the general case. Then it is the forward scattering amplitude of eq. (5.1) that is antisymmetric in the particles. Let us write

$$A = B + B' \boldsymbol{\tau}_1 \cdot \boldsymbol{\tau}_2 + C \boldsymbol{\sigma}_1 \cdot \boldsymbol{\sigma}_2 + C' \boldsymbol{\sigma}_1 \cdot \boldsymbol{\sigma}_2 \boldsymbol{\tau}_1 \cdot \boldsymbol{\tau}_2, \quad (\text{A.6})$$

where

$$B = \sum_l \frac{F_l P_l(\mathbf{k} \cdot \mathbf{k}')}{1 + F_l/(2l+1)}, \quad (\text{A.7})$$

and corresponding expressions for B' , C and C' . Let

$$P = P_{\mathbf{k}_1 \leftrightarrow \mathbf{k}'_2} P_\sigma P_\tau \quad (\text{A.8})$$

be an exchange operator. Here

$$P_\sigma = \frac{1}{2}(1 + \boldsymbol{\sigma}_1 \cdot \boldsymbol{\sigma}_2), \quad P_\tau = \frac{1}{2}(1 + \boldsymbol{\tau}_1 \cdot \boldsymbol{\tau}_2), \quad (\text{A.9})$$

and $P_{\mathbf{k} \leftrightarrow \mathbf{k}'}$ changes the momenta of, say, the outgoing particles. The antisymmetry of A is then expressed by

$$PA = -A. \quad (\text{A.10})$$

Now performing the operations involved in (A.10), using the operator identities as

$$(\boldsymbol{\sigma}_1 \cdot \boldsymbol{\sigma}_2)^2 = 3 - 2 \boldsymbol{\sigma}_1 \cdot \boldsymbol{\sigma}_2, \quad (\boldsymbol{\tau}_1 \cdot \boldsymbol{\tau}_2)^2 = 3 - 2 \boldsymbol{\tau}_1 \cdot \boldsymbol{\tau}_2 \quad (\text{A.11})$$

one obtains for $\mathbf{k} = \mathbf{k}'$ the equations

$$\begin{aligned} 5B + 3B' + 3C + 9C' &= 0 \\ B + 3B' + 3C - 3C' &= 0 \\ B + 3B' + 3C - 3C' &= 0 \\ B - B' - C + 5C' &= 0. \end{aligned} \quad (\text{A.12})$$

We see that the second and third equation are the same. Hence, we have

$$\begin{aligned} \text{I} \quad 5B + 3B' + 3C' + 9C' &= 0 \\ \text{II} \quad B + 3B' + 3C - 3C' &= 0 \\ \text{III} \quad B - B' - C + 5C' &= 0. \end{aligned} \quad (\text{A.13})$$

There is one further linear dependence. It is easily seen that, e.g., $+3 \times \text{III} + 2 \times \text{II}$ gives us I. Hence we have at most two sum rules. By adding I and II and inserting the expansions (A.7) with $\mathbf{k} = \mathbf{k}'$ we get back (5.2),

$$\sum_l \left(\frac{F_l}{1 + F_l/(2l+1)} + \frac{F'_l}{1 + F'_l/(2l+1)} + \frac{G_l}{1 + G_l/(2l+1)} + \frac{G'_l}{1 + G'_l/(2l+1)} \right) = 0. \quad (\text{A.14})$$

Now, by forming $\frac{1}{2} \times \text{I} - \frac{3}{2} \times \text{II}$ we obtain the second sum rule obtained by Friman and Dhar [48],

$$\sum_l \left(\frac{F_l}{1 + F_l/(2l+1)} - \frac{3F'_l}{1 + F'_l/(2l+1)} - \frac{3G_l}{1 + G_l/(2l+1)} + \frac{9G'_l}{1 + G'_l/(2l+1)} \right) = 0 \quad (\text{A.15})$$

where we have used (A.7) with $\mathbf{k} = \mathbf{k}'$. That we prefer (A.14) and (A.15) as sum rules instead of some linear combinations of them has to do with the appealing interpretation of singlet odd and triplet odd wave functions vanishing* for $\mathbf{k} = \mathbf{k}'$. See our discussion above for a potential. There are other cases with several sum rules. For example, in spin-polarized liquid ${}^3\text{He}$ the different spin projections of the

* In a two-body collision, $\mathbf{k} = \mathbf{k}'$ means that when one transforms to the center-of-mass system, the relative momentum is zero; then, clearly, P-wave scattering is zero.

forward scattering amplitude in triplet spin states are not the same. However, they all vanish for $\mathbf{k} = \mathbf{k}'$ leading to several sum rules [95].

In appendix B we are going to have a look at how the stability criteria are modified when we take into account the tensor invariants. At present we remember that the isovector tensor invariants obviously are not very important. Hence we can from (A.14) and (A.15) form the approximate constraint

$$\sum_l \frac{F_l}{1 + F_l/(2l+1)} = -3 \sum_l \frac{G'_l}{1 + G'_l/(2l+1)}. \quad (\text{A.16})$$

Now assume that $G'_0 = 1.35$, which may be too small and that $G'_l = 0$ for $l > 0$. The right-hand side of (A.16) then equals -1.72 . It is very hard to see how (A.16) could be satisfied with an effective mass equaling the free mass. We take this as an indication that the effective mass in nuclear matter is, say, $0.8 m$ and that the effective mass in nuclei is enhanced to m by coupling to surface vibrations as mentioned earlier. If the nuclear matter m^* comes out to be about the free mass the possibilities are either that some $G'_l < 0$ for $l > 0$ or some $F_l < 0$ for $l \geq 2$ or both. We gave arguments earlier that G'_l , for $l > 0$, should be small, however.

Friman and Dhar have derived the sum rules, that correspond to (A.14) and (A.15), including the tensor components [48].

Appendix B. Stability criteria

We shall first have a look at what a so-called normal Fermi liquid is. Let us consider a noninteracting homogeneous gas of fermions in a large box. The single-particle wave functions are plane waves, since the system has translational invariance. The eigenstates of the system are antisymmetric combinations of those plane waves, each characterized by its momentum k . An eigenstate of the system is defined by enumerating which plane waves are occupied. This is done by means of a distribution function $n(k)$. The ground state of the system corresponds to an isotropic distribution function $n_0(k)$ such that

$$\begin{aligned} n_0(k) &= 1, & \text{for } k \leq k_F, \\ n_0(k) &= 0, & \text{for } k > k_F, \end{aligned} \quad (\text{B.1})$$

where k_F is the Fermi momentum. In symmetric nuclear matter we furthermore have four degenerate spin and isospin states corresponding to a momentum k . The density ρ is given by

$$\rho = 2k_F^2/3\pi^2. \quad (\text{B.2})$$

Landau's basic assumption was that an invariant classification of states in the system remains when the interaction is adiabatically switched on. In the case of symmetric nuclear matter this means that in the interacting system the single-particle wave functions remain the plane waves mentioned above; the distribution function of quasiparticles in the interacting ground state is given by (B.1) and the density by (B.2). If a system obeys Landau's assumption, the system is said to be a normal Fermi liquid.

Now, in a normal Fermi liquid one has a spherical Fermi surface with the distribution function given

in eq. (B.1). For the state to be a ground state the free energy

$$A = E - \mu N \quad (\text{B.3})$$

has to have a minimum for a spherical Fermi surface. Let us define a direction in momentum space by its polar angles θ and φ and let us displace the Fermi surface in this direction by [96]*

$$u = \sum_{lm} u_{lm} y_{lm}(\theta, \varphi), \quad (\text{B.4})$$

where u is infinitesimal and $y_{lm}(\theta, \varphi)$ are spherical harmonics in conventional notations. According to (3.6) the resulting variation in the free energy is given by

$$\begin{aligned} \delta A = & \frac{1}{(2\pi)^3} \sum_{\sigma\tau} \int d\Omega \int_{k_F}^{k_F+u} (\varepsilon_k - \mu) k^2 dk \\ & + \frac{1}{2} \frac{1}{(2\pi)^6} \sum_{\substack{\sigma_1\sigma_2 \\ \tau_1\tau_2}} \int \int d\Omega_1 d\Omega_2 \int_{k_F}^{k_F+u} k_1^2 dk_1 \int_{k_F}^{k_F+u} k_2^2 dk_2 f(k_1, k_2), \end{aligned} \quad (\text{B.5})$$

in obvious notation. The integrations over momenta give

$$\delta A = \frac{k_F^2}{2 \cdot (2\pi)^3 m^*} \sum_{\sigma\tau} \int d\Omega u^2(\theta, \varphi) + \frac{1}{2} \frac{k_F^4}{(2\pi)^6} \sum_{\substack{\sigma_1\sigma_2 \\ \tau_1\tau_2}} \int \int d\Omega_1 d\Omega_2 u(\theta_1, \varphi_1) u(\theta_2, \varphi_2) f(\xi), \quad (\text{B.6})$$

where ξ is the angle between (θ_1, φ_1) and (θ_2, φ_2) . According to (4.12) we have

$$f = \sum_l f_l P_l(\cos \xi). \quad (\text{B.7})$$

Inserting (B.7) and (B.4) into (B.6) and using the properties of spherical harmonics and Legendre functions gives

$$\delta A = \frac{k_F^3}{(2\pi)^3 m^*} \frac{2}{l_m} \sum_{lm} |u_{lm}|^2 \left(1 + \frac{F_l}{2l+1} \right), \quad (\text{B.8})$$

where

$$F_l = (2k_F m^*/\pi^2) f_l = N_0 f_l. \quad (\text{B.9})$$

* We comment on the separation of Fermi surfaces of spins and isospins later on. We suppress these quantum numbers for the moment.

In the derivation of (B.8) we have demanded the reality condition

$$u_{lm}^* = (-1)^m u_{l-m}. \quad (\text{B.10})$$

Now, for δA to be always positive, it is necessary that all of the following conditions are satisfied:

$$1 + F_l/(2l+1) > 0 \quad (\text{B.11})$$

or

$$F_l > -(2l+1). \quad (\text{B.12})$$

The condition (B.11) is no surprise. It assures that there is no pole in the forward scattering amplitude, eq. (5.1). Obviously, the 1's in (B.11) represent the relative increase in kinetic energy when the Fermi surface is deformed by (B.4), whereas the second term gives the change in potential energy.

Above we derived the stability criteria for the $S = 0, T = 0$ particle-hole channel. The derivations in other channels go in much the same way. Again defining a direction in momentum space by its polar angles θ and φ and displacing the surface in this direction by

$$u\tau_z, \mathbf{u} \cdot \boldsymbol{\sigma} \text{ and } \mathbf{u} \cdot \boldsymbol{\sigma} \tau_z, \quad (\text{B.13})$$

gives criteria for the stability of the spherical Fermi surface in the $S = 0, T = 1; S = 1, T = 0$ and $S = 1, T = 1$ particle-hole channels respectively. In the absence of a tensor force we arrive at criteria identical to (B.11) for the F_l, G_l and G'_l . In the presence of a tensor force the $S = 1$ stability criteria are modified [42]. We will not go through the derivation in detail in this context. The interested reader is referred to ref. [42] for details.

Migdal dropped the tensor components using arguments based on the uncertainty principle (see pp. 238 and 253 in ref. [1]). Those arguments, however, apply only to the direct terms of a potential, whereas in the Landau limit the contributions to the tensor degrees of freedom come from the exchange terms [42].

The derivation of the stability criteria is straightforward. It is convenient to write

$$\mathbf{u} \cdot \boldsymbol{\sigma} = -u^-(\theta, \varphi) \sigma^+ - u^+(\sigma, \varphi) \sigma^- + u^z(\sigma, \varphi) \sigma^z = \sum_{\mu=-1}^{+1} (-1)^\mu u^\mu \sigma^{-\mu} \quad (\text{B.14})$$

where σ^+ and σ^- are spin raising and lowering operators, respectively. For each of the components $u^\mu(\theta, \varphi)$ of the infinitesimal distortions we make the expansion (B.4). The reality condition (B.10) is naturally generalized to

$$u_{lm}^{\mu*} = (-1)^{m-\mu} u_{l-m}^{-\mu}. \quad (\text{B.15})$$

Let us demonstrate some results for the $S = 1, T = 0$ part of the interaction,

$$G(\mathbf{k}_1, \mathbf{k}_2) \boldsymbol{\sigma}_1 \cdot \boldsymbol{\sigma}_2 + \frac{q^2}{k_F^2} H(\cos \theta_L) S_{12} \quad (\text{B.16})$$

where $\mathbf{q} = \mathbf{k}_1 - \mathbf{k}_2$. For a given particle-hole total angular momentum J there is only one 2×2 matrix with Landau l, l' values $J \pm 1$ to diagonalize. The first such matrix is for $J = 1$ and given by

$$\begin{aligned}\langle 01|A|01\rangle &= 1 + G_0, \\ \langle 21|A|01\rangle = \langle 01|A|21\rangle &= -\sqrt{2}(H_0 - \frac{2}{3}H_1 + \frac{1}{3}H_2), \\ \langle 21|A|21\rangle &= 1 + \frac{1}{3}G_2 - \frac{7}{15}H_1 + \frac{2}{5}H_2 - \frac{3}{35}H_3,\end{aligned}\tag{B.17}$$

where A is, up to a positive factor, the change in free energy due to the distortion (B.14). Hence, in (B.17) the criterion for stability is that both eigenvalues be positive.

In the case $J = l = l'$ there is no coupling as in the case $J = 0$ and $l = l' = 1$. The first two uncoupled eigenvalues give the stability criteria: $l = l' = 1, J = 0$

$$1 + \frac{1}{3}G_1 - \frac{10}{3}H_0 + \frac{4}{3}H_1 - \frac{2}{15}H_2 > 0\tag{B.18}$$

and for $l = l' = J = 1$

$$1 + \frac{1}{3}G_1 + \frac{5}{3}H_0 - \frac{2}{3}H_1 + \frac{1}{15}H_2 > 0.\tag{B.19}$$

Obviously if we switch off the tensor in (B.17), (B.18) and (B.19) we get back stability criteria of the form (B.11) for the G_l .

Now back to some physics. In symmetrical nuclear matter the most interesting state, from the point of view of stability, is the $J = 0$ state in (B.18) [31] as mentioned in section 6.4. As noted there, the corresponding 0^- state in ^{208}Pb has a high unperturbed energy due to the spin-orbit splitting. The counterpart of the $J = 1, T = 0$ nuclear matter state eq. (B.17) is, however, seen. In ref. [75] the low-lying isoscalar 1^+ state at 5.51 MeV in ^{208}Pb was studied. It was found that for a weak ρ -coupling (about half of that corresponding to Höhler and Pietarinen [30]) the state goes to zero energy, which speaks in favor of a strong ρ -coupling.

In passing, a few words on neutron star matter: In the past some investigations were carried out as to whether neutron matter might become ferromagnetic at some critical density. The answer seems to be no. It may, however, be worthwhile to note that the tensor interaction in (B.17) will push one state downwards and the other upwards in energy. So if there is a tendency toward ferromagnetism in neutron star matter there would presumably be at a lower density a phase transition due to a negative eigenvalue in (B.17).

We have in this appendix dealt with the stability of a spherical Fermi surface in the long-wavelength limit. Even if the criteria are satisfied that does not guarantee that there is not a finite-wavelength instability leading to another ground state. As an example of this possibility we mention a pion condensate at a critical momentum k_c . Although this does not occur in nuclei, we may well have a π^- -condensate in neutron stars (see some contributions in “Mesons in nuclei” mentioned in refs. [19, 22]).

References

- [1] A.B. Migdal, Theory of Finite Fermi Systems and Applications to Atomic Nuclei (Interscience, New York, 1957).
- [2] G.E. Brown and Mannque Rho, Phys. Lett. 82B (1979) 177;
G.E. Brown, Mannque Rho and V. Vento, Phys. Lett. 84B (1979) 383;
G.E. Brown, Mannque Rho and V. Vento, Phys. Lett. 97B (1980) 423.

- [3] G. 't Hooft, Nucl. Phys. B72 (1974) 461; B75 (1974) 461.
- [4] E. Witten, Proc. Workshop on Solitons in Nuclear and Particle Physics at the Lewes Center for Physics, June 1984 (World Scientific Publ. Co., Singapore).
- [5] E. Witten, Nucl. Phys. B160 (1979) 57.
- [6] T.H.R. Skyrme, Proc. Roy. Soc. A260 (1961) 127.
- [7] G. Adkins and C.R. Nappi, Phys. Lett. 137B (1984) 251.
- [8] D. Klabučar, work in progress.
- [9] Manque Rho, Proc. Int. School of Physics “Enrico Fermi”, 18–23 June 1984 (Varenna, Italy);
K. Iketani, Kyushu University Preprint, 1984.
- [10] V. Vento, M. Rho, E. Nyman, J.H. Jun and G.E. Brown, Nucl. Phys. A345 (1980) 413.
- [11] G.E. Brown, A.D. Jackson, M. Rho and V. Vento, Phys. Lett. 140B (1984) 285.
- [12] A. Jackson, A.D. Jackson and V. Pasquier, Nucl. Phys. A432 (1985) 567;
R. Vinh Mau, M. Lacombe, B. Loiseau, W.N. Cottingham and P. Lisboa, Phys. Lett. 150B (1985) 259.
- [13] V. Vento, M. Rho and G.E. Brown, Phys. Lett. 103B (1981) 285.
- [14] G.E. Brown, Australian Journal of Physics 36 (1983) 591; Proc. Workshop on the Interaction Between Medium Energy Nucleons in Nuclei, Bloomington, India, 22–30 Oct. 1982, A.I.P. Conf. Proc. No. 97.
- [15] V. Vento and M. Rho, Nucl. Phys. A412 (1984) 413.
- [16] G.E. Brown and A.D. Jackson, *The Nucleon–Nucleon Interaction* (North-Holland, Amsterdam, 1976).
- [17] T.T.S. Kuo and G.E. Brown, Phys. Lett. 18 (1966) 54. A factor of 2 is corrected in ref. [18].
- [18] G.E. Brown, *Unified Theory of Nuclear Models and Forces* (North-Holland, Amsterdam, 3rd ed., 1971).
- [19] G.E. Brown, *Mesons in Nuclei*, Vol. I, eds. M. Rho and D. Wilkinson (North-Holland, Amsterdam, 1979).
- [20] J. Durso, M. Saarela, G.E. Brown and A.D. Jackson, Nucl. Phys. A278 (1977) 445.
- [21] J. Durso, A.D. Jackson and B. VerWest, Nucl. Phys. A345 (1980) 471.
- [22] R. Vinh Mau, *Mesons in Nuclei*, Vol. I, eds. M. Rho and D. Wilkinson (North-Holland, Amsterdam, 1979).
- [23] M. Rho, A.S. Goldhaber and G.E. Brown, Phys. Rev. Lett. 51 (1983) 747.
- [24] G. Breit, Proc. Nat'l. Acad. Sci. U.S.A. 46 (1960) 746; Phys. Rev. 120 (1960) 287.
- [25] B. VerWest and D.O. Riska, Phys. Lett. 48B (1974) 17.
- [26] W. Grein, Nucl. Phys. B131 (1977) 255.
- [27] F. Iachello, A.D. Jackson and A. Lande, Phys. Lett. 43B (1973) 191.
- [28] G.E. Brown, Prog. in Particle and Nuclear Physics 8, Proc. Int. School of Nuclear Physics, Erice, 21–30 April 1981 (Pergamon Press, 1981);
E. Oset, Nucl. Phys. A, to be published.
- [29] M.M. Nagels et al., Nucl. Phys. B109 (1976) 1.
- [30] G. Höhler and E. Pietarinen, Nucl. Phys. B95 (1975) 210.
- [31] M.R. Anastasio and G.E. Brown, Nucl. Phys. A285 (1977) 516.
- [32] G.E. Brown, S.-O. Bäckman, E. Oset and W. Weise, Nucl. Phys. A286 (1977) 191.
- [33] G. Love, M. Franey and F. Petrovich, Proc. Int. Conf. on Spin Excitations in Nuclei Telluride, Co., 25–27 March 1982 (Plenum Press, N.Y., 1984).
N.Y., 1984).
- [34] T.D. Lee, Rev. Mod. Phys. 47 (1975) 267;
A.D. Jackson, M. Rho and E. Krotschek, Nucl. Phys. A407 (1983) 495.
- [35] E. Nyman and M. Rho, Nucl. Phys. A268 (1976) 408.
- [36] A.D. Jackson, Annual Reviews of Nuclear and Particle Science (1983) 105.
- [37] A.A. Abriksov and I.M. Khalatnikov, Reports on Progress in Physics 22 (1959) 329.
- [38] D. Pines and P. Nozières, *The Theory of Quantum Liquids*, Vol. I (W.A. Benjamin, N.Y. and Amsterdam, 1966).
- [39] L.D. Landau, Zh. Eksp. Teor. Fiz. 30 (1956) 1058; 32 (1957) 59; 35 (1958) 97.
- [40] G.E. Brown, Rev. Mod. Phys. 43 (1971) 1.
- [41] S.-O. Bäckman, Nucl. Phys. A130 (1969) 427.
- [42] S.-O. Bäckman, O. Sjöberg and A.D. Jackson, Nucl. Phys. A321 (1979) 10.
- [43] J. Dabrowski and P. Haensel, Ann. Phys. (N.Y.) 97 (1976) 452.
- [44] J. Speth, V. Klemt, J. Wambach and G.E. Brown, Nucl. Phys. A343 (1980) 382.
- [45] Y. Futami, H. Toki and W. Weise, Phys. Lett. 77B (1978) 37.
- [46] W.H. Dickhoff, Nucl. Phys. A399 (1983) 287;
W.H. Dickhoff, A. Faessler, J. Meyer-ter-Vehn and H. Müther, Phys. Rev. C 23 (1981) 1154.
- [47] S.-O. Bäckman, A.D. Jackson and J.A. Niskanen, unpublished Stony Brook results (1979).
- [48] B.L. Friman and A.K. Dhar, Phys. Lett. 85B (1979) 1.
- [49] S.-O. Bäckman and W. Weise, Phys. Lett. 55B (1975) 1.
- [50] K.A. Brueckner and J.L. Gammel, Phys. Rev. 109 (1958) 1023.
- [51] Z.-Y. Ma and T.T.S. Kuo, Phys. Lett. 127B (1983) 137.
- [52] O. Sjöberg, Ann. Phys. 78 (1973) 39.
- [53] O. Sjöberg, Nucl. Phys. A209 (1973) 363.
- [54] S.-O. Bäckman, Nucl. Phys. A120 (1968) 593.

- [55] N.F. Berk and J.R. Schrieffer, Phys. Rev. Lett. 17 (1966) 433.
- [56] S. Doniach and S. Engelsberg, Phys. Rev. Lett. 17 (1966) 750.
- [57] S. Babu and G.E. Brown, Ann. Phys. 78 (1973) 1.
- [58] S. Krewald and J. Speth, Phys. Rev. Lett. 45 (1980) 417.
- [59] M.W. Kirson, Ann. Phys. (N.Y.) 66 (1971) 624.
- [60] D.W.L. Sprung and A.M. Jopko, Can. Journ. Phys. 50 (1972) 2768.
- [61] J. Bardeen, G. Baym and D. Pines, Phys. Rev. 156 (1967) 207.
- [62] N. Marty, M. Morlet, A. Willis, V. Comparat and R. Frascaria, Proc. Int. Symp. on Highly Excited States in Nuclei, Julich, 1975, ed. A. Faessler.
- [63] D.H. Youngblood, C.M. Rozsa, J.M. Moss, D.R. Brown and J.D. Bronson, Phys. Rev. Lett. 39 (1977) 1188.
- [64] J.P. Blaizot, D. Gogny and B. Grammaticos, Nucl. Phys. A265 (1976) 315.
- [65] J.P. Blaizot, D. Cogney and B. Grammaticos, Nucl. Phys. A355 (1981) 115.
- [66] G.E. Brown, J.H. Gunn and P. Gould, Nucl. Phys. 46 (1963) 598.
- [67] G.F. Bertsch and T.T.S. Kuo, Nucl. Phys. A112 (1968) 204.
- [68] J.P. Jeukenne, A. Lejeune and C. Mahaux, Phys. Reports 25C (1976) 83.
- [69] V. Bernard and N. Van Giai, Nucl. Phys. A348 (1980) 75.
- [70] P.F. Bortignon and R.A. Broglia, Nucl. Phys. A371 (1981) 405.
- [71] J. Wambach, V.K. Mishra and Li Chu-hsia, Nucl. Phys. A380 (1982) 285.
- [72] H.M. Sommermann, T.T.S. Kuo and K.F. Ratcliff, Phys. Lett. 112B (1982) 108.
- [73] G.E. Brown, C.J. Pethick and A. Zaringhalam, J. Low Temp. Phys. 48 (1982) 349.
- [74] D. Greywall and P. Busch, Phys. Rev. Lett. 49 (1982) 146;
D. Greywall, Phys. Rev. B27 (1983) 2747.
- [75] A. Bohr and B.R. Mottelson, Nuclear Structure, Vol. I (W.A. Benjamin, Inc., N.Y., Amsterdam, 1969).
- [76] H.A. Bethe, G.E. Brown, J. Applegate and J.M. Lattimer, Nucl. Phys. A324 (1979) 487.
- [77] G.E. Brown, J. Speth and J. Wambach, Phys. Rev. Lett. 46 (1981) 1057.
- [78] G.E. Brown and Mannque Rho, Nucl. Phys. A372 (1981) 397.
- [79] C.D. Goodman et al., Phys. Rev. Lett. 44 (1980) 1755.
- [80] B.L. Friman and E.M. Nyman, Nucl. Phys. A302 (1978) 365.
- [81] J. Wambach, A.D. Jackson and J. Speth, Nucl. Phys. A348 (1980) 221.
- [82] A.B. Migdal, Zh. ETF 61 (1971) 2210; JETP (Sov. Phys.) 34 (1972) 1184.
- [83] W. Weise and G.E. Brown, Phys. Lett. 48B (1974) 297.
- [84] W.G. Love, in: The (*p, n*) Reaction and the Nucleon-Nucleon Force, eds. C.D. Goodman et al. (Plenum, N.Y. 1980);
F. Petrovich, ibid.
- [85] T.N. Taddeucci et al., Phys. Rev. C 25 (1982) 1094.
- [86] S.-O. Bäckman and O. Sjöberg, private communication.
- [87] G.E. Brown, J.S. Dehesa and J. Speth, Nucl. Phys. A330 (1979) 290.
- [88] C. Mahaux and H.M. Sommermann, Nucl. Phys. A411 (1983) 27.
- [89] W.H. Dickhoff, A. Faessler, H. Müther and S.S. Wu, Nucl. Phys. A405 (1983) 534.
- [90] E. Oset and A. Palanques-Mestre, Nucl. Phys. A359 (1981) 289.
- [91] W.H. Dickhoff, A. Faessler, J. Meyer-ter-Vehn and H. Müther, Nucl. Phys. A368 (1981) 445.
- [92] K. Nakayama, S. Krewald, J. Speth and G.E. Brown, Phys. Rev. Lett. 52 (1984) 500.
- [93] G.M. Carneiro and C.J. Pethick, Phys. Rev. B16 (1977) 1933.
- [94] O. Sjöberg, Phys. Lett. 142B (1984) 229.
- [95] K.S. Bedell and K.F. Quader, Phys. Lett. 96A (1983) 91.
- [96] J.Ia. Pomeranchuk, JETP (Sov. Phys.) 8 (1959) 361.